ESTABLISHING A BIM FRAMEWORK FOR INTEGRATING PASSIVE DESIGN STRATEGIES FOR DESIGNING ENERGY-EFFICIENT RESIDENTIAL HIGH-RISE BUILDINGS IN SRI LANKA

Panagoda Widanalage Udara Sachinthana Perera

228086C

Degree of Master of Science

Department of Civil Engineering

University of Moratuwa

Sri Lanka

November 2024

ESTABLISHING A BIM FRAMEWORK FOR INTEGRATING PASSIVE DESIGN STRATEGIES FOR DESIGNING ENERGY-EFFICIENT RESIDENTIAL HIGH-RISE BUILDINGS IN SRI LANKA

Panagoda Widanalage Udara Sachinthana Perera

228086C

Thesis submitted in partial fulfillment of the requirements for the degree Master of Science in Civil Engineering.

Department of Civil Engineering

University of Moratuwa

Sri Lanka

November 2024

DECLARATION

I hereby witness that this thesis represents my original research work conducted after registration for the degree of M.Sc. at the Department of Civil Engineering, University of Moratuwa. It has not been submitted elsewhere or for any degree or diploma, and the collaborative contributions and previous work related to the current study have been stated and properly acknowledged.

Also, I hereby grant a non-exclusive right to the University of Moratuwa and its agents to archive and make accessible this dissertation, in whole or in part, in print, electronic, or another medium. However, I retain all the ownership to use this content in whole or part in publications (Article/ Book).

Signature: Date: 25.11.2024

The above candidate has carried out research for the Master's degree under my supervision

Name of the supervisor: Prof. C. S. Lewangamage

Signature of the supervisor: Date: 26.11.2024

Name of the supervisor: Dr. A. U. Weerasuriya

Signature of the supervisor: Date: 26.11.2024

Name of the supervisor: Dr. R. Ruparathna

Signature of the supervisor: Date: 26.11.2024

ACKNOWLEDGEMENT

I dedicate this thesis to the following individuals whose unwavering support and guidance have been imperative for the success of my Master’s research:

- To my esteemed supervisors, Prof. C.S. Lewangamage, Dr. Asiri Weerasuriya, and Dr. Rajeev Ruparathna, whose mentorship and expertise paved the way for the accomplishments of my Master's degree. Dr. Asiri's immense support enhanced my scientific thinking and writing, guiding me to a successful completion. Prof. Sujeewa, my thesis supervisor, supported me by coordinating progress reviews, ensuring the smooth progression of my academic endeavors. Dr. Rajeev's insights into building information modeling expanded the horizons of my research scope.
- To Eng. Ishan Tharaka, for his contribution to preparing the early version of the questionnaire survey and the data collection.
- To Dr.(Ms) Nilanka Weerasinghe (UOM), Dr. Rajeev Mallawarachchi (SLTC), Dr. Senaka Dharmatilleke (Havelock City), and Mr. Rohitha (Havelock City), whose assistance in the field measurement campaign was invaluable. I thank all the undergraduates who helped me collect field measurement data.
- To Dr. Hasitha Hidallanagamage and Dr. Nimal Wijerathna for their support and insightful feedback during the progress reviews.
- To Eng. Pasindu Meddage and Eng. Imesh Ekanayake, whose assistance in understanding and developing machine learning models to enrich my research.
- To my beloved parents and friends, your unwavering support and encouragement have strengthened me throughout my MSc journey.

P.W.U.S. Perera

Department of Civil Engineering

University of Moratuwa

ABSTRACT

Sri Lanka expects a surge in demand for residential high-rise buildings (RHBs). Energy-intensive heating, ventilation, and air conditioning (HVAC) systems are relied on for the indoor thermal comfort of these buildings. The HVAC dependency can be minimized by integrating Passive Design Strategies (PDS) that leverage natural resources to control heat transfer and ventilation. Despite their potential, the efficacy of PDS is sparsely studied for Sri Lankan buildings. Addressing this knowledge gap, this study introduces a novel Building Information Modeling (BIM)-based Building Performance Analysis (BPA) framework for an energy-efficient building design workflow. Eight popular PDS were identified through a questionnaire survey among local building designers. These strategies were then applied to a typical RHB in three distinct sub-climates in Sri Lanka. The comparison between the survey findings and simulation results highlights a discrepancy between the popularity of PDS and their actual performance, emphasizing the need for enhanced awareness among Sri Lankan building designers. The local and global sensitivity analyses revealed low e-coating glasses and solar reflective wall paints as the energy-efficient PDS for Colombo and Kandy. In contrast, low conductivity walls and multiple/thick glazing are the most effective PDS for Nuwara Eliya. The multi-objective optimization of this study demonstrated that the optimum PDS design could substantially reduce operational energy consumption by 41.4%, 61%, and 29.4% and investment costs by 7.5%, 4%, and 4% compared to original designs in Colombo, Kandy, and Nuwara Eliya. Importantly, prioritizing low operational energy PDS design over the investment cost proves crucial for achieving sustainable metrics, such as carbon emission reduction and green rating scores. While the output of this study sets basic guidelines for Sri Lankan building designers in integrating passive design strategies for RHBs, the novel BIM-based BPA framework stands as a solution for existing technical gaps in BIM-based building design workflows.

Keywords: Passive design strategies, Building Information Modelling, Energy Simulation

TABLE OF CONTENTS

LIST OF FIGURES

LIST OF TABLES

LIST OF ABBREVIATIONS

RHB – Residential High-rise Building

PDS – Passive Design Strategies

BIM- Building Information Modelling

BPA – Building Performance Simulation

EUI – Energy Use Intensity

LSA – Local Sensitivity Analysis

GSA – Global Sensitivity Analysis

LHS – Latin Hypercube Sampling

OH – Window Overhang

SF- Window Sidefin

EC – Reflective Walls

GU – Multiple/thick glazing

WS – High thermal walls

CW - Low conductivity walls

WC – Low-E glazing

WAPE – Weighted Absolute Percentage Error

MAE – Mean Absolute Error

MSE – Mean Squared Error

OE – Operational Energy

IC – Investment Cost

HVAC – Heating, Ventilation, and Air Conditioning

EE – Elementary Effect

CC – Construction Cost

MOO – Multi-Objective Optimization

R^2 – Coefficient of Determination

$E_{equipment}$ – Annual Energy Demand for equipment

$E_{lighting}$ – Annual Energy Demand for lighting

E_{hvac} – Annual Energy Demand for HVAC

CC_r – Construction Cost of r^{th} PDS design

MC_r – Material Cost of r^{th} PDS design

OC – Construction and Material Costs of the rest of the building element

FA – Total area of a typical floor

D_i – Euclidian Distance

f_{IC} – Investment Cost function

f_{OE} – Operational Energy function

NDS – Non-Dominated Solution

EF- Emission Factor

EPD – Environmental Product Declaration

AUC – Additional Upfront Carbon Emission

ANNEXURE

CHAPTER 1

1. INTRODUCTION

The urban population has significantly grown over the past decade, and now nearly 54% of the world's population lives in urban habitats. This figure is anticipated to increase to 68% by the end of 2050 (World Bank, 2022). About 50% will be in the tropics, the region near the equator, bounded by Tropics of Cancer and Capricorn in the Northern and Southern Hemisphere (Harding et al., 2020). The Tropic is heavily populated; thus, providing shelters for a large population using scarce land is a perpetual problem. As a feasible solution, residential high-rise buildings (RHB) have been constructed in urban areas in the tropics. Following the same trend, RHBs have been built in Sri Lanka in past decades as never before. For instance, the number of approved RHB projects in Sri Lanka has risen almost three times from 2010 to 2017. About 90% of RHBs were constructed in Colombo, the commercial capital of Sri Lanka (Prathapasinghe et al., 2018). It is anticipated that this trend will continue at a higher rate.

Although RHBs maximize the utilization of scarce land in cities, they also increase energy consumption in the Tropics. RHBs consume much energy to maintain indoor thermal comfort for building occupants because of the year-round high ambient temperature and humidity in the Tropics. As a result, there is a high demand for Heating, ventilation, and air conditioning (HVAC) systems in the Tropics (Karunathilake et al., 2018). These HVAC systems consume an average of 35% of the total building energy consumption, making RHBs an energy hotspot (González-Torres et al., 2022). Besides, the regular maintenance of such systems is an additional recurring cost for building occupants. The increased energy consumption burdens building occupants and degrades the environment due to fossil fuel burning for electricity production, leading to severe environmental impacts, such as global warming (Zhong et al., 2021). Therefore, designing energy-efficient RHBs in Sri Lanka is imperative to achieve sustainability goals.

Passive design strategies (PDS) are well-accepted methods of minimizing the dependence on HVAC systems. PDSs modify the thermos-physical properties of buildings, thus decreasing indoor heat gain. PDSs often involve altering envelop configurations, changing ventilation patterns, controlling occupancy parameters (set point temperature, schedules, etc.), and changing building orientations (Nandapala et al., 2020a; Udawattha & Halwatura, 2018a). PDSs have long been a part of the vernacular architecture in tropical regions, especially in Asia, where their effectiveness has been proven (Mendis et al., 2020; Nguyen et al., 2011a, 2011b; Pathirana et al., 2019; Santy et al., 2017). Ancient residential buildings in Sri Lanka also adopted PDSs, such as central courtyards, window shadings, low conductivity walling, etc.(Mehjabeen Ratree et al., 2020). However, scientific evidence on the integration of PDS for RHBs in the tropics is rare, and no evidence in the literature is found for Sri Lanka.

Three problems frequently confront the integration of PDS in residential high-rise buildings. The first problem is the climate sensitivity of PDSs, resulting in various degrees of building energy saving in different climate zones (Harkouss et al., 2018a). This prevents the direct application of PDS across different climate zones without conducting a comprehensive assessment of PDSs' energy-saving effectiveness. The second problem is the redundancy or adverse effect caused by the interaction of several PDSs with non-linear relationships between PDS design parameters. Moreover, some PDSs can hinder positive features, such as daylight penetration(Freewan, 2014a) and natural ventilation(Elshafei et al., 2017). The third problem is the high payback period associated with PDS applications, discouraging potential investment in PDS (Sun et al., 2018). However, these problems can be addressed early in the building design process. During this stage, designers analyze building performances (From here, the term "building performance analysis will be used to refer to it) when PDS are integrated into RHBs to make crucial decisions. Physics-based building performance analyses assess different design scenarios and provide all the information needed to make the best decision.

However, building performance analyses (BPA) are time-consuming and require high computing performance and storage, as their workflows are iterative and involve ample data storage and complex decision-making in diverse environmental conditions. Building Information Modelling (BIM) offers a promising solution for designers to integrate building simulations, data analysis, and visualization into a single platform.

However, BIM-based BPA workflows experience technical challenges like interoperability and lack of visualization tools. Therefore, a compatible and efficient workflow should be invented before using a BIM-based BPA environment to evaluate the energy efficiency of PDS in RHBs.

1.1 Scope and Objectives

The research aims to establish a BIM-based framework to perform BPA to support designing energy-efficient and cost-effective buildings by integrating passive design strategies. This aim is achieved by fulfilling four objectives as stated below:

- To identify popular passive design strategies to reduce energy consumption, enhance thermal comfortability, and improve daylight performance in RHBs' living spaces by conducting a comprehensive literature review and questionnaire survey.
- To develop a BIM-based framework to identify suitable PDSs by conducting a cost-benefit analysis and rate building sustainability after adopting PDSs.
- To evaluate the performance of passive strategies in building energy saving, thermal comfort, and daylight performance of RHBs in three climate zones in Sri Lanka.
- To propose a ready-to-use holistic framework to integrate suitable PDSs into RHB designs to save energy, improve thermal comfortability and daylight performance, and achieve sustainability goals.

The study fulfilled the abovementioned objectives by investigating PDSs, RHBs, and BIM-based design frameworks. To make the study more specific, it defined the scope for all three domains, illustrated in Figure 01.

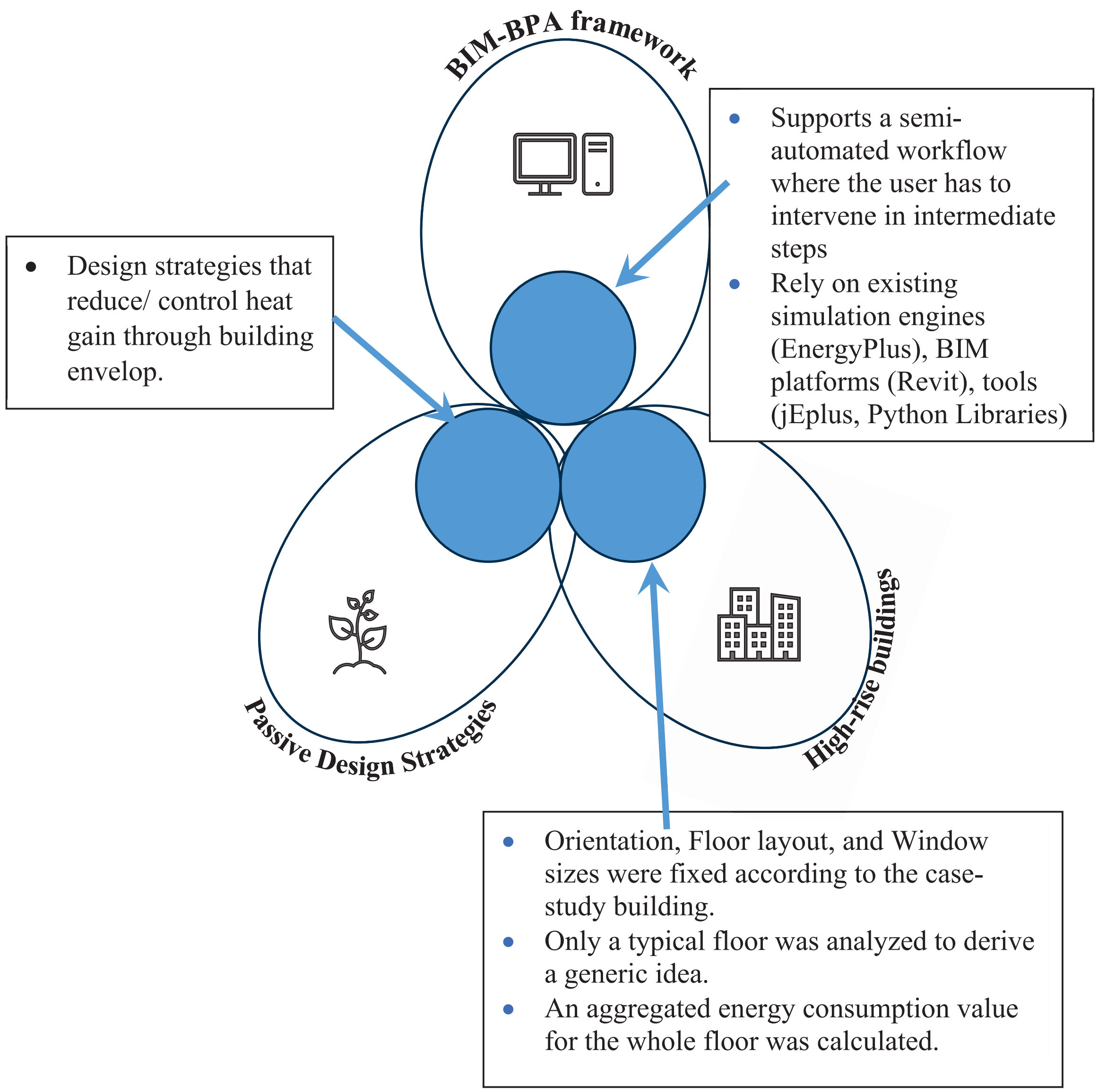

Figure 1:Scope of the study

1.2 Methodology

Figure 2 shows the entire research methodology with three distinct phases. In the first phase, eight passive design strategies, popular among Sri Lankan building designers, were selected from a questionnaire survey. The second phase consists of developing a BIM-based framework. This framework introduces a novel building design workflow tailored to enhance the sustainability of building designs by integrating PDS and facilitating the BPA of RHBs. The BPA workflow consists of daylight and energy simulations, global and local sensitivity analyses, and multi-objective optimization. To ensure the completeness of the workflow, five middleware tools were developed utilizing Autodesk Dynamo and Python programming language. The primary goals of this framework are to recommend energy-efficient PDSs for specific climatic conditions and to choose the optimal PDS based on investment cost, operational energy consumption, and achieving sustainability goals. The third phase of the research project aims to demonstrate the framework's performance by conducting a case study on a typical RHB in Sri Lanka. The case study considered three sub-climate zones to investigate the impact of local climate conditions on the energy savings of PDSs. The third phase is divided into two stages. In the first stage, the energy-saving efficiency of PDS is estimated for each sub-climate zone by considering variations in energy-saving efficiency in the three sub-climates. In the second stage, the optimum PDS design is identified by considering the minimum investment cost of operational energy and the maximum sustainability goals. Finally, the study proposes recommendations for integrating PDSs for RHBs in Sri Lanka by highlighting the importance of BIM-based approaches in designing RHBs in the Tropics.

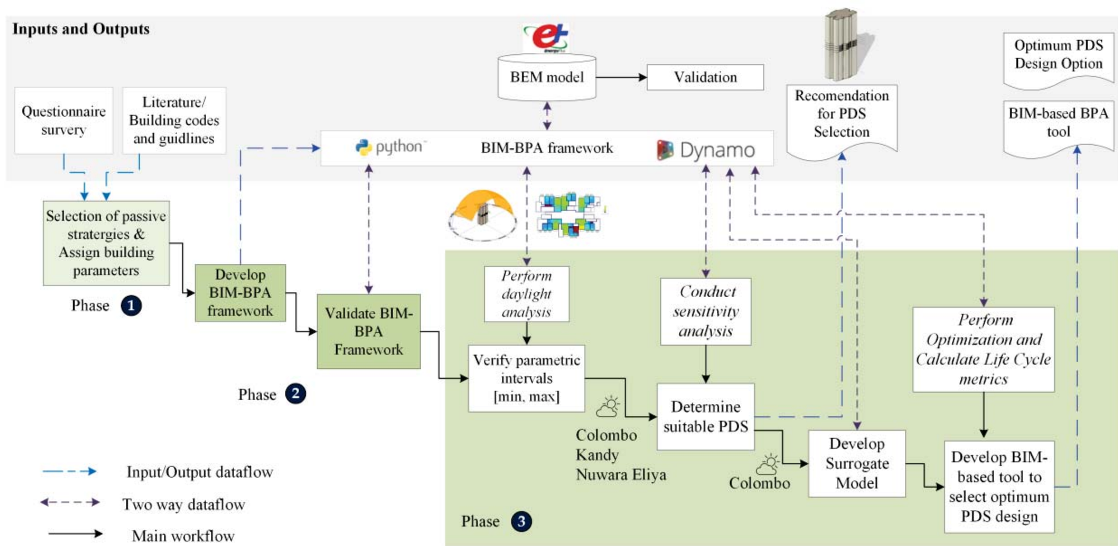

Figure 2: Graphical representation of the research methodology.

1.3 Arrangement of the Thesis

The thesis is arranged as follows:

Chapter 01 introduces the research topic, discusses the background of the study area and the research gap, and finally presents the study's aim, objectives, and methodology of fulfilling research objectives, including the scope of the study.

Chapter 02 presents a comprehensive literature review to understand the existing scientific knowledge on applying PDSs in tropical climates and BIM-based RHB design workflows. The review concludes by showing the limitations of existing research works.

Chapter 03 explains the process of selecting Passive Design Strategies (PDS) for this study. The local designer's preferences for PDS are presented based on the survey results of the questionnaire. Finally, this chapter summarizes building variables and their thresholds based on the findings of previous studies.

Chapter 04 outlines the novel BIM-based BPA framework proposed in this study. First, it presents the ideal BIM-based BPA-aided building design workflow and details the BIM template, simulation sub-frameworks, and middleware tools developed to achieve the proposed workflow.

Chapter 05 presents the details of the case study conducted in this research. The chapter includes the construction, thermal, and operational details of the case study building, baseline settings, and the validation of the building energy model. Then, the chapter describes the details and validation of the energy prediction meta-model, weather details of three case-study climates, and the verification of PDS thresholds from daylight simulations.

Chapter 06 presents the results of the analysis performed in this study. This chapter consists of two parts. First, it describes the sensitivity analysis and the recommendations for PDS for the best energy savings under three climates. Second, it shows the results of optimum PDS combinations.

Chapter 07 presents the limitations of adopting the results and BIM-based framework for future studies.

Chapter 08 presents the conclusions and recommendations based on the results of the analysis.

CHAPTER 2

2. LITERATURE REVIEW

This chapter focuses on two areas of previous research: passive design strategies for tropical climates and BIM-based building design frameworks. This chapter presents a detailed literature review of existing scientific knowledge in these two areas.

2.1 Passive Design Strategies in Tropical Climates

Numerous studies have explored the usefulness and efficiency of PDS in tropical climates. Tropical (also referred to as equatorial) climate classification first appeared in the Koppen-Geiger climate zoning map. The tropical zone is again divided into four sub-climates: fully humid (A_f), winter dry (A_w), summer dry (A_s), and monsoonal(A_m). This zoning is not compatible with building thermal comfort studies due to a lack of representation of heating/cooling degree days, solar radiation, and humidity. ASHARE Standard-169 provides better climate zoning for creating thermal and energy studies to address this issue. In this climate zoning, 8 thermal zones are defined based on heating or cooling degree days, denoted by the first letter. The second letter of the zone represents the type of climate, whereas the tropical region is denoted by A, which is characterized by high humidity. The existing research encompasses different sub-climates (ranging from 0A to 4A according to ASHRAE 169) in tropical countries. The following chapters present the findings of the literature review on PDS applications, which are categorized into three types. The first research type discusses the application of a single PDS in a specific sub-climate zone. The second research type analyzes the impacts of integrating multiple PDS into buildings. The third research type examines how the effectiveness of PDS varies across different sub-climate zones in the tropical region.

2.1.1 Application of a single PDS

A simulation study by (Rajapaksha et al., 2003) found that an adequately ventilated courtyard acts as a passive cooling strategy that minimizes indoor overheating of houses (Santy et al., 2017), increasing natural ventilation and shading devices save the building's cooling energy in extremely hot, humid climates (0A). A study conducted by Wong & Baldwin (2016a) has concluded that double-skin green facades can substantially save energy in high-rise residential buildings in Hong Kong, which have sub-tropical (2A) climates. Ohene et al. (2022) found that passive design strategies like natural ventilation, sun-shading, and airtightness can reduce the energy demand of residential buildings by 50% in tropical (0A) climates. If passive design strategies are coupled with solar PV systems, Ohene et al. (2022) further confirm the potential of constructing net-zero energy buildings. A study on an extremely hot, humid (0A) climate emphasizes the importance of using thick mud-concrete blocks (low conductivity and high thermal mass) as passive building envelops to reduce energy consumption and enhance structural cooling effects(Udawattha & Halwatura, 2018b). A study inspired by vernacular tropical architecture indicates that earth-based walling materials and exterior shading can improve thermal comfort and reduce carbon footprint in low-rise residential buildings (Mehjabeen Ratree et al., 2020). Another study in Sri Lanka introduced an innovative insulated roof slab system that includes an EPS (Expanded Polystyrene) layer. The field measurements show that it can reduce 20% peak cooling loads and 5% life-cycle cost in tropical climates (Nandapala et al., 2020b).

These studies have concentrated on implementing only a single PDS. Nonetheless, it is common practice to apply multiple PDSs to enhance their energy-saving ability simultaneously.

2.1.2 Application of Multiple Passive Design Strategies

Cheung et al. (2005) are one of the early researchers who showed the importance of applying multiple PDS for buildings in hot, humid (2A) climates. The simulation results for a residential high-rise building indicate that using a light color for exterior walls is the most effective strategy, which saves 19.4% of annual energy demand. This saving increased by 31.4% if light-colored walls had EPS wall insulation, low e-window glazing, and window shadings. Rana et al. (2021) propose a low window-to-wall ratio in South and West facades and double glazing with Low E coating to reduce about 9.14% energy consumption (0A) of buildings in the tropics. Anwar et al. (2021) found that natural ventilation and green walls were efficient passive strategies to reduce cooling (by 27.75%) and heating (35%) demands of buildings (0A) in the tropics. Another study (Huang & Hwang, 2016) highlights the importance of combining several passive design strategies to reduce high cooling loads caused by future extreme climates in tropical countries (2A). Y. Chen et al. (2021) discovered that operable window shadings can effectively mitigate excessive daylight penetration while preserving a favorable thermal indoor environment in hot and humid (0A) climates. Furthermore, the study suggests that buildings should incorporate operable windows, thermal insulation, and airtightness for optimal effectiveness. A case study analysis in tropical regions(0A) indicates that passive strategies reduce 5% energy consumption(Sun et al., 2018). However, the study pinpoints that the higher investment cost and, thus, the higher payback period can discourage stakeholders from integrating passive strategy into buildings. Hence, the payback period of passive design integration is an essential factor in the design process.

Previous research predominantly employed trial-and-error methods to determine an appropriate combination of passive design strategies. However, Prieto et al. (2018)proposed that this approach may result in redundant maximum energy savings; hence, adopting a mathematical approach to evaluate how passive design strategies interact is crucial.

Global sensitivity analysis (GSA) is a popular mathematical approach in passive design studies. It helps designers to understand both the importance of each variable and the interaction effect with each other. For example, Liu et al. (2020) employed the Morris method for GSA to identify the highest sensitive variables for solar protection passive strategies. Furthermore, the findings suggest that the thermal transmittance (U-value) of walls and windows exhibit interactions, implying that coupling highly insulated walls and windows may not yield optimal energy savings. Neale et al. (2022) found that building orientation, window-to-wall ratio, and coefficient of performance (COP) of cooling & heating systems are interacting parameters according to the Morris global sensitivity analysis. Hence, designers are advised to carefully select compatible passive design strategies as combinations. Multiple regression is another approach employed for GSA. A simulation-based study by X. Chen et al. (2015) shows that building orientation is a non-linear and interacting variable. This interaction effect reduces the cooling energy sensitivity, which cannot be discovered using a local sensitivity analysis. While the GSA is a valuable guide for selecting compatible variables and achieving a more effective passive design combination, mathematical approaches, such as optimization, offer optimal PDS combinations to minimize building energy consumption. More importantly, multiple objectives of various stakeholders (government, client, utility suppliers, etc.) should be satisfied in building designs. Hence, studies on applying a combination of passive design strategies have followed multi-objective optimization (MOO). For example, Alsharif et al. (2023a) show an optimum window shading combination, which saves about 7% of Heating and Cooling Loads and reduces 28 discomfort hours using the MOO approach. A study on South Korean residential buildings in a mixed humid (4A) climate has employed sensitivity analysis and MOO (Jung et al., 2021). The results indicate airtightness, number of occupants, and window-to-wall ratio as the most sensitive variables in passive design integration. Moreover, the study shows that an optimum PDS combination can save energy demand by 52.7%.

2.1.3 Dependency of climatic parameters for PDS effectiveness

A review by Bhamare et al. (2019) emphasizes that climatic conditions significantly influence the efficacy of passive design strategies. Harkouss et al. (2018b) reached a similar conclusion, suggesting that strategies to insulate exterior walls effectively reduce energy consumption in heating-dominant climates but may yield contrasting results in cooling-dominant regions. Moreover, while studies discussed in previous sections broadly illustrate the energy-saving effectiveness of various passive design strategies for tropical climates, some research highlights variations in effectiveness across sub-climates within the tropical region.

A study has investigated how sub-climates in tropical Brazil affect the energy saving of passive roof designs (Filho & Santos, 2014a). The findings indicate that a roof coated with reflective paint is effective for subtropical (3A) and tropical (0A) regions. In contrast, adding an insulation layer combined with reflective paint is solely practical for the tropical (0A) region. Nguyen & Reiter (2014) have investigated the effectiveness of passive design strategies for thermal comfort improvement in buildings under different sub-climates in tropical Vietnam. They found that natural ventilation is an effective passive strategy for tropical sub-climates (0A and 1A), while passive solar heating is only effective for warm, humid (2A) tropical regions. In their study, Gamero-Salinas et al. (2021) designed strategies that reduced energy consumption in both current and projected future weather scenarios across tropical lowland (0A) and tropical upland (2A) sub-climates in Honduras. Despite discovering that a comparable combination of natural ventilation, wall absorptance, and solar heat gain coefficients proves effective for both climates, they note a distinction difference in this combination to eliminate the overheating risk in 2A climates but only a risk reduction in 0A climates.

A non-exhaustive summary of the reviewed literature in this study is shown in Table 1 below,

Table 1: Summary of a literature review on Passive Design Strategies

Journal	**Types of Passive Designs**	**Country**	**ASHRAE 169-2020 climate zone**	**Reference**
Renewable Energy	Courtyards	Sri Lanka	0A	(Rajapaksha et al., 2003)
Buildings	Natural Ventilation, Shading, Walls and Roof, Orientation	Indonesia	0A	(Santy et al., 2017)
Building and Environment	Green walls	Hong-Kong	2A	(Wong & Baldwin, 2016a)
Energy and Buildings	Green walls	Hong-Kong	2A	(K. W. D. K. C. Dahanayake & Chow, 2017)
Energy and Buildings	Natural Ventilation, Sun Shading, Daylight, Airtightness	Ghana	0A	(Ohene et al., 2022)
Advances in Building Energy Research	Walling material	Sri Lanka	0A	(Udawattha & Halwatura, 2018b)
3rd International Conference of Contemporary Affairs in Architecture and Urbanism	4 traditional passive design strategies	Bangladesh and Sri Lanka	0A	(Mehjabeen Ratree et al., 2020)
Energy and Buildings	Roofing materials	Sri Lanka	0A	(Nandapala et al., 2020b)
Energy and Buildings	Envelope	China	2A	(Cheung et al., 2005)
International Journal of Building	Passive designs	Bangladesh	0A	(Rana et al., 2021)

Pathology and Adaptation				
Building Simul	7 strategies	Pakistan	0A	(Anwar et al., 2021)
Applied Energy	Envelop passive strategies	Taiwan	2A	(Huang & Hwang, 2016)
Journal of Asian Architecture And Building Engineering	Shading and Natural ventilation	Indonesia	Hot and humid climate	(Y. Chen et al., 2021)
Journal of Cleaner Production Journal	Building retrofit strategies to enhance daylight and decrease AC	Singapore	0A	(Sun et al., 2018)
Energy and Buildings	Building Envelop strategies and infiltration	Hong-Kong	2A	(Liu et al., 2020)
Applied Energy	25 building parameters	Ireland	5A	(Neale et al., 2022)
Energy and Buildings	Envelop passive strategies	Netherlands	4A	(Prieto et al., 2018)
Energy	9 passive design strategies	Hong Kong	2A	(X. Chen et al., 2015)
Energy and Buildings	Window shading	Australia, Melbourne	3A	(Alsharif et al., 2023a)
Building and Environment journal	Building envelops and airtightness	South Korea	4A	(Jung et al., 2021)
Energy and Buildings	Passive designs	Many countries	Many Climate zones	(Bhamare et al., 2019)
Energy	Envelop passive strategies	Many Countries	Köppen-Geiger climates	(Harkouss et al., 2018b)
Energy and Buildings	Roof insulation and reflectivity of the roof	Brazil	3A and 0A	(Filho & Santos, 2014a)
Energy and Buildings	Ventilation strategies	Vietnam	0A and 1A	(Nguyen & Reiter, 2014)
Energy and Buildings	5 passive strategies	Honduras	0A and 2A (Current and future climate)	(Gamero-Salinas et al., 2021)

2.2 Studies on BIM-based design workflows for BPA

BIM-based designing workflows integrated into building performance analysis (BPA) is an emerging research area (Jin et al., 2019). Performance-related data storage and management and better data visualization are key characteristics of the BIM-based BPA approach. Chang & Hsieh (2020) pinpoint four main steps in a BIM-based designing workflow: BIM authoring, BIM to simulation model translation, Building Performance Analysis, and Visualize and Update the BIM model. In the existing literature, three study types can be identified covering the four stages of BIM-based designing workflow, as highlighted in Figure 3. The subsequent sections present the details of the BIM-based designing workflow.

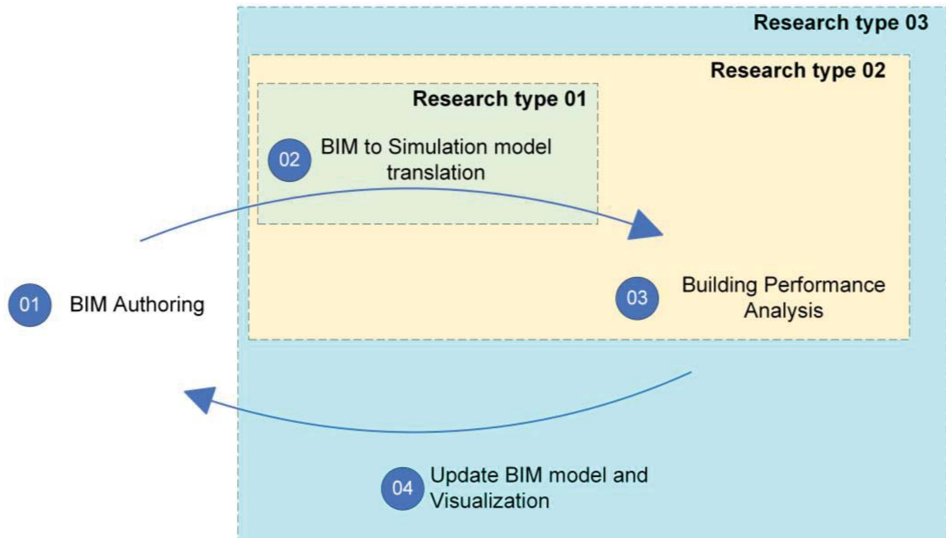

Figure 3: Summary of BIM-based design stages and existing research types.

2.2.1 Studies on BIM to Building Performance Simulation Model Translation.

Many studies have attempted to avoid remodeling buildings using building simulation tools by directly developing tools to translate BIM into building simulation models. Their focus is to bridge the gap in data exchange between the BIM authoring software and building performance simulation engines. The BIM to Building Energy Model (BEM) translation is frequently studied from the referred articles.

Ahn et al. (2014) are some of the earliest researchers to develop a practical interface for BIM to complete building energy simulation interoperability. They have introduced a BIM (IFC) to BEM (Energy Plus – IDF) file converter, enabling accurate geometry conversion. This allows automated building energy modeling, which saves cost and time when many design options (i.e., BIM models) are to be explored. Hou et al. (2022) have developed a method to translate initial building geometries and element properties to a Computation Fluid Dynamics (CFD) model and Building Energy Model

(BEM). Those models are then used to create a database to train an extreme learning machine model (ELM). This further enables faster thermal comfort prediction, indoor air quality, and energy consumption prediction. Shen & Pan (2023) also utilized BIM to create a database of energy simulation to train machine learning models. An open-source file format specialized for green building simulations: gbXML schema has been used to exchange data from BIM to energy simulation software (Design Builder). Unfortunately, the study does not support open-source data exchange and is limited to commercial software (e.g., Design Builder). Moreover, the abovementioned studies support only geometry and material data exchange out of many important parameters, such as building schedules, HVAC details, people, lighting, equipment heat gains, etc., for energy simulations. A study introduces a BIM (IFC) to a building energy model (Open Studio) translation (Ramaji et al., 2020), which can translate lighting fixture data in addition to geometry and material data. The case study presented in the research shows the importance of utilizing BIM to build simulation model translation for cloud-based simulations. Chong et al. (2019a) introduced an open-source BIM to create an energy model translator based on Java, which overcomes the limited data translation in other research works. It can convert geometry, schedules, HVAC details, and heat gain data from gbXML schema to building energy simulation input files (IDF). A practical application of the model for real-time calibration of energy models is demonstrated in the study.

A few scholars have developed BIM daylight model translators, which map geometrical and optical properties for daylight simulation models. Kota et al. (2014) have developed a plug-in (Autodesk Revit) to translate the BIM model to the Radiance model (lighting simulations) and validated it for several test cases. The dependence on commercial BIM software platforms is a main limitation of this tool, where researchers suggest exploring translation through open-source schema like IFC. Another study demonstrated data exchange for daylight simulation via Microsoft Excel and utilized the workflow to assess the visual comfort of apartment buildings (Amoruso et al., 2019).

The ability to 1) skip reworks in simulation modeling and 2) conduct detailed physics-based simulations are advantages of translating BIM to building simulation models. Nonetheless, the need for users to switch between multiple platforms (Ex-BIM, performance simulation engines) for iterative design processes remains a drawback of these tools and frameworks.

2.2.2 Studies on BIM-integrated Performance Analysis

Another domain of literature has studied how a BIM-based approach can translate and perform simulations in one click without switching between BIM and performance simulation engines.

A study introduces a new IFC-based framework to read BIM model data and give feedback about scores achieved under the material section of the BREAM green rating system (Ilhan & Yaman, 2016). A software tool developed under the framework runs a rule-based algorithm that checks the criteria of BREAM rating. Alwan & Ilhan Jones (2022) have developed a tool called pycab, which calculates the embodied carbon of the building from a BIM(IFC) file. As an example of practical usage, they have shown how the tool can be compared with the 2030 Climate Challenge Benchmarks set by RIBA. Bracht et al. (2021) have developed an application to obtain building properties from BIM (gbXML) files and predict thermal loads using a metamodeling approach. Thermal load predictions of test cases stand as proof of concept for the proposed approach, where the error of predictions is satisfactory (0-15%). However, the study pinpoints that gbXML files exported from different BIM authoring software (Autodesk Revit, ArchiCad, Open Buildings) do not follow typical standards, which hinders open-source data exchange. Yan et al. (2022) have developed a visual programming script (Grasshopper) that can translate the BIM model (Rhino) and perform daylight and energy simulations. Rad et al. (2021) attempted to utilize BIM-based building data to calculate the life cycle cost (LCC) of disaster-resilient building designs. Particularly noteworthy is their introduction of a failure cost component for LCC based on the probability of earthquake occurrence. Their Plug-In integrates energy simulation with earthquake simulation results, enabling a comparative analysis of building design options based on LCC.

Compared to the previous research, these studies have enabled faster BIM modeling to perform analysis workflow with minimum human intervention. Although BIM has appealing information visualization capability, the discussed tools failed to integrate results into BIM. For example, Truong et al. (2017) have showcased the importance of results visualization by developing a tool to illustrate the space-wise energy consumption of an apartment.

2.2.3 Studies on BIM-integrated building performance analysis and output visualization

The last domain in this section summarizes BIM-integrated sustainability performance analyses, which integrate 1) BIM authoring, 2) performance simulation, and 3) result visualization & updating BIM.

The Intelligent Green Building Rating (iGBR) introduces an innovative BIM-based framework for automatically assessing the green rating of buildings (D. Zhang et al., 2019). Utilizing the cloud platform, iGBR facilitates real-time monitoring of updates to BIM models. Moreover, it offers a unique feature by suggesting design ideas through group chat, thus presenting innovative solutions beyond current research paradigms. J. Zhang et al. (2021) have developed an algorithm that automatically generates an optimum building layout using a generative design approach. This algorithm visualizes viable design options inside the BIM platform with the total thermal load of each option. Building designers are given more leverage to choose design options based on quantitative metrics like thermal load and qualitative metrics like aesthetics and human-building interaction. A study by Singh et al. (2022a)developed a BIM-based tool to integrate building performance data for selecting optimal design options (appropriate geometrical and material properties) at early stages. In this tool, while performance analysis guides users to quantify the energy consumption of each design option, the BIM model visualizer provides valuable information to imagine how the building looks. The Performance-integrated BIM (P-BIM) framework Zhuang et al. (2021) represents another method for achieving an optimal envelope configuration that enhances both Indoor Environmental Quality (IEQ) and minimizes Life-Cycle Costs (LCC). While this framework encompasses a broad range of IEQ parameters in its optimization objective function, the authors propose enhancing it by incorporating IEQ parameters based on customer satisfaction. Moreover, they recommend developing tools that concentrate on the early stages of the design process to refine the framework further. Seghier et al. (2022) have introduced a BIM-based approach (RBIM) to choose the optimum envelope retrofit option. The developed prototype tool enables designers to select wall and window types that minimize overall thermal transfer value (OTTV) and retrofit cost. A summary of reviewed articles is shown in Table 2.

Table 2 : Summary of the studies on BIM-based design workflows

Journal	Stage	BIM Authoring	Performance Analysis	Pushback results and update	Input Parameters	Energy Consumption	IEQ	LCA	Day-Light	Green Rating	Open Source	Ref.
Energy and Buildings	Early Stage				Building parameters						Yes	(Ahn et al., 2014)
Energy and Building	Operational Stage										No	(Hou et al., 2022)
Applied Energy	Early-Stage				Whole Building						Partial	(Shen & Pan, 2023)
Journal of Computing in Civil Engineering	Early-Stage				Whole Building						Yes	(Ramaji et al., 2020)
Energy & Buildings	Early-Stage				Validation test cases						Yes	(Chong et al., 2019a)
Energy & Buildings	Case Study				Whole Building							(Kota et al., 2014)
Sustainability	Operational Stage				Whole Building							(Amoruso et al., 2019)
Automation in Construction	Early Stage				Building Model						Yes	(Ilhan & Yaman, 2016)
Automation in Construction	Early Stage				Whole Building						Yes	(Alwan & Ilhan Jones, 2022)
Automation in Construction	Early Stage				Whole Building						Yes	(Bracht et al., 2021)
Building and Environment	Early-Stage				Geometry Parameters Extreme weather files						Partial	(Yan et al., 2022)
Automation in Construction	Early-Stage				Whole Building						Partial	(Rad et al., 2021)
Energy and Buildings	Early Stage				Floor layout, Space loads, Door/Window sizes(WWR)						Partial	(J. Zhang et al., 2021)
Automation in Construction	Early Stage				Layout options, Envelop Parameters, Space heat loads						Yes	(Singh et al., 2022a)
Automation in Construction	O&M				Building Envelop construction						Yes	(Zhuang et al., 2021)
Automation in Construction	Retrofit				Envelop retrofit methods						Partial	(Seghier et al., 2022)
Sustainability	Early-Stage				Whole Building						No	(D. Zhang et al., 2019)

2.3 Summary of the chapter

This chapter presents the findings of a comprehensive literature review on Passive Design Strategies in tropical climates and BIM-based design workflows for building performance analysis. The literature survey is presented under two categories: (1) studies on passive design strategies (PDS) and (2) studies on the BIM-based design workflow for building performance analysis (BPA).

The findings of studies on PDS can be summarized as follows,

- Passive design strategies (PDS) are proven design integrations that minimize residential high-rise buildings' heating and cooling energy demand. A combination of PDS can enhance this energy reduction, yet careful selection is vital to avoid any redundancy effects. Sensitivity analysis and optimization are frequently cited mathematical approaches that help designers choose compatible and most effective PDS combinations. Building energy simulations are commonly employed to predict heating and cooling energy demand under different scenarios.
- The suitability of PDS is highly dependent on climatic parameters; thus, selecting compatible PDS for a particular region is necessary by conducting specified studies. To our knowledge, no study has been conducted on the suitability of PDS for RHBs in Sri Lanka.

The findings of studies on BIM-based design workflows can be summarized below,

- An ideal BIM-integrated building design process should facilitate three steps:1) BIM authoring, 2) Building Performance Analysis, and 3) Results visualization and updating the BIM model. Although few studies have covered all three steps, those studies have not focused on PDS integration into buildings. Many also have failed to incorporate building performance analysis and green rating assessment of buildings.
- The existing BIM-based workflows have still failed to support the open-source data format, which is essential for full-scale interoperability in BIM-based approaches.

CHAPTER 3

3. SELECTION OF PASSIVE DESIGN STRATEGIES

The task of selecting suitable Passive Design Strategies (PDS) for various climate regions around the world can be tedious. For this study, national-level guidelines, local studies in Sri Lanka, and research on tropical areas were referred to identify a list of PDS as a starting point. This chapter discusses the selection process PDS for this study, including its variables and their minimum and maximum values.

3.1 National guideline for Passive Design Strategy selection

The Sustainable Energy Residences Guidelines in Sri Lanka have provided essential guidance for choosing suitable Passive Design Strategies (PDS) tailored to the Sri Lankan context(Sri Lanka Sustainable Energy Authority, 2019). Figure 4 shows the recommended strategies. These strategies are categorized into four groups:

1. Start at the neighborhood/ Site

This group encompasses strategies for selecting appropriate building orientations and site layouts to optimize passive cooling and minimize solar gains in frequently occupied spaces. Initial site planning involves arranging land plots and streets to enhance natural ventilation and reduce solar exposure.

2. Shade (Avoid Sun)

Shading is a commonly employed PDS type to reduce direct solar radiation entering buildings. Various methods are suggested, including:

- External features include vegetation, complex landscaping elements, and neighboring structures.
- Building features like more extensive roof eaves and verandas.
- Incorporating green facades and green roofs.
- Providing shading for windows through external (window overhangs and side fins) or internal means (curtains, room blinds, or ventilated blinds).

3. Ventilate thoroughly.

This category of PDS aims to improve thermal comfort and indoor air quality by increasing airflow velocity and replacing heated indoor air with fresh, cool air. The guideline recommends orienting buildings to maximize wind exposure and promoting indoor airflow through well-designed building shells and openings.

4. Select materials wisely

Four PDS measures are outlined in the guideline under this category:

- Insulating exterior walls.
- Utilizing materials with high thermal mass.
- Opting for light-colored exterior walls.
- Applying films to reduce solar heat gains through glass surfaces.

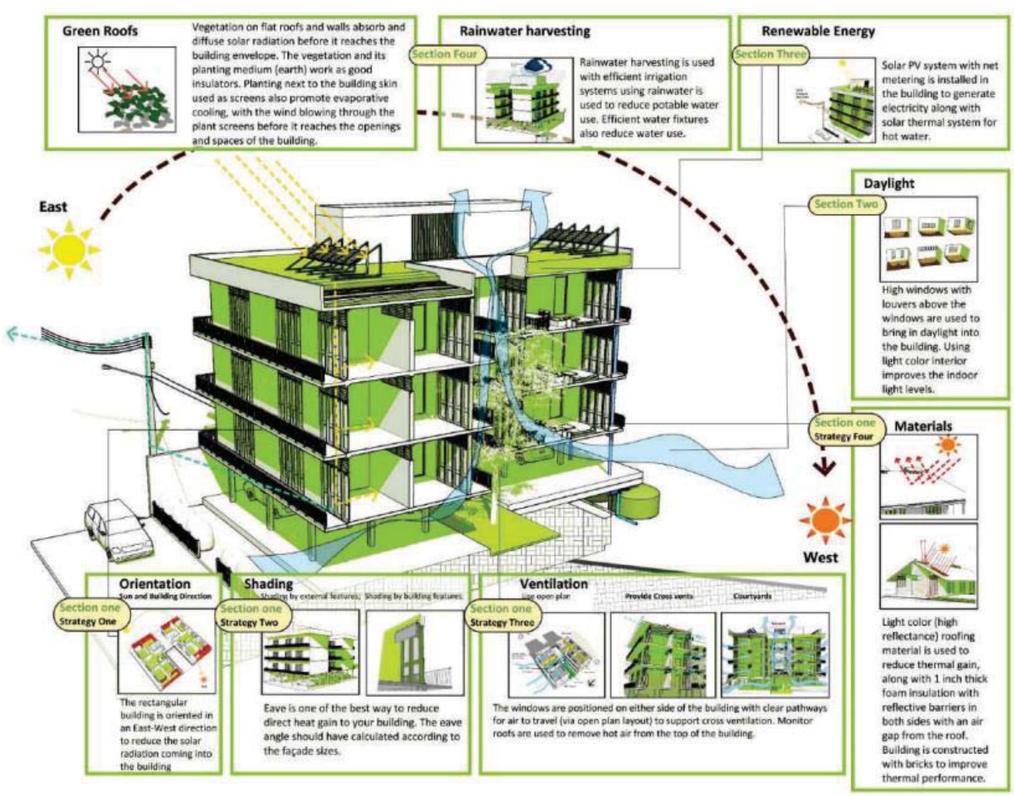

Figure 4: Graphical representation of guidelines to select PDS in Sri Lankan Buildings (Source: (Sri Lanka Sustainable Energy Authority, 2019)).

One notable limitation of these strategies is that they primarily apply to tropical climates with high temperatures, focusing on minimizing heat gains. Regions such as Nuwara Eliya and Bandarawela, characterized by cooler climates, may necessitate additional PDS, such as passive solar heating, to maintain adequate thermal comfort inside buildings, which are not covered in this guideline.

It is essential to consider the Passive Design Strategies (PDS) mentioned under "Start at Neighborhood" and "Ventilate Thoroughly" during the early stage of building design. This is because designers have more flexibility to make significant changes, such as changing the orientation, increasing the size of openings, and adjusting their locations. However, these two categories are out of the scope of this study. Instead, the PDS mentioned under "Shade" and "Select Material Wisely" are applicable. Therefore, 14 passive design strategies were initially selected (Table 3). PDSs are grouped according to building element (e.g., Exterior walls, Windows) or function (e.g., Airtightness).

Table 3: List of PDS outlined in the local guideline.

Category	**Passive Design Strategy**
Exterior walls	1.1 Solar reflective wall paints
	1.2 Light-colored exterior paints
	1.3 Green Walls
	1.4 External wall insulation
	1.5 Internal wall insulation
	1.6 Floor insulation
	1.7 High thermal mass walls
Windows	2.1 Apply coating on windows
	2.2 Internal shutters
	2.3 Double/multiple glazing
	2.4 Window frames with thermal breaks
	2.4 Louvers

	2.5 Vertical fins
	2.6 Overhangs
Airtightness	3.1 Joint sealing

3.2 Questionary survey

The next task of this study was to filter the most popular PDS among local designers. This was to add practical sense to the current research and to check whether the prevalent PDS performs well in the Sri Lankan context. The task was completed through an online questionnaire survey.

The questionnaire was sent to architects, designers, and consultants as a Google form and collected 74 responses. The respondents had various professional backgrounds, such as architecture (30%), structural engineering (15%), civil engineering (20%), and MEP engineering (15%), with expertise in energy simulations, architectural designs, green building consultation, etc. About 53% confirmed an excellent understanding of passive design strategies for over 15 years. This questionnaire allowed respondents to vote for preferred or commonly used PDS out of a list of 14 PDS obtained from the literature.

From the 14 common PDS strategies list, the survey narrowed down to the eight most popular PDS. The selected PDSs, their rank, and the number of votes are shown in Figure 5. Notably, reflective exterior surfaces and high-mass walls emerged as the most and least favorite choices. Green and insulated exterior walls followed closely reflective exterior surfaces and high-mass walls. Interestingly, when it came to window modifications, adding side fins proved more popular than other options like overhangs, low e-coatings, or thicker glazing.

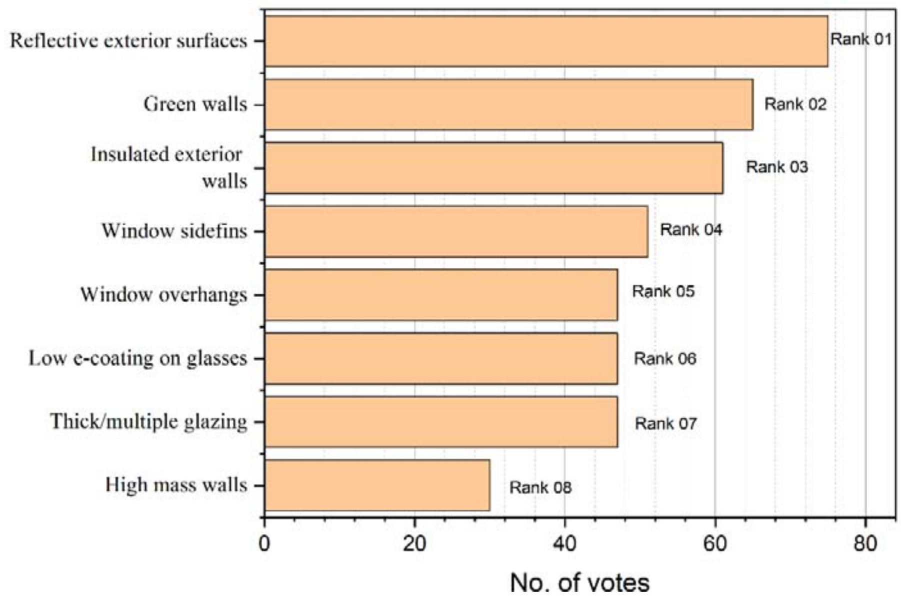

Figure 5: Most popular PDS among local designers and votes received for each PDS.

3.3 Selected Passive Design Strategies

To evaluate the impact of PDSs on building performance, relevant building parameter(s) for each PDS must be identified. Performance metrics are then calculated by assigning different values to these parameters. The selection of parameters is based on their compatibility with energy and lighting simulations, their usage in previous studies, and recommended threshold values. The following subsections provide a detailed description of parameters and their thresholds.

3.3.1 Window overhangs (OH) and side fins (SF)

Window overhangs and side fins are common PDS adopted for RHBs. These PDSs avoid direct heat gains through windows. Studies conducted by Alsharif et al., (2023b) and Freewan, (2014b) have chosen the length of overhangs and side fins as the variable to numerically model window overhangs and side fins in building energy modeling. Considering no window overhangs and side fins, the lower limit is 0, whereas the upper limit is 0.8m, considering daylight blocking and construction limitations. The upper limit is verified by performing daylight simulation in the proposed workflow.

3.3.2 Green walls (GW)

Applying green facades reduces the cooling energy demand of high-rise buildings (Malys et al., 2014; Wong & Baldwin, 2016b). Passive green walls, which have vegetation grown on a supportive structure attached to the façade, are a popular method of constructing green walls. Green walls reduce the cooling energy demand owing to four (4) effects: Shading, cavity insulation, wind barrier effect, and cooling due to evapotranspiration (Charoenkit & Yiemwattana, 2016; Manso & Castro-Gomes, 2015). However, modeling all these effects in energy modeling is technically tricky. Due to this limitation, only the shading impact of green walls is considered by adding a shading panel outside the exterior wall in the building energy model. The variable being considered is the area of facade coverage with green walls, which ranges from 0% to 100% of the exterior walls. The baseline design assumes 0% or no green wall coverage.

3.3.3 Reflective exterior surfaces (EC)

The amount of heat a material absorbs from solar radiation is an important variable when implementing Passive Design Strategies (PDS) in tropical regions. Special solar reflective paints are applied to exterior walls to reduce solar absorptance. Several studies Dias et al.(2014), Filho & Santos, (2014b) and Yew et al(2013) have identified solar absorptance, a non-dimensional parameter, as the variable to model PDS in simulation models. These studies suggest a range of 0.2 to 0.8 for this variable.

3.3.4 Thick/multiple glazing (GU)

Designers of green buildings can choose the thickness and composition of glazing. While clear glass with 3mm thickness is typically used, designers may opt for larger thicknesses or multiple layers with an air gap, such as Double/Triple glass, to reduce the glass's thermal transmittance (U-Value). Therefore, the U-value is a variable that can be used for energy simulation models. Previous research and the availability of different glass types suggest the upper, 5.8 W/m^2K, and lower, 0.8 W/m^2K, limits for U-Value.

3.3.5 High thermal mass walls (WS)

The high thermal mass wall is another prevalent PDS in literature. They increase the lagging time and reduce direct heat transfer during the daytime (Udawattha & Halwatura, 2018b). In other words, heat takes longer to pass through high thermal mass walls. Specific heat capacity is recommended in previous studies for energy simulation models. This study adopts a particular heat capacity of 800-1800 kJ/kg-K considering various wall construction materials (Muñoz et al., 2022).

3.3.6 External wall insulation/ Low conductivity walls (CW)

The conductive heat transfer is another controlling variable in the building. This heat transfer is mainly controlled using low thermal conductive walling materials or applying insulation layers. This is a popular strategy in both cooling and heating dominant regions. Thermal conductivity is the variable used to represent CW in building energy simulation models. The lower limit is taken as 0.035W/mK, representing innovative EPS concrete, while the upper limit of 2.1W/mK is assumed for reinforced concrete as recommended by (CIBSE, 2015; Shiveswarran et al., 2023).

3.3.7 Low e-coating on glasses (WC)

Applying low e-coatings and films on glasses to have a smaller solar heat gain coefficient (SHGC) is another technique to minimize heat transfer through windows. This technique is particularly effective in reducing the cooling energy demand in buildings in tropical climates (Harkouss et al., 2018; Jung et al., 2021). Although a small SHGC of 0.2 is advantageous in minimizing heat gain through windows, low e-coating glasses have small visual transmittance (VT), compromising daylight penetration to buildings (Pilkington North America, 2017). Hence, a lower SHGC limit of 0.5 is recommended.

The selected PDS, associated building variables, thresholds, and baseline values are summarized in Table 4.

Table 4: Summary of selected Passive Design Strategies (PDS)

Abb.	**Passive Strategy**	**Variable**	**Interval**	**Baseline**
OH	Window overhangs	Overhang length (m)	[0.0-0.8]	0
SF	Window side fins	Left and right overhang length (m)	[0.0-0.8]	0
GW	Green walls	Green wall percentage (%)	[0 – 100%]	0
EC	Reflective exterior surfaces	Solar Absorptance (Ratio)	[0.2-0.8]	0.8
GU	Thick/multiple glazing	U-Factor of glass (W/m^2K)	[1.7-5.7]	5.7
WS	High thermal mass walls	Specific Heat of walls (J/kg-K)	[800-1800]	860
CW	External wall insulation/Use low conductivity walling materials	Conductivity of walls (W/m-K)	[0.1-2.1]	2.1
WC	Low e-coating on glasses	Solar Heat Gain Coefficient (Ratio)	[0.5-0.83]	0.83

3.4 Summary of the chapter

This chapter presented the selection process for the current study of passive design strategies (PDS). First, 14 PDS were identified based on the national guidelines published by the Sustainable Energy Authority of Sri Lanka. Then, the most popular 8 PDS were filtered by conducting an online questionnaire survey among Architecture, Engineering, and Construction (AEC) professionals in Sri Lanka. Finally, a discussion on selected PDS, corresponding variables, and their thresholds was presented, referring to previous research and available construction materials.

CHAPTER 4

4. BIM-BASED BPA FRAMEWORK FOR SELECTING THE OPTIMUM PDS DESIGN OPTION

This section discusses the framework developed for the BIM-based building performance analysis (BPA) to select the best PDS for residential high-rise buildings. Previous studies have shown (Section 2.2) that building performance simulation and analysis tools are often disconnected and not integrated into a unified environment. This poses a challenge, particularly when building design workflows to enhance sustainability. To address this issue, this study introduces a four-step BIM-based designing workflow: BIM authoring, BIM to simulation model translation, Building Performance Analysis, and Visualize and Update the BIM model. The framework uses several software tools and interfaces listed in Figure 06.

Autodesk Revit is the most common BIM authoring software in BIM-based BPA approaches. Therefore, it was chosen as the BIM authoring software for this study. Once the BIM model is prepared, the next step is to translate it into a simulation model (e.g., energy, lighting). The only ready-to-use and open-source software available to facilitate this task is gbEplus (https://github.com/weilixu/gbEplus). However, the tool is not compatible with the current BIM environment. Therefore, one of the primary objectives of this study is to develop a BIM-compatible, open-source, and ready-to-use BIM toolset.

Several tools, such as Design Builder, Transys, and Open Studio, are available to facilitate building performance analysis, which runs on the Energy Plus simulation engine and enables advanced modeling and simulations. However, these tools fail to support parametric simulations in a BIM environment. Surplus tool (Y. Zhang & Korolija, 2010), famous among energy simulation research communities, is an open-source interface that runs on the EnergyPlus simulation engine and has a high potential for integration into the BIM environment. Therefore, jEplus was selected as the energy simulation engine for this study. Although few software tools are available for carbon emission and life-cycle costs, they do not yet support the BIM environment. Besides, calculating carbon emissions and life cycle costs is not complex; it only requires a database of default values and factors. Therefore, as proof of concept for the BIM-based BPA framework, the study developed its script to facilitate this task.

Visual programming embedded in modern BIM software can facilitate updating the BIM model in parametric analysis. For example, Grasshopper for Rhino and Dynamo for Revit are popular visual programming software in the BIM environment. For this study, Dynamo (compatible with Revit) was selected to facilitate the last step in the design workflow.

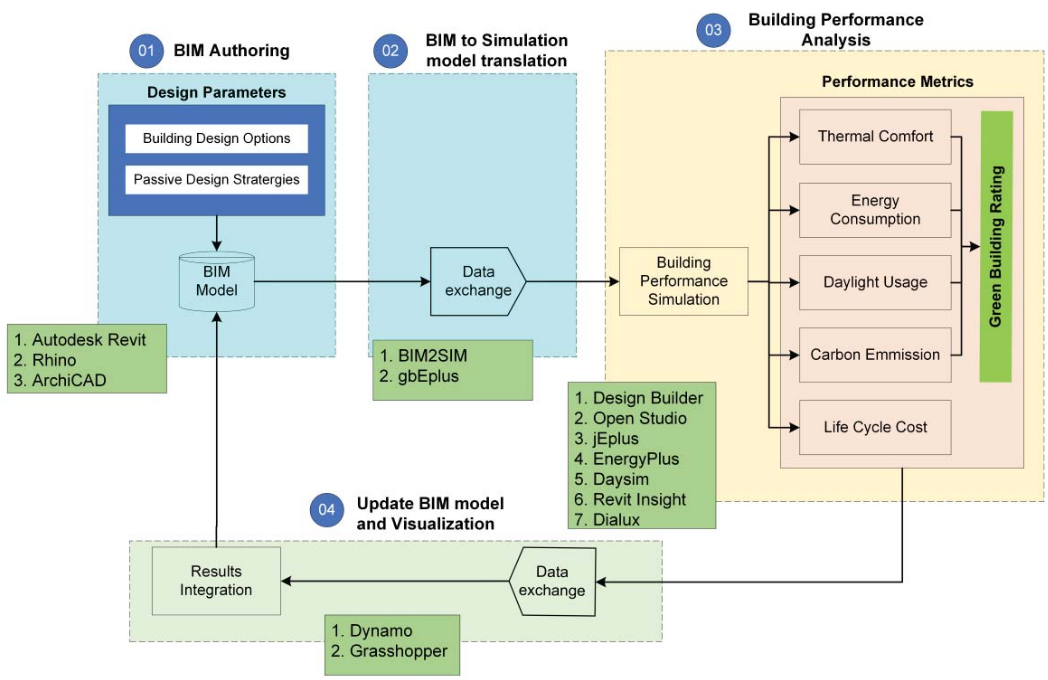

Figure 6: Ideal BIM-based BPA-aided building designing workflow.

The BIM-based Building Performance Analysis (BPA) framework unifies building design workflows by incorporating all necessary tools, including BIM templates, simulation sub-frameworks and interfaces, databases, and middleware tools. The popular BIM authoring platform, Autodesk Revit, uses the widely recognized parametric energy simulation interface jEplus coupled with the EnergyPlus engine. The Autodesk Insight daylight analysis tool for daylight simulations is the commonly used BIM tool. All these tools were integrated into a novel BIM-based BPA framework. The following subsections describe the newly developed supportive tools to achieve a unified building design workflow.

4.1 BIM template

The first step of the proposed workflow is creating a BIM model of the baseline building. Standardizing data is essential for BIM modeling to maintain consistency and interoperability in the later steps of the design workflow. Hence, a BIM template was prepared using Autodesk Revit software and included the following features,

1. Revit family components with additional life-cycle parameters
2. Wall and floor family components for adiabatic walls
3. Operating schedules and heat gain data for different types of spaces (Bedroom, Living room, and other rooms)

An example of the BIM interface is shown in Figure 07.

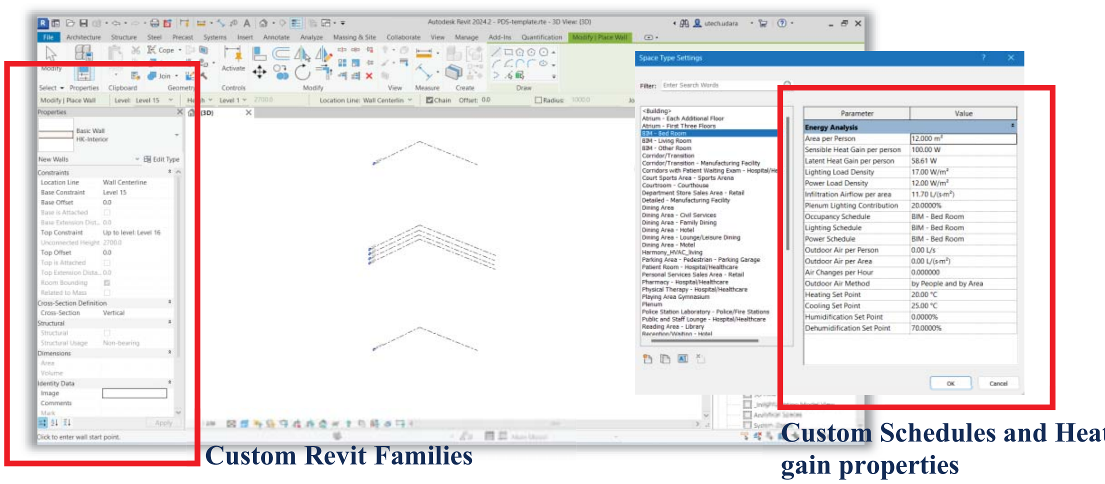

Figure 7: Interface of BIM template prepared in Autodesk Revit.

The BIM-based BPA framework consists of two simulation sub-frameworks: energy simulation and daylight simulation. Figure 08 illustrates the relationships between each component and the data flow structure. The subsequent sections describe each of the sub-frameworks.

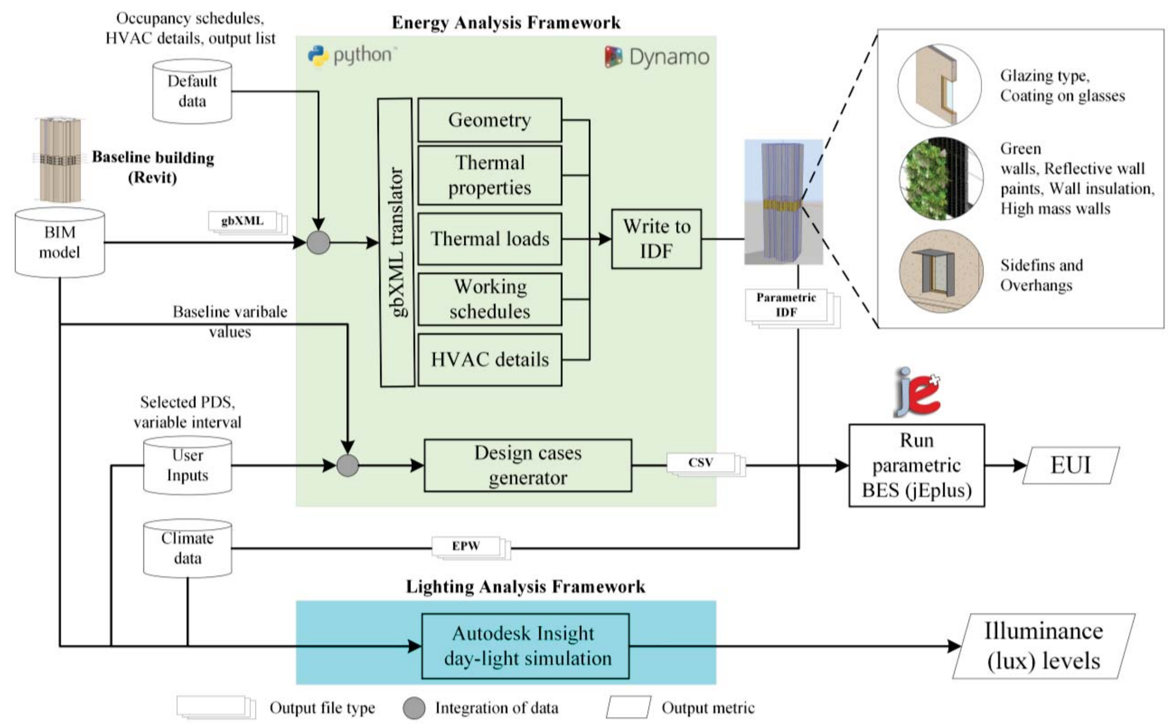

Figure 8: Illustration of energy simulation and daylight simulation sub-frameworks based on the BIM model.

4.2 Energy simulation sub-framework

This sub-framework facilitates parametric energy analysis in the proposed design workflow. Many energy simulations must be performed to conduct sensitivity analyses and develop ML-based metamodels. Using JEplus, an open-source software interface that offers parametric simulation capability, users can define variables and simulation cases and run multiple energy simulations simultaneously. It is a popular interface used in parametric simulations among the scientific community as it also helps to summarize simulation results into a single file. However, JEplus requires users to input a building energy model (BEM) in IDF format, a weather file in EPW format, and an analysis case file in CSV format to perform parametric simulation. This sub-framework includes an important middleware tool that addresses the interoperability issue that arises when data is exchanged from the BIM model to the Building Energy Model (BEM), i.e., one mandatory input of plus.

4.2.1 gbXML translator

The gbXML translator is a newly developed middleware tool based on Python. This script is used to convert BIM models in gbXML format. gbXML is an open-source schema that is popularly used for BIM-based energy simulations. It was specifically designed to contain data required for energy simulations. On the other hand, IDF is an input BEM file format supported by the EnergyPlus simulation engine.

The translator maps various building properties from gbXML schema to IDF data format. The tool extracts details of geometry, thermal properties, heat gains, occupancy/lighting/equipment schedules, and HVAC details from the gbXML file and converts them into IDF data classes. Additionally, the translator reads the library's default schedules, HVAC objects, and output objects to fill in any missing data. To integrate the gbXML translator into the BIM environment, a user interface has been developed and deployed as a BIM tool (Figure 09). The mapping of data classes is shown in Figure 10.

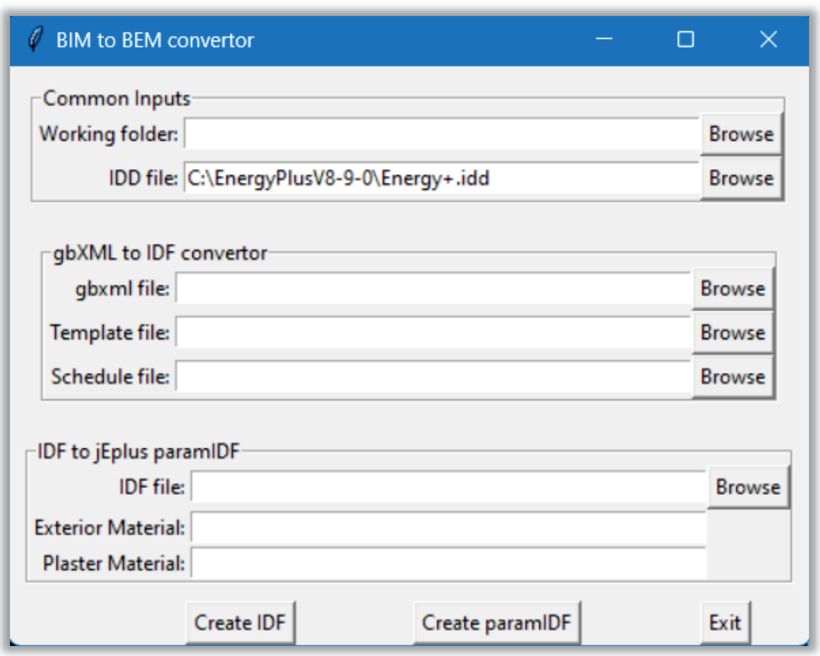

Figure 9: User interface of the gbXML translator.

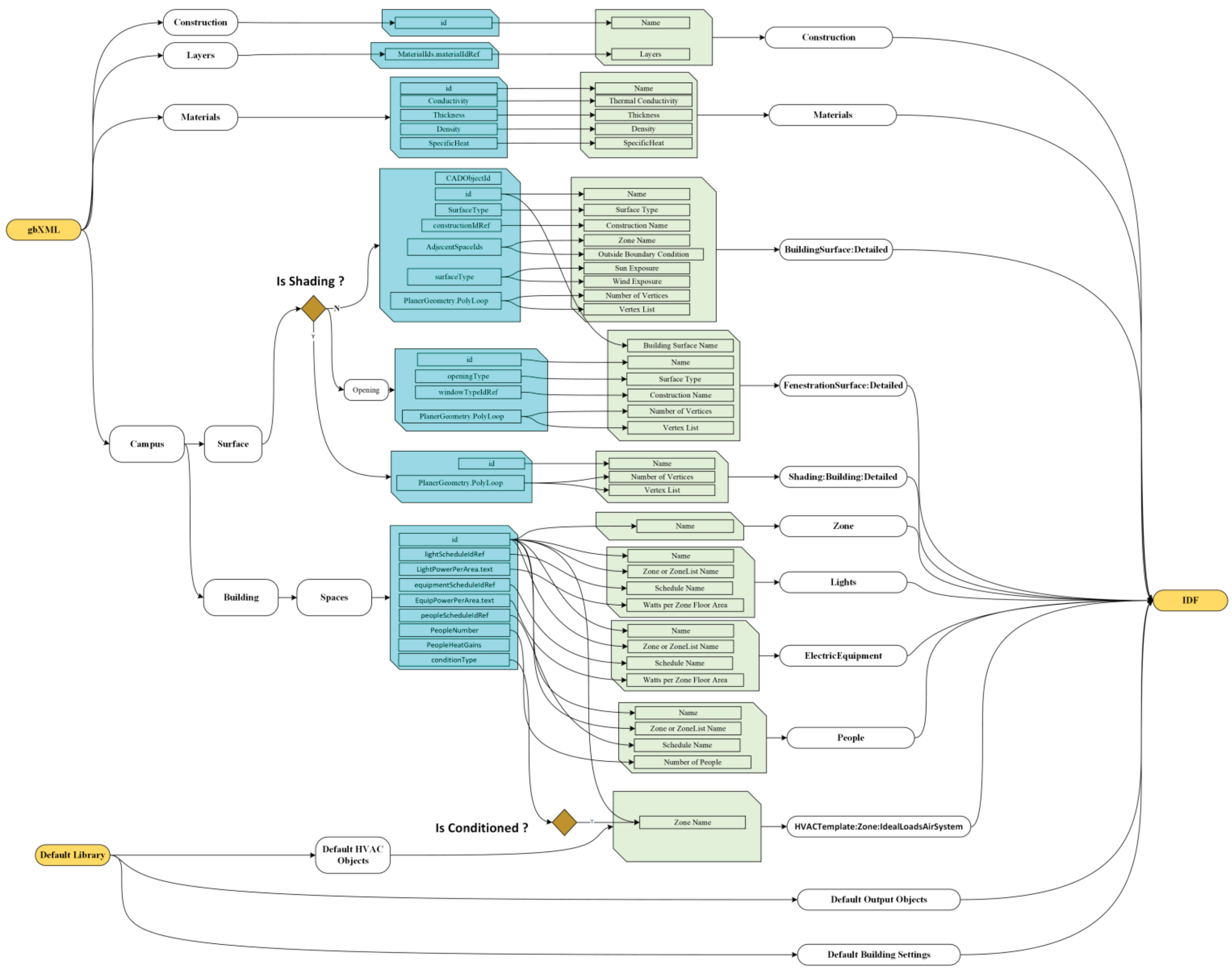

Figure 10: Data mapping from gbXML classes to IDF classes.

4.2.2 Validation of gbXML translator

To confidently simulate results according to a Building Information Model (BIM), it is crucial to ensure minimal data loss and accurate data mapping during translation of Green Building XML (gbXML) to Integrated Design Environment (IDF). Chong et al. (2019b) Validated a similar BIM to BEM converter for gbXML test cases and compared the accuracy of translation using visual appearance and Weighted Absolute Percentage Error (WAPE) of model elements.

Four test cases were obtained from the gbXML Green Building—Test Cases, based on the ASHRAE 1810-RP gbXML Test Case Research Project, to validate the BIM to BEM converter. Based on the geometry and thermal properties in the documentation, a BIM model was created for each test case using Autodesk Revit and then translated using the new BIM to BEM converter.

As the first step in validation, both BIM and BEM models were visualized using Autodesk Revit and the gbXML online viewer. Table 5 summarizes the visual representations.

Table 5: Visual representation of test cases

Case	*BIM(Revit)*	*BEM (IDF)*
01	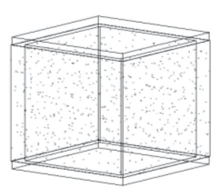	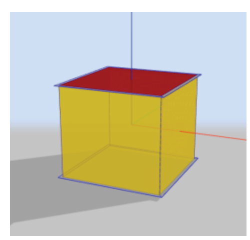
02	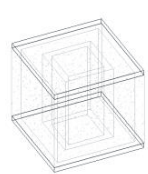	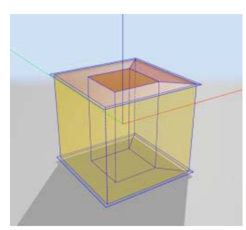

Case	*BIM(Revit)*	*BEM (IDF)*
03	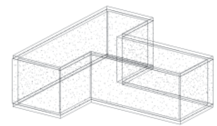	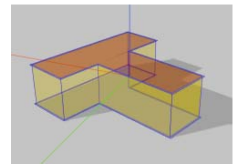
04	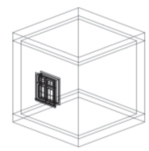	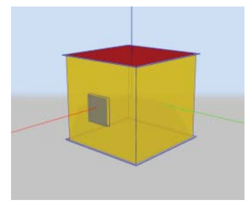

For the second validation step, the Weighted Absolute Percentage Error (WAPE) was computed for the BIM wall area, roof area, glazing area, and floor area (Ai), the corresponding area values of BEM (F_i) using Eq. (1).

$$WAPE = 100 \times \frac{\sum_{i=1}^{n} |A_i - F_i|}{\sum_{i=1}^{n} A_i} \tag{10}$$

The WAPE falls from 3% to 8% due to the differences in spatial area computation methods in Revit and EnergyPlus models. To ensure precision, this study thoroughly inspected each surface's thermal properties (Conductivity, Thermal Mass, and Thickness). The manual inspection affirmed that the proposed BIM to BEM converter achieved 100% accuracy in transferring thermal data.

4.2.3 Analysis Case Generator

An analysis case generator is a middleware tool developed using Python script. The output file of this generator provides commands for jEplus to run several simulations and assign values to variables in each simulation run. This tool supports the following three analysis types:

- Local sensitivity analysis (LSA)—This analysis combines variables while changing one variable at a time. The user must select variables (n) to be analyzed, their minimum and maximum values, and the number of divisions (*p*). Thus, it creates a CSV file that contains $n \times p$ number of analysis cases. More details about this analysis are shown in Section 6.1.

- Global sensitivity analysis (GSA)—GSA requires combining variables while changing the values of multiple variables at a time. The users need to select several variables (k) and several trajectories (r) as the inputs; thus, the generator creates $r \times (k+1)$ analysis cases for the simulation. More details about this analysis are shown in Section 6.1.
- Latin Hypercube Sampling (LHS)—This popular method uses a statistical approach to generate near-random samples. It is often employed for machine learning meta-model developments. The Python library pyDOE (https://github.com/clicumu/pyDOE2) is integrated into this method as the analysis case generator module.

The user interface of the Analysis case generator is shown in Figure 11.

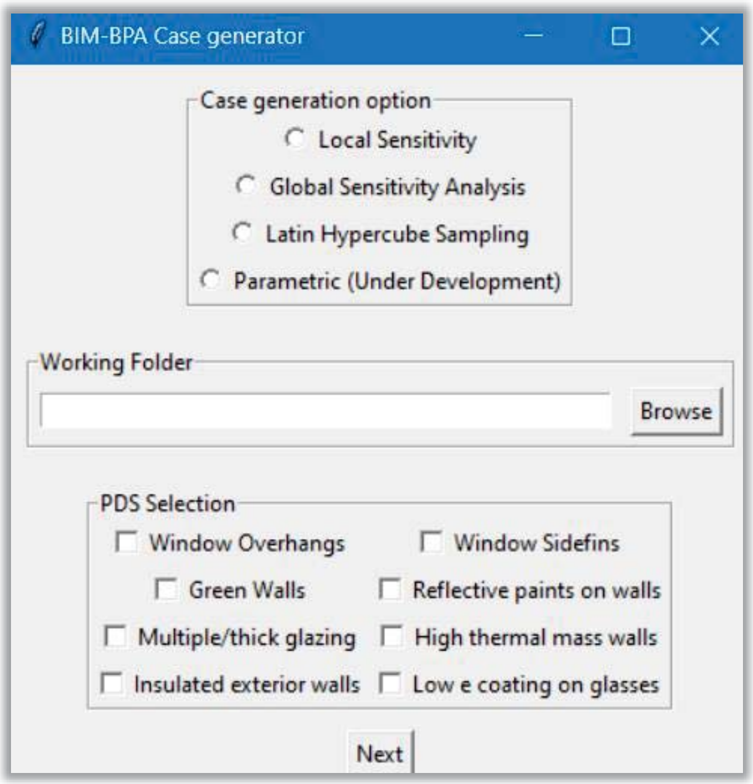

Figure 11: User interface of analysis case generator.

4.3 Daylight simulation sub-framework

Autodesk Insight is a BIM tool developed for cloud-based daylight simulations. Autodesk Insight uses Lighting Analysis for Revit (LAR) as the daylight simulation engine, which uses a bidirectional ray-tracing light modeling technique. This tool reads optical data (wall, floor, and ceiling colors, visual transmittance of glasses) and climate data (solar illumination) from the BIM model and performs simulations in Autodesk Cloud. As an output, the tool calculates the illuminance level in each room of the BIM model. However, one limitation is the designer needs to follow a trial-error approach by simulating different cases sequentially. This plug-in is directly employed in this study since this is an already integrated BIM tool for BIM-based performance analysis workflows.

4.4 Multi-objective optimization module

Multi-objective optimization can find the best possible solutions while achieving multiple objectives without compromising each other. Genetic algorithms are often used for this purpose, and Non-sorted Genetic Algorithm – II (NSGA-II) is a popular and validated genetic algorithm for energy simulation-based studies. NSGA-II can effectively find solutions for non-linear and discontinuous functions.

To implement NSGA-II in energy simulation-based studies, a Python script with constraints and equations was written to calculate objective functions, constraints, and stop criteria. Pymoo (https://pymoo.org/) Python library was used to select the NSGA-II algorithm as a function. The algorithm calculates the energy consumption of each design option by calling a Machine Learning metamodel, which is more efficient in predicting energy demand than using physics-based energy simulations. More details about the meta-model are presented in Section 5.2. The cost of investment is also calculated by calling the LCA database prepared from the BIM model of the building. Once the stop criteria are met, in this case, the maximum generations, all the evaluated solutions in the process were written to a CSV file. The second algorithm was written to search for non-dominated solutions from those searched in the NSGA-II algorithm. These solutions were then separately written to a CSV file for later use. The user interface developed to run this middleware tool is shown in Figure 12.

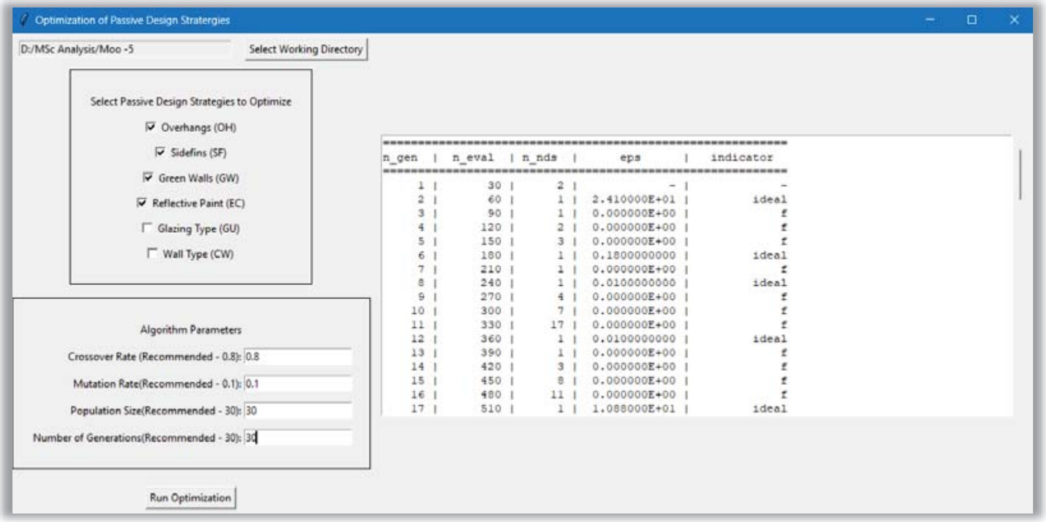

Figure 12: User interface of multi-objective optimization middleware tool.

4.5 Results Integrator

Dynamo is an interface that allows users to manipulate BIM models and read data in Autodesk Revit. This research developed a Dynamo script called the "results integrator module" to visualize PDS design options from multi-objective optimization. The integrator has three main parts, as shown in Figure 13.

The first part is the input interface, allowing users to set different design options, such as adding window overhangs, side fins, and green walls, and choosing building materials, such as glazing types, walling materials, and exterior wall colors. When the Dynamo script was run, the second part called a machine-learning model, predicted the energy consumption of the building design and calculated the cost per design option by calling the BIM-LCA database. The script also calculates the lifecycle carbon emission and the number of LEED green rating points that can be obtained for each design option. Finally, the third part of the Dynamo script updates the BIM model for each design option, saves and displays the results, energy consumption, investment cost, lifecycle carbon emission, and LEED green rating points to a CSV file. More details about the equations used in calculations are presented in Section 06 of this thesis.

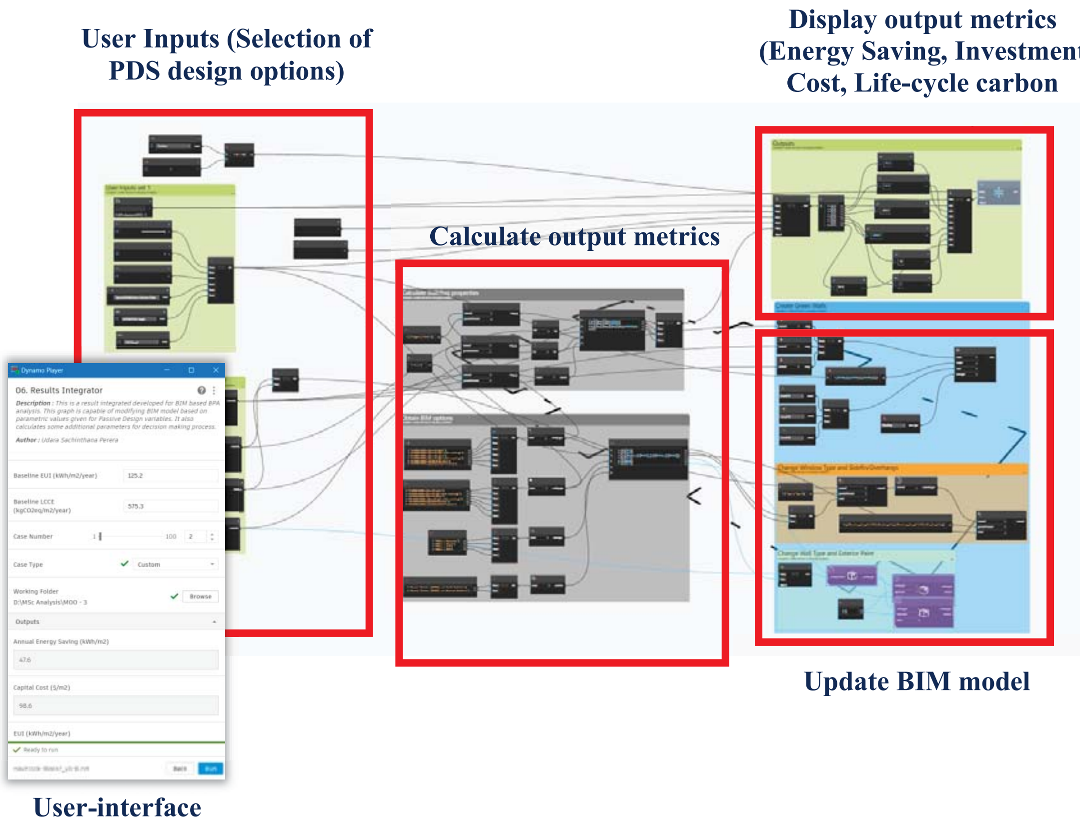

Figure 13: Dynamo script and user-interface.

4.6 Building design workflow using BIM-based BPA framework

The completed building design workflow is introduced after developing the necessary templates, sub-frameworks, and middleware tools (Figure 14). The proposed workflow involves developing the BIM model of the baseline building on the prepared template. In the BIM model, accurate thermal and physical properties and life-cycle values should be input for each building element. Then, the designers should select a set of PDS and the corresponding building variables. If any objects obstruct daylight penetration to the building, it is recommended that a daylight simulation be performed using the Autodesk Insight simulation tool. The simulation results can determine each variable's minimum and maximum values. Next, a sensitivity analysis should be conducted using the energy analysis sub-framework. The designers can then use the sensitivity analysis results to decide which building variables should be modified using PDS. The modifications should be evaluated for their energy-saving potential and compatibility with other building variables. This step further allows designers to simplify optimization by removing ineffective variables in calculations. This is the first decision-making instance of the proposed BIM-based BPA framework. After a sensitivity analysis, designers can choose PDS design options for multi-objective optimization. The optimization process produces non-dominated solutions, which are displayed through the results integrator. From these options, the designers can select the optimal PDS design that meets the criteria of low investment cost, EUI, and high marks for the green rating system. This decision-making process constitutes the second instance of the BIM-based BPA framework. Once the best design option is determined, designers can update the baseline BIM model using the results integrator tool.

4.7 Summary of the chapter

This chapter introduced a new BIM-based BPA framework for sustainable residential high-rise building design. The building should be modeled using the BIM template (Section 4.1) proposed in this study. Two sub-frameworks were developed to address technical gaps in the building design workflow: energy analysis and daylight analysis. Additionally, five middleware tools were developed to improve interoperability in the BIM environment. Finally, Section 4.6 presents the proposed building design workflow with the help of the BIM-based BPA framework.

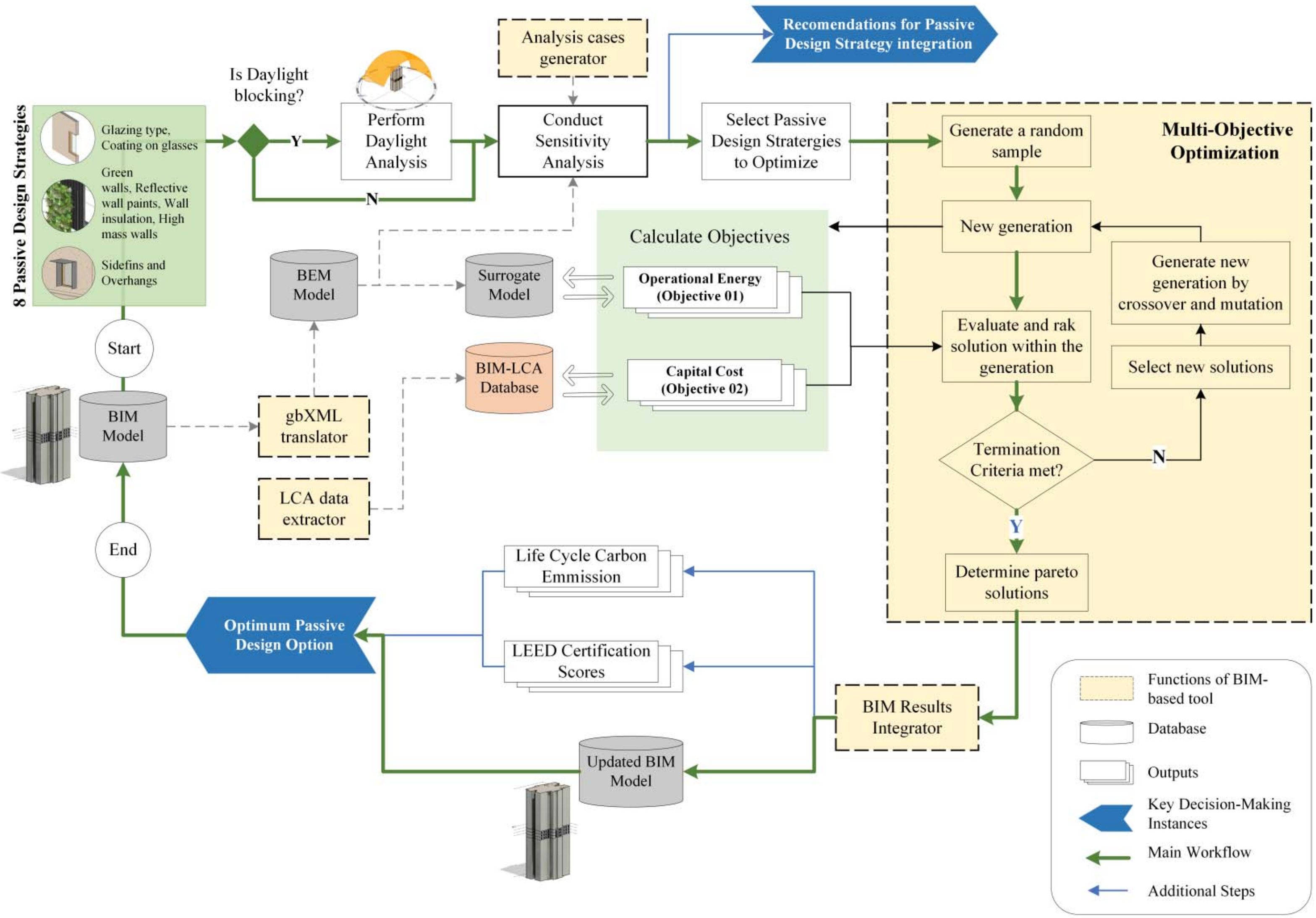

Figure 14: Proposed BIM-based design workflow.

CHAPTER 5

5. CASE-STUDY BUILDING AND CLIMATE DATA

5.1 Baseline Settings of the BIM Model and Building Energy Model

For this study, we have selected the Havelock City apartment building as a typical high-rise building (Figure 15) in Sri Lanka. The building has 32 floors; each has six luxurious apartments. A central lobby area connects these apartments. The six apartments on each floor comprise four double-bedroom apartments with floor areas ranging from 87 m^2 to 109 m^2 and two triple-bedroom apartments with 105 m^2 and 130 m^2 floor areas. We have sourced construction details from the building's as-built drawings, and occupancy schedules and heat gains data were obtained from the recommended sources (Karunathilake et al., 2018; Shiveswarran et al., 2023), as outlined in Table 6.

Table 6: Summary of construction properties of the baseline building

Type	Variable	Value
Orientation	Longer axis direction	East-West
Exterior wall (Reinforced concrete wall with cement-sand plaster on both sides)	Conductivity of core walling material Conductivity of plasters	2.1 W/m-K 0.72 W/m-K
Partition walls (Cement-sand block wall with cement-sand plaster on both sides)	Conductivity of core walling material	1.2 W/m-K
Interior floor (Reinforced concrete floor with top tile finish and bottom cement-sand plaster finish)	Conductivity of core floor material Conductivity of floor finishes	2.1 W/m-K 1.2 W/m-K
External window	U-value of glass SHGC of glass	5.7 W/m^2-K 0.83 (ratio)

Heat gains	Lighting power density	2.5 W/m^2
	Equipment power density	1.5 W/m^2
	Average people's heat gain	110 W/person
	Number of people per apartment	3

It is assumed that the bedrooms and living spaces in the apartments are equipped with air-conditioners, while kitchens and bathrooms are naturally vented spaces. A study conducted in Sri Lanka by Jayasinghe & Priyanvada (2002) found that occupants feel comfortable at a neutral temperature of 26°C in tropical lowlands (such as Colombo) and 22°C in tropical uplands (such as Nuwara Eliya). Therefore, heating and cooling setpoints for buildings that use HVAC systems should be set at 20°C (Shiveswarran et al., 2023) and 27°C (Energy Efficiency Building Code of Sri Lanka, 2021), respectively.

This study assumed that the building operates in a mixed-mode condition where occupants can open windows to increase natural ventilation up to 3 each if the indoor temperature is within the comfort temperature threshold of 20°C - 27°C. Suppose the indoor temperature falls outside of this range. In that case, the Energy Plus simulation activates the HVAC system under a minimum ventilation rate of 1 ach and calculates the annual energy consumption of HVAC (E_{hvac}). The simulation also calculates the yearly lighting (Lighting) and equipment (Equipment) energy consumption based on occupancy schedules. Finally, the annual operational energy of the building is normalized per unit floor area, referred to as Energy Use Intensity (EUI), of the building according to Eq. (2). The EUI is directly obtained as an output from EnergyPlus simulations.

$$Annual\,Operational\,Energy\,Consumption = EUI = \frac{\sum (E_{hvac} + E_{lighting} + E_{equipment})\,\mathrm{kwh}}{Total\ \ floor\ area(m^2)} \qquad (2)$$

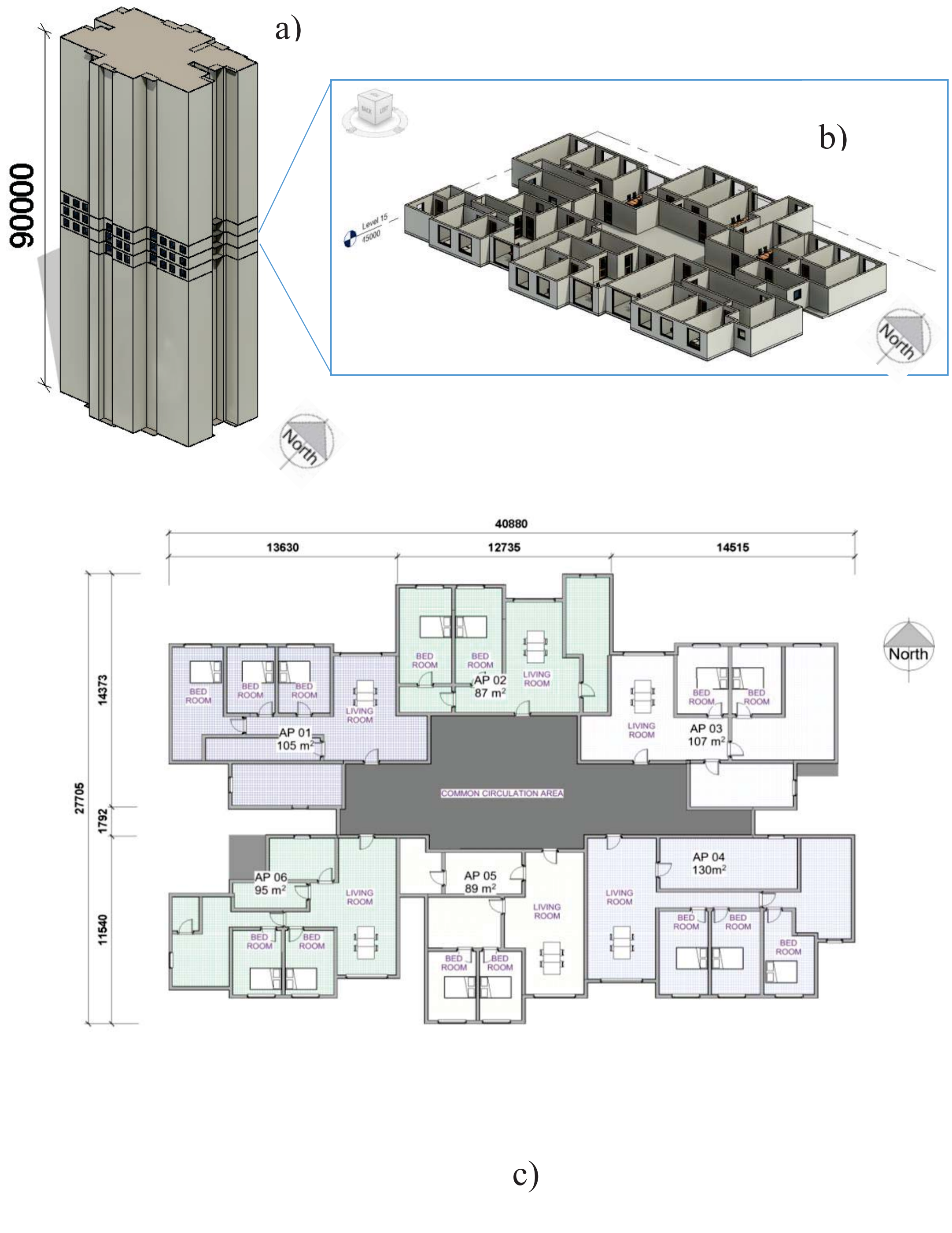

Figure 15:a) 3D view of the BIM model, b) 3D view of a typical floor, 3) detailed plan view of a typical floor (All dimensions are in millimeters).

5.1.1 Validation of building energy model (BEM)

Building energy simulations are used for several purposes, such as predicting the energy consumption of different design options, studying the energy consumption of extrapolated scenarios, and making scientific pronouncements on energy consumption patterns (Trucano et al., 2006). However, the building energy modeling process involves making many assumptions about the building's thermal properties, schedules, heat gains, and weather parameters, making it highly error-prone and deviations from reality. Therefore, to obtain realistic energy predictions, it is essential to validate the building energy model (BEM), which is the primary source of information for simulations.

The National Renewable Energy Laboratory (NREL) recommends empirical validation as a reliable method for validating models, but it can be expensive and time-consuming (Judkoff et al., 2008). Previous studies have carried out empirical validation by comparing actual energy consumption (Harkouss et al., 2018a; Singh et al., 2020, 2022b; Weerasuriya et al., 2019a) or actual temperature measurement (Chong et al., 2019b; K. C. Dahanayake & Chow, 2018; Krüger & Givoni, 2008; Liu et al., 2021; Mahar et al., 2020; Ohlsson & Olofsson, 2021; Royapoor & Roskilly, 2015; Thapa et al., 2023). In cases where records on energy consumption, internal heat gains, and schedules are not available, it is recommended to conduct a validation study using actual temperature measurements.

The Havelock City building layout was studied in this research as a case study. To achieve accurate energy predictions for different PDS design scenarios, the BEM model of the case-study building was validated with actual indoor temperature measurements. A ten-day field measurement campaign was conducted in a representative apartment of the Havelock City building, which was kept unoccupied throughout the campaign period to comply with NREL guidelines. A temperature and humidity data logger, Elitech (RC-4HC), was placed 1.2m above the floor level and 2m away from windows to avoid direct solar heat gains. Layouts, orientation, and the sensor location are indicated in Annexure 01.

In the BEM, building parameters were set according to the details outlined in Annexure 01. To simulate similar outdoor weather conditions, the outdoor temperature in

Colombo in the Energy Plus weather file (EPW) was replaced with the 10-day outdoor temperature data obtained from the meteorological department of Sri Lanka.

Figure 16 summarizes the comparison between simulated and observed temperatures. The simulated temperature slightly overestimated the actual temperature. However, the Root Mean Square Error (RMSE) is about 2%, and the normalized mean biased error (NMBE) is -0.7%, within the acceptable limits recommended by ASHRAE guideline 14.

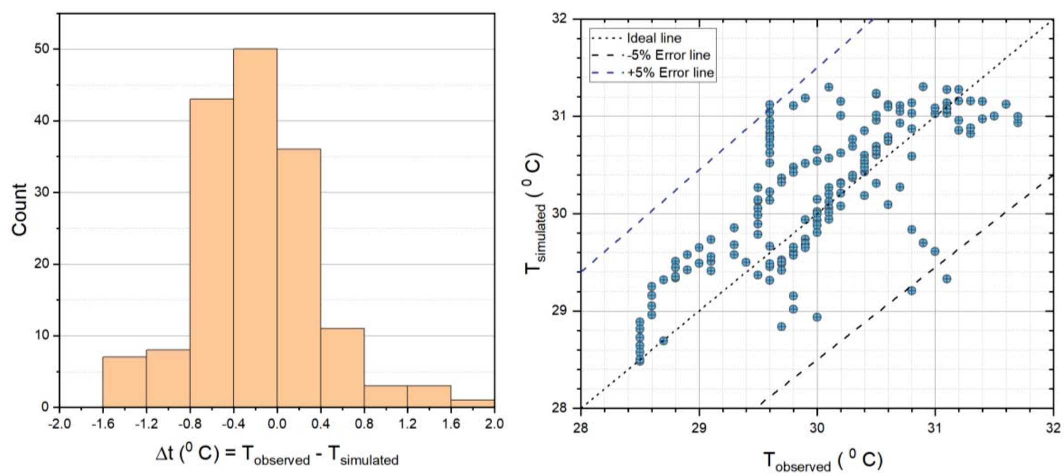

Figure 16:a) Frequency of the difference between measured and simulated temperature (Tobserved – Tsimualted), and b) comparison between simulated and measured temperatures.

5.2 Energy Prediction using Metamodel.

Surrogate energy modeling, or meta-modeling, is widely used to reduce computational costs by replacing exhaustive physics-based simulations (Bracht et al., 2021; X. Chen et al., 2017). High computational power, price, and time are required to execute energy simulations, posing a significant obstacle when dealing with numerous scenarios, such as multi-objective optimization problems, for making informed decisions on building designs. Moreover, in a BIM-integrated environment, the efficiency of building performance prediction is essential. Surrogate energy modeling offers a viable solution for iterative design problems by training a statistical model using a training dataset.

Among various statistical approaches, machine learning techniques have gained popularity among researchers due to their accuracy and efficiency (X. Chen et al., 2017; Østergård et al., 2018). In this study, a machine learning approach was employed to develop a surrogate model containing variables corresponding to Passive Design Strategies (PDS), thus providing flexibility to alter variable values and examine their effects more rapidly.

A database of 200 design cases for each climate scenario was generated using the Latin Hypercube Sampling (LHS) technique, a recommended method for the meta-model approach (Afzal et al., 2017). Each scenario's energy consumption (EUI) was predicted by conducting physics-based energy simulations using the energy simulation sub-framework (Section 4.2). This database was then used as the training dataset for developing surrogate models using XGBoost, a popular machine-learning algorithm.

To ensure the model's accuracy, it was trained and validated with performance metrics, a common step in machine learning. The dataset was randomly divided into a 70% training and 30% testing ratio. Mean squared error (MSA), mean absolute error (MAE), and coefficient of determination (R^2) were used as performance indicators to evaluate the model's accuracy. A summary of these performance indicators for the selected dataset is shown in Table 7.

Table 7: Performance indices of ML model training and testing

Performance Indices		**Colombo**	**Kandy**	**Nuwara Eliya**
MAE	**Training**	1.04	0.71	0.56
	Testing	1.59	1.31	1.18
MSE	**Training**	1.73	0.85	0.49
	Testing	4.42	2.97	2.09
R^2	**Training**	0.98	0.96	0.99
	Testing	0.96	0.90	0.95

The performance indices indicate that the machine learning (ML) model was not overfitted. For example, the maximum Mean Absolute Error (MAE) in both training (1.04) and testing (1.59) of the Colombo ML model confirmed that the ML model predicted the Energy Use Intensity (EUI) for any value within the trained thresholds with an error less than 1.59 kWh/m^2. The Mean Squared Error (MSE) also confirmed that there were few outliers within the ML prediction of randomly selected testing cases. Finally, the low difference (<0.06) and high R^2 value (>0.9) of both training and testing confirmed that the fitting accuracy was generic without limiting it to the training dataset. The comparison of simulated and predicted EUI for both the training and testing datasets is shown in Figure 17.

The trained surrogate model was then utilized in the multi-objective optimization stage, where EUI predicted 2600 design cases per climate scenario. Leveraging the surrogate model significantly reduced the computational burden of conducting physics-based simulations for each design iteration, enabling efficient design space exploration and facilitating informed decision-making regarding building designs.

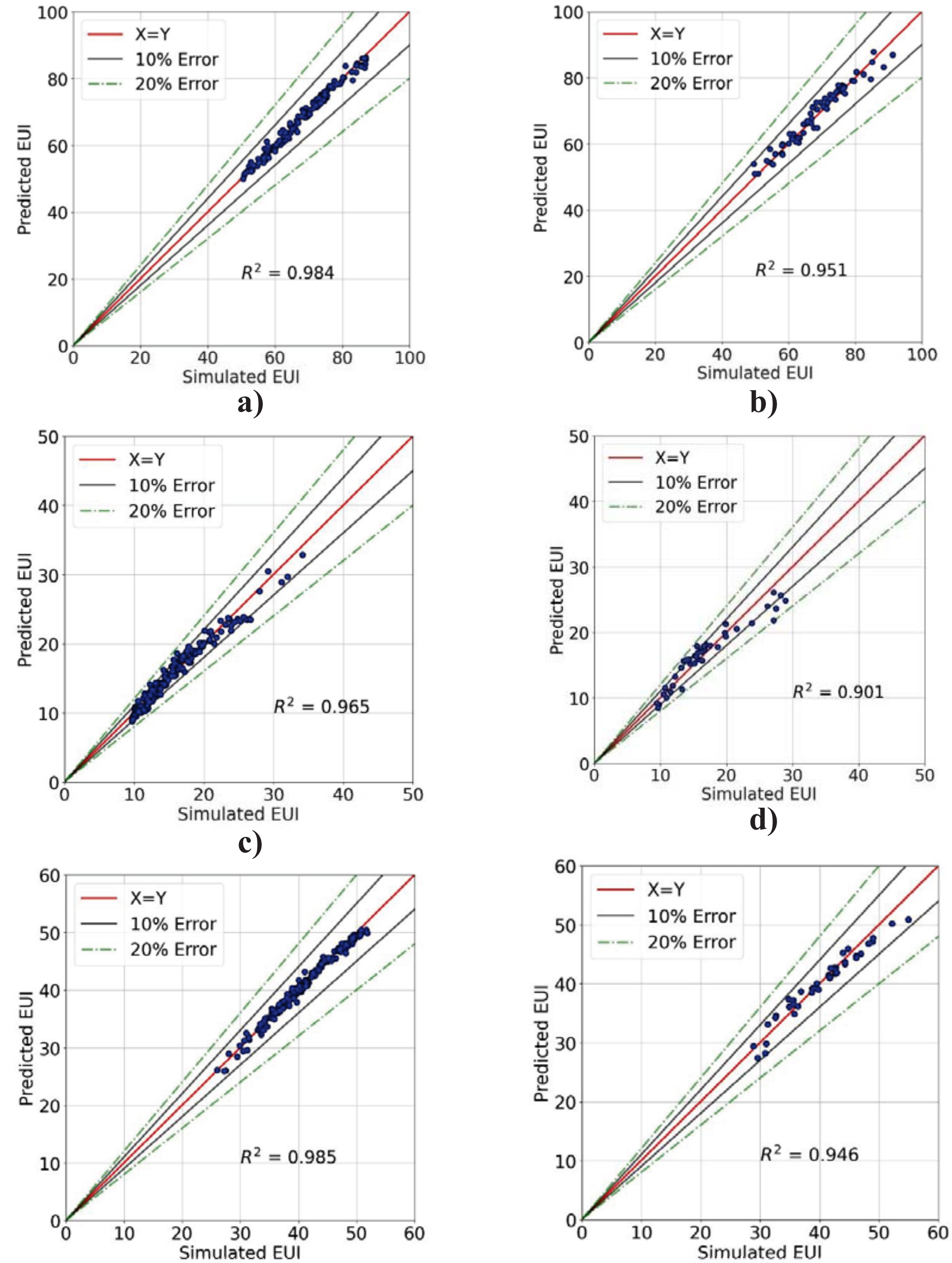

e) f)

Figure 17: Predicted vs. Simulated EUI for Colombo: training(a) and testing(b), Kandy: training(a) and testing(b), Nuwara Eliya: training(a) and testing(b) dataset.

5.3 Weather data

Sri Lanka, an island nation located closer to the equator, is an ideal example of a tropical country that is characterized by several distinct sub-climates due to its altitude difference from the coastal region to the uplands (Jayasinghe & Attalage, 1999; Jayasinghe & Priyanvada, 2002) (Figure 18). Hence, Sri Lanka has been chosen as the case study for the tropical region to investigate how passive design strategies adopted for residential high-rise buildings perform in distinct local climates. A famous climate classification for HVAC designs, ASHRAE 169, classifies Sri Lanka under three different climate zones, namely, extremely hot-humid (0A), very hot-humid(1A), and warm-humid (3A) (ANSI/ASHRAE, 2021). Colombo, Kandy, and Nuwara Eliya are representative examples of cities of the above climates in Sri Lanka.

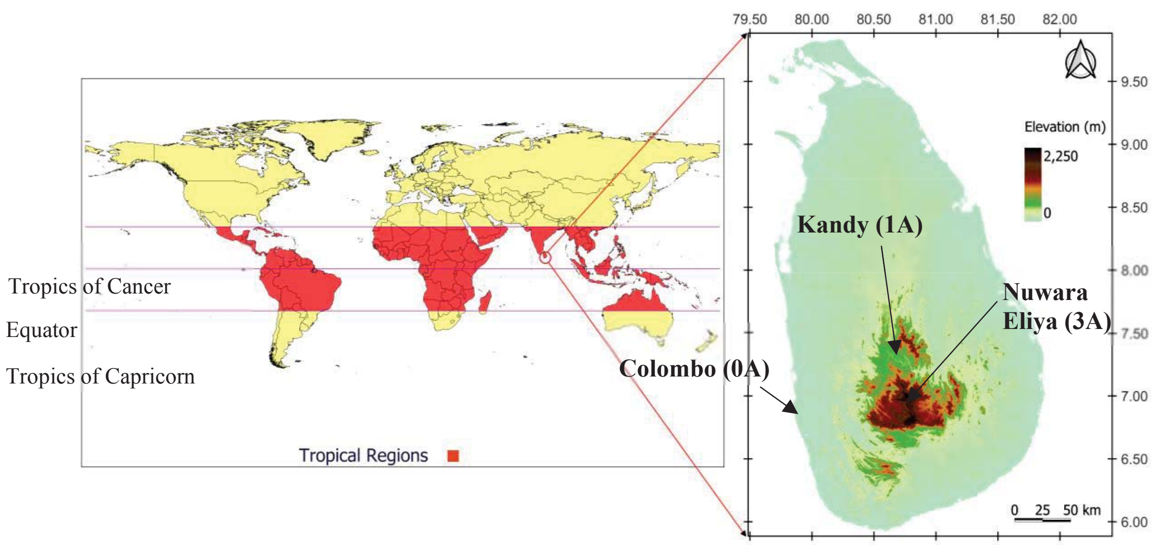

Figure 18: Tropical region, Sri Lanka's location, and elevation variation throughout the country.

The weather data of three locations, Colombo, Kandy, and Nuwara Eliya, in the sub in Sri Lanka were obtained as TMYx EPW weather files. EPW file format downloaded from http://onebuilding.climate.org (Crawley et al., 2022). These distinct climate conditions show a high variability in climate parameters, as indicated in Figure 19. According to Figure 19(a), the mean hourly average dry-bulb temperature fluctuates from 26.3ºC to 28.4ºC in Colombo (0A). A slight temperature drop is in Kandy (1A), which ranges between 23.2ºC - 25.5ºC, and a significant drop in Nuwara Eliya (3A), which varies between 14.9ºC - 17ºC. On a typical day, hourly temperature variation and comfort threshold indicate that Nuwara Eliya is a heating-dominant region while Colombo is a cooling-dominant region (Figure 19(b)). However, Kandy has a higher potential for operating as a naturally vented space owing to temperature variations within the comfort threshold. The relative humidity of all three regions shows a year-round high average (>69%) that agrees with the humid climate condition specified in the ASHRAE classification. Moreover, direct normal radiation (DNI) variation on a typical day (Figure 19(d)) further shows solar radiation differences over the three regions selected for this study.

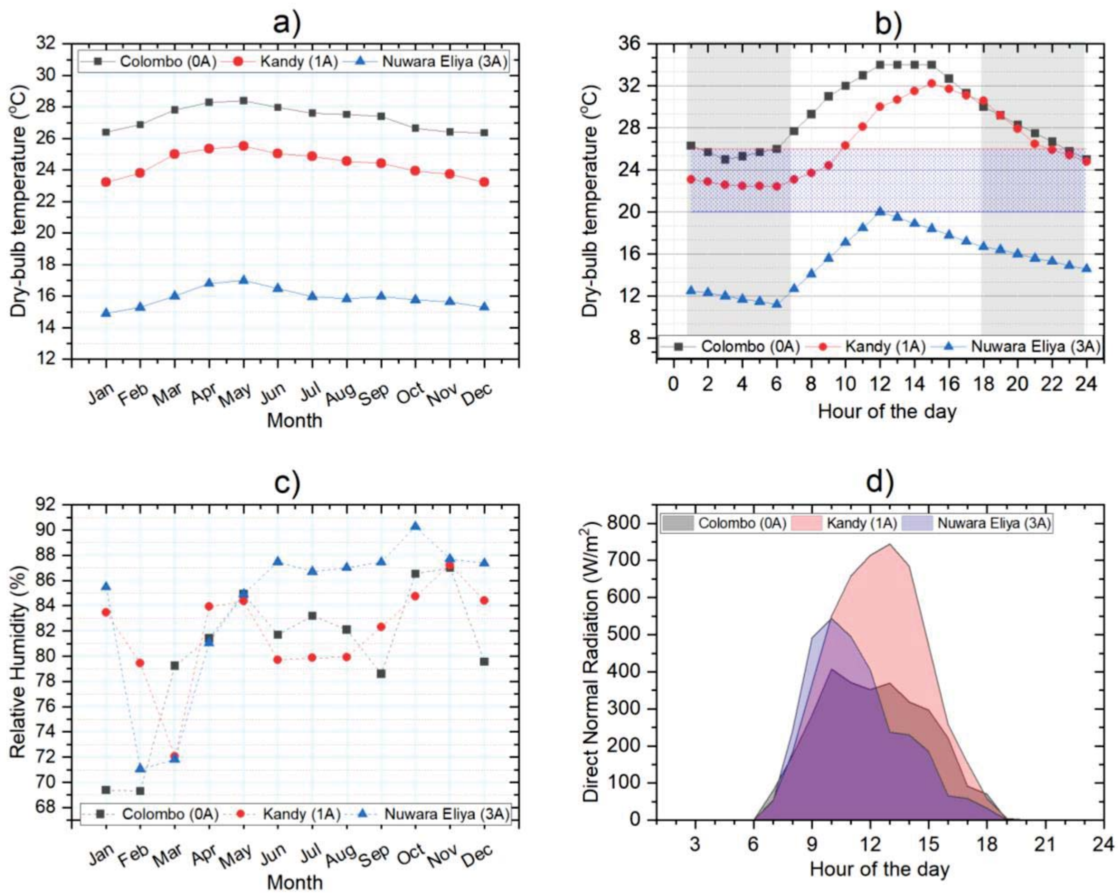

Figure 19: Key climate characteristics of Colombo, Kandy, and Nuwara Eliya - a) Monthly mean of hourly average dry-bulb temperature over 12 months, b) hourly average of dry-bulb temperature variation over a typical day, c) Monthly mean of hourly relative humidity, d) Direct Normal Radiation of a design day.

5.4 Verification of PDS variable thresholds from daylight simulations

PDS, as identified in Chapter 4 of this thesis, requires a verification step to ensure minimum daylight is not compromised when integrated into buildings. Out of eight

PDS, three PDS- overhangs (OH), side fins (SF), and coating on windows (WC)- block natural daylight, affecting the daylight performance of the building. To minimize this effect, this study conducted a series of daylight simulations. It determined either maximum (OH, SF) and minimum (WC) variable values that satisfy the minimum daylight requirement of green building ratings. A popular green LEED rating v3(U.S. Green Building Council, 2016) recommends that at least 75% of regularly occupied floors be within an illuminance level of 110-5400 lux on a clear-sky day. According to the LEED v3 set of simulations were performed on a clear sky day (i.e., September 21, from 9.00 AM to 3.00 PM) where three sky models (Colombo, Kandy, and Nuwara Eliya) were downloaded from the Autodesk sky model database. The scope of the simulation included only bedrooms and living areas, which are assumed to be regularly occupied. Notably, the baseline building achieves 95%, 94%, and 94% floor area for Colombo, Kandy, and Nuwara Eliya. Then, a trial-and-error approach was adopted by increasing OH and SF variable values and decreasing WC values till it reached the lowest acceptable daylight threshold.

The results of daylight simulation indicate a PDS design consisting of a maximum of 0.8m long side fins/ overhangs and a minimum of 0.5 SHGC will not affect the minimum daylight performance of the building (Table 8).

Table 8: Summary of daylight calculations of three climates selected for this study (According to LEED v3).

	Floor area (m^2) within the daylight threshold (percentage %)	
Location	**Baseline** Overhang & Side fin – 0.8m SHGC – 0.5	**PDS option** Overhang & Side fin – 0.8m SHGC – 0.5
Colombo	339 (94%)	310 (86%)
Kandy	339 (94%)	275 (77%)
Nuwara Eliya	339 (94%)	276(77%)

[Figure 20](#) shows the floor areas of bedrooms and living rooms within the acceptable daylight threshold in shades of blue when the PDS design option (Table 8) is applied. The red color area of the figures indicates the regions of low daylight within the design day. Figure 20d) represents an annual sun path over the case-study building. According to Figure 20, it can be visually confirmed that the majority of the regularly occupied area meets the daylight requirements.

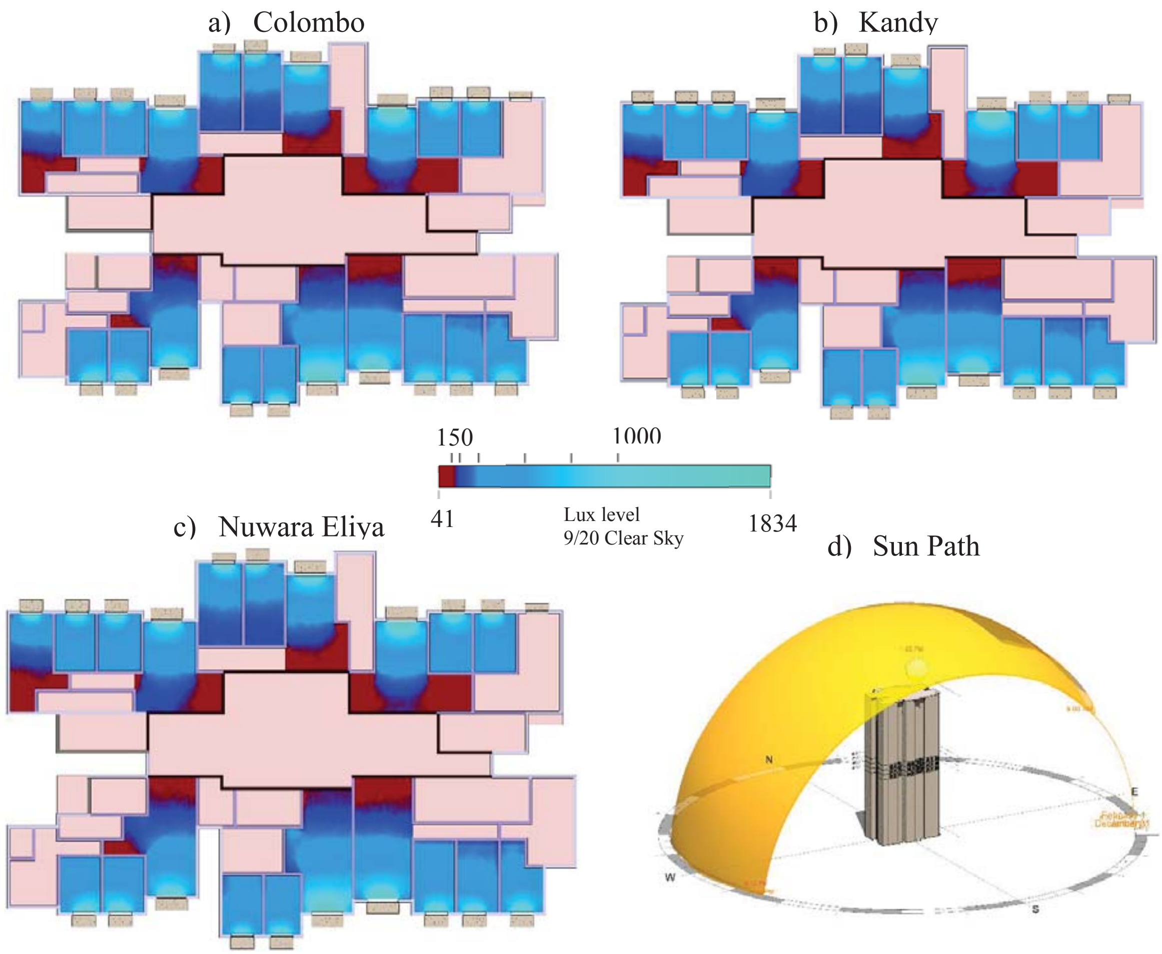

Figure 20: Results of the daylight performance analysis where shades of blue indicate the floor area within 110-5400 lux levels on a design day. a) Results of Colombo, b) Results of Kandy, c) Results of Nuwara Eliya, d) an example of yearly - sun path variation over the building site

5.5 Summary of the chapter

This chapter first presented the details of the case study building and its physical and thermal properties. Then, it showed the field measurement data and the validation of the building energy model (BEM) prepared for the case study building. After that, the development process of the energy-predicting meta-model and its validation were discussed. Then, it presented the weather parameters of the case study climate zones. Finally, the thresholds of daylight-blocking passive design strategies were verified with the study's daylight analysis sub-framework.

CHAPTER 6

6. ANALYSIS OF RESULTS

In the final phase of the study, a BIM-based BPA framework was employed to integrate Passive Design Strategies (PDS) into the case-study building in three climate zones. This phase was conducted in two stages, involving two decision-making instances in the building design workflow. In the first stage, the best energy-saving PDS combinations were determined with sensitivity analyses.

As a starting point, the energy savings of PDS at their best design variable values (i.e., minimum or maximum values) were tested by running eight simulations per climate zone (i.e., building locations in Colombo, Kandy, and Nuwara Eliya). The energy-saving potential of each PDS was then compared with the ranking of their popularity identified in Section 3.2. The results of this step are shown in Figure 21. The energy saving is expressed as a percentage difference in annual operational energy consumption, also named as Energy Use Intensity (ΔEUI (%)) of the building with PDSs for the same building without any PDS.

Figure 21 illustrates three critical aspects of Passive Design Strategies (PDS) and their impact on building energy consumption in three locations. The first aspect shows a weak correlation between the popularity of a PDS and its energy-saving potential. For instance, in Colombo and Kandy, the second-best energy-saving PDS is WC, but it is only ranked 6th in popularity. Surprisingly, the second and third most popular PDS, GW and CW, have the lowest energy-saving potential in these two cities. Notably, in Nuwara Eliya, PDS's popularity and energy-saving potential do not have any relationship. Hence, it is reasonable to assume that construction industry professionals in Sri Lanka tend to adopt prevalent PDS without adequately considering their efficiency.

The second aspect highlights the significant variation in the energy-saving efficiency of PDSs in different climate zones. The energy saving of PDS varies from 15.9% (EC) to 0.98% (CW) in Colombo. Notably, three PDS (GW, CW, and WS) can only save <1% of the energy consumption of buildings in Colombo. Therefore, selecting PDSs with high energy-saving potential is essential to achieve maximum energy-saving without incurring additional costs.

The third aspect of the study illustrates the variation in the energy-saving efficiency of PDSs in sub-climate zones, which indicates that PDSs' energy-saving efficiency depends on local climate conditions. For example, GU showed an additional demand for energy in Colombo and Kandy but saved energy in Nuwara Eliya. Similarly, PDSs like EC, SF, OH, and WC saved energy in Colombo and Kandy but demanded additional energy for buildings in Nuwara Eliya. Hence, the results confirmed the importance of analyzing the energy-saving effectiveness of PDS in local climates.

However, the study does not reveal the advantages of other PDS designs or how energy-saving varies with PDSs' properties. To address this, a local sensitivity analysis was conducted to quantify the variation and the type of relationship between PDS' property and building energy demand.

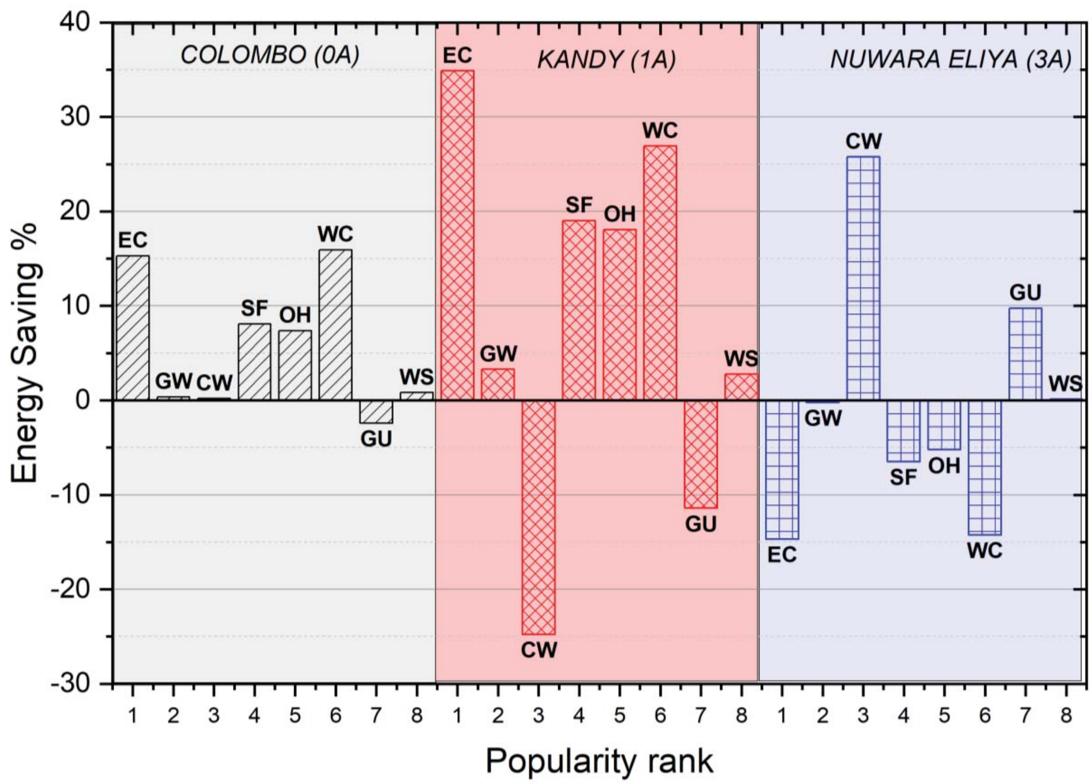

Figure 21: Energy saving percentage of each PDS at its extreme variable value vs. popularity rank in the questionnaire survey.

6.1 Sensitivity Analysis

Local Sensitivity Analysis (LSA) can provide valuable insights into changes in energy consumption when a single building variable is changed while all other variables are kept at their baseline values. Similarly, LSA can demonstrate the energy-saving trend of applying a single PDS to a building design.

On the other hand, Global Sensitivity Analysis (GSA) can provide insights into the variations in energy demand when multiple building variables are altered simultaneously, such as adding various PDS to building designs. To examine both scenarios, this study performed local and global sensitivity analyses, and the results are presented in the following sub-sections.

6.1.1 Local sensitivity analysis (LSA) using partial derivatives.

The output objective (OP_i), or Energy Use Intensity (EUI), of a PDS design option (i), can be mathematically shown as a function of eight PDS variables ($x_1, x_2, \ldots \ldots x_8$).

$$OP_i = f\ (x_1, x_2, \ldots \ldots x_8) \tag{3}$$

The LSA method assumes that each variable is independent of the others. To calculate each PDS's sensitivity coefficient (SC), the energy-saving variation is quantified by dividing the variable threshold into four equal parts.

$$SC_{PDSi} = \frac{1}{n}\sum_{i=1}^{n=5} \frac{\Delta OP / (\frac{OP_i + OP_{i+1}}{2})}{\Delta IP / (\frac{IP_i + IP_{i+1}}{2})} \tag{4}$$

where OP_i, OP_i+1, ΔOP are the output (i.e., EUI) in the previous and current PDS magnitudes and their difference. Similarly, IP_i, IP_i+1, and ΔIP are the input (the PDS' magnitude) during the last and current intervals and their difference. n is the number of intervals equal to four in this study. Then, a linear regression curve is used to approximate each variation. The coefficient of regression (R^2) is calculated to determine whether the variation is linear.

According to Figure 22 (a) & (b), Overhang length (OH) and Side fin length (SF) linearly (R^2 =0.98) decrease EUI by 10 kWh/m^2 and 7 kWh/m^2 over the variable value changed from 0 to 0.8m in both Colombo and Kandy. These two variables ranked third in both regions in the degree of sensitivity (SC= 0.04 and SC=0.04 in Colombo, SC= 0.1 and SC=0.11 in Kandy), showing that both PDS: window overhangs and window side fins can significantly save building energy in Colombo and Kandy. In contrast, OH and SF increased EUI from 35.36 kWh/m^2 (baseline) to 37.21 kWh/m^2 (OH) and 37.65 kWh/m^2 (SF) when the length of the overhang and side fins were increased from 0 to 0.8m. Thus, having shorter or no overhangs and side fins is recommended for residential high-rise buildings (RHB) in Nuwara Eliya.

Energy demand (EUI) linearly decreased from 96.23 kWh/m^2 to 94.85 kWh/m^2 when green walls percentage (GW) changed from 0 to 100% in the residential high-rise buildings in Colombo (Figure 22(c)). Similarly, EUI was reduced by 1.0 kWh/m^2 when 100% GW was added to buildings in Kandy. EUI tended to increase by 0.5 kWh/m^2 if a 100% green wall area was added to buildings in Nuwara Eliya, indicating it is unsuitable for reducing operational energy in the Nuwara Eliya climate.

Solar absorptance ratio (EC) is the second most sensitive variable in Colombo (SC=0.08) and Kandy (SC=0.23). Within the full range of solar absorptance ratio (EC), EUI was reduced by 14 kWh/m2 in Colombo and 11 kWh/m2 (Figure 22 (d)). However, an opposite correlation with an EUI increase of 17.3 kWh/m^2 was shown for RHBs in Nuwara Eliya. Therefore, applying reflective wall paints proves to be an effective PDS in Colombo and Kandy but ineffective in Nuwara Eliya.

Figure 22(e) shows that the changing U-Factor of glass (GU) only reduces EUI in Nuwara Eliya, i.e., from 35.4 kWh/m^2 to 33 kWh/m^2 with a robust linear relationship. Hence, adding thick/multiple window glazing is advantageous for the buildings in Nuwara Eliya. The LSA results indicate that adding multiple/thick window glazing is a poor PDS choice in Colombo and Kandy owing to the increase of EUI by 1.25 kWh/m^2 and 2.0 kWh/m^2 when the U-value of glass is decreased from the baseline value of 5.7 W/m^2/K to 1.3 W/m^2/K.

The lowest sensitive variable, the specific heat of walls (WS), reduced EUI by only 0.8%, 0.8%, and 2.7% in the baseline cases in Colombo, Kandy, and Nuwara Eliya (Figure 22 (f)). Therefore, integrating high thermal mass walls signaled a less energy-effective integration of PDS into residential high-rise buildings than the other seven PDS.

Conductivity of walls (CW) linearly reduces (R^2=0.91) EUI by 9 kWh/m^2 (25.7%) in residential buildings in Nuwara Eliya, as shown in Figure 22 (g). Notably, CW is the highest sensitive variable in Nuwara Eliya, demonstrating the importance of applying low conductive walls for residential high-rise buildings. RHBs in Colombo showed an insignificant EUI reduction of 0.17 kWh/m^2 with a non-linear variation (R^2=0.32); adding low conductive walls is not an energy-efficient strategy for this region. This PDS failed to reduce EUI in Kandy, too.

According to Figure 22(h), solar heat gain coefficient (WC) is the highest sensitive variable in Colombo and Kandy that can linearly reduce EUI by 16 kWh/m^2 (15.8%) and 8.4 kWh/m^2 (27%). These results suggest that adding low e-coating on window glasses is an ideal PDS to reduce the EUI of residential high-rise buildings in Kandy and Colombo. However, residential high-rise buildings in Nuwara Eliya showed an opposite relationship, reducing SHGC from 0.83 to 0.5 and increasing EUI by 5.0kWh/m^2 (14.2%) compared to the baseline case.

This section discusses LSA's ability to estimate the energy saving of various PDS applications on a building's energy use intensity (EUI) when PDSs were applied individually. However, LSA does not reveal which PDS is the most influential or how PDSs interact with each other when multiple PDS are integrated into the building design. To address this, the study conducted a global sensitivity analysis to quantify the influence of PDSs and their mutual relationships when they were applied as groups to the building.

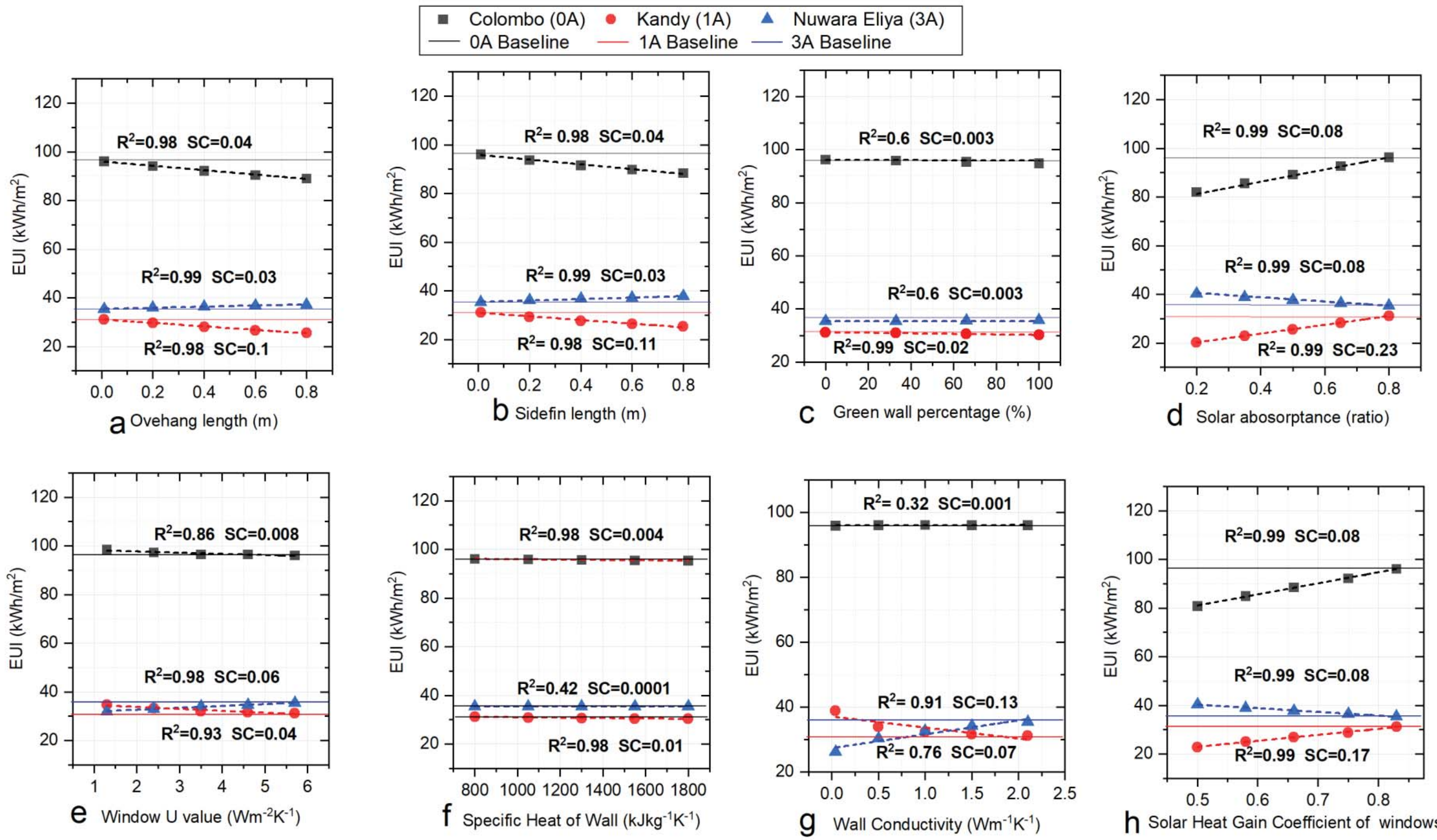

Figure 22: Summary of local sensitivity analysis where the change of EUI is shown for one-at-a-time change of a) Overhang, b) Sidefin, c)Green walls, d) Reflective exterior paint, e) Multiple/thick glazing, f) High thermal mass walls, g) Low Conductive walls and h) Low-e glazing

6.1.2 Global sensitivity analysis using the Morris method.

This study employed the Morris method for the global sensitivity analysis. The Morris method calculates the Elementary Effect (EE) (Eq. 05) for the "*r*" number of trajectories in N-dimensional input space. Here, *N* represents the number of building variables corresponding to PDS, and the parametric range of each strategy is scaled into an interval of [0,1] and discretized into *p* grid levels, which allows the change a parametric value of each strategy by equal steps of Δ (where $\Delta = p/2(p-1)$). An analysis of (N+1) × r design cases is required to obtain three sensitivity measures to assess each passive strategy's global sensitivity.

- μ_i – Mean of the distribution of EEs of the *i*th parameter. The mean value overall impacts the output of each input parameter.
- σ_i^* – standard deviation of the distribution of EEs of the *i*th parameter.
- μ_i^* - Absolute mean of the distribution of EEs of the *i*th parameter.

$$EE_i = \frac{y(x + e_i\Delta_i) - y(x)}{\Delta_i} \tag{5}$$

where *y* is the output (i.e., EUI), *x* is a vector of actual input variables with k coordinates, e_i is a vector of zeros but with its *i*th component equal to ±1, and $\Delta_i = p/2(p-1)$ with *p* even number of intervals of parameter *x*.

The mean (μ) and standard deviation (σ) of each parameter are calculated as:

$$\mu_i = \frac{1}{r}\sum_{i=1}^{r} EE_i \tag{6}$$

$$\sigma_i = \sqrt{\frac{1}{(r-1)}\sum_{i=1}^{r}\left(EE_i - \mu\right)^2} \tag{7}$$

Generally, *r* is assigned a value between 4 to 10, depending on the input parameters (Heiselberg et al., 2009; Liu et al., 2020). Because eight PDSs were used as input parameters, this study chose $r = 10$ with four gird levels ($p = 4$) for reliable GSA results (Saltelli et al., 2008). For this study, 270 EnergyPlus simulations were conducted using the energy analysis sub-framework (Section 4.2) for ten elementary effects, eight PDSs, and three climate zones. GSA estimates the importance of PDSs based on the absolute mean of EE_i (μ^*) and the mutual relationship type among PDSs using the covariance (σ/μ^*). A relationship is linear if $\sigma/\mu^* < 0.1$, monotonic if $0.5 > \sigma/\mu^* > 0.1$, almost monotonic if $1.0 > \sigma/\mu^* > 0.5$, or non-linear, non-monotonic or/and interaction effects if $\sigma/\mu^* > 1.0$ (Garcia Sanchez et al., 2014).

Overhang length and side fin length (OH and SF) have a negative ($\mu<0$) and monotonic relationship with EUI in Colombo (σ/μ^* = 0.21 and 0.33) and Kandy (σ/μ^* = 0.33 and 0.47) respectively. Hence, adding window overhangs and side fins indicates that EUI can be reduced in residential high-rise buildings in Colombo and Kandy, even in a PDS design combination with the rest of the strategies. However, in both Colombo and Kandy, OH showed a high influence (μ^*=5.2 and μ=3.3) on EUI reduction over SF (μ^*=5.2 and μ=3.2), compared to an almost similar influence in LSA. In contrast, these two PDS did not reduce EUI for buildings in Nuwara Eliya, agreeing with LSA outputs.

In Colombo, the Green Wall percentage (GW) is the 5th most influential variable, exhibiting a monotonic relationship with Energy Use Intensity (EUI), with a negative mean (μ) of -0.7. Similarly, in Kandy, GW is the 7th influential variable with a mean (μ) of -0.4. GW reduces EUI when applied alongside other PDS without any redundancy effect in Colombo and Kandy. However, GSA results revealed the unsuitability of GW for residential high-rise buildings in Nuwara Eliya due to a positive μ value, indicating an increase in EUI.

In both Colombo and Kandy, a negative μ and high influence (second highest μ^*) associated with solar absorptance (EC) suggests a potential reduction in Energy Use Intensity (EUI) at a greater rate. Conversely, EC was ineffective in Nuwara Eliya owing to a negative μ value.

U-Factor of glass (GU) monotonically (σ/μ^* = 0.21) decreased EUI (μ = -3.4) in residential high-rise buildings in Nuwara Eliya when the variable's value decreased. Therefore, thick/multiple window glazing is a compatible addition to a PDS design combination. In contrast, GU indicated a nonlinear, nonmonotonic, and interaction effect for buildings in Colombo (σ/μ^*=1.21) and an almost monotonic relationship in Kandy (σ/μ^*=0.96). Hence, a designer may need to explore the optimum value of GU to achieve the minimum EUI.

Like local sensitivity analysis results, GSA shows that the specific heat of walls (WS) is the least influential variable in all three regions since σ and μ are very close to zero. Hence, applying high thermal mass walls did not considerably alter EUI in three climates.

The conductivity of walls (CW) was the highest influential variable in Nuwara Eliya (μ* = 11.1) that reduced EUI monotonically (σ/μ*=0.32) over the variable interval. Hence, insulating exterior walls or adding low conductive walling material is a promising PDS that can be concurrently applied with other PDS. Although CW indicated a strong influence in Kandy and Colombo, it was not an effective PDS due to a positive (μ = +8.5, μ = +3.5) impact on the output for the tested variable's value. Resistance due to the low conductivity of walls that avoid dissipation of heat trapped in the daytime can be the main reason for this phenomenon. Besides, CW is a nonlinear, nonmonotonic, and interacting variable (σ/μ*=1.06) in Colombo, making EUI saving predictions uncertain.

GSA indicates solar heat gain coefficient (WC) as the most influential variable in Colombo (μ* = 16.2) and Kandy (μ* = 9) that reduce EUI monotonically. This result recommends applying low e-coating on window glasses as a beneficial PDS addition. The results in Kandy ranked WC as the second most influential variable, yet it tended to increase EUI when altered from the baseline value. In other words, designers should keep SHGC at its maximum value, similar to a case with no PDS.

Table 9: Summary of the Morris metrics

		Colombo (0A)			**Kandy (1A)**			**Nuwara Eliya (3A)**		
Variable		**μ**	**μ***	**σ/μ***	**μ**	**μ***	**σ/μ***	**μ**	**μ***	**σ/μ***
Overhang length	OH	-5.2	5.2	0.21	-3.3	3.3	0.33	**1.5**	**1.5**	**0.2**
Left and right-side fin length	SF	-5.2	5.2	0.33	-3.2	3.2	0.47	**1.7**	**1.7**	**0.29**
Green wall percentage	GW	-0.7	0.7	0.29	-0.4	0.4	0.5	**0.2**	**0.2**	**0.5**
Solar Absorptance	EC	-9.3	9.3	0.41	-6.4	6.4	0.36	**3.9**	**3.9**	**0.54**
U-Factor of glass	GU	**0.3**	**1.9**	**1.21**	**1.9**	**2.4**	**0.96**	-3.4	3.4	0.21

Specific Heat of walls	WS	-0.5	0.5	0.4	-0.4	0.4	0.5	0.05	0.06	0.04
Conductivity of walls	CW	**3.5**	**3.5**	**1.06**	**8.5**	**8.5**	**0.76**	-11.1	11.1	0.32
Solar Heat Gain Coefficient	WC	-16.2	16.2	0.17	-9	9	0.32	**5.1**	**5.1**	**0.18**

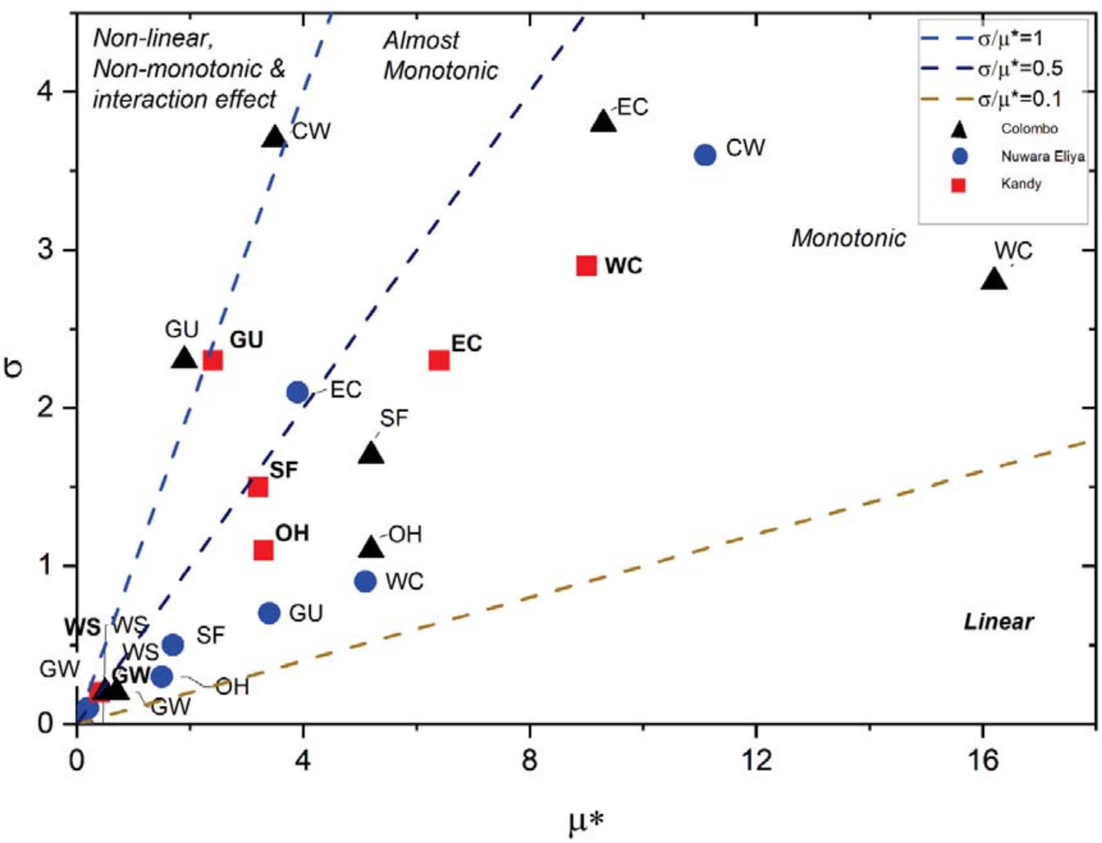

Figure 23: The covariance plot (σ vs. μ) of eight passive design strategies in Colombo (0A) (black triangles), Kandy (1A) (Red squares), and Nuwara Eliya (3A) (Blue circles).*

6.2 Sensitivity Analysis aided recommendations for selecting the best energy-saving PDS combinations for local climates.

Sensitivity analyses are a mathematical approach that helps designers form an effective PDS combination by checking their energy-saving efficiency and compatibility. This study followed three criteria to make this decision based on sensitivity analyses presented in the previous sections. The first criterion recommends avoiding integrating PDS, which causes an increase in the EUI when modifying the corresponding building variables. For example, reducing the GU (U-value of glasses) and CW (conductivity of walls) tends to increase EUI in RHBs in Kandy. This implies that integrating PDS, like multiple/thick window glazing and low-conducting walling materials, requires more energy in RHBs than its baseline building. The second criterion is to neglect PDSs that do not significantly reduce EUI after application. For example, increasing WS (the thermal mass of walls) using high thermal mass walling material reduces EUI by less than 1% in Colombo and Kandy. Since this involves additional investment costs in integrating this PDS, it may not provide sufficient client benefits. The third criterion is carefully selecting an optimum PDS with interacting and non-linear relationships with other PDSs. For instance, GU (U-value of windows) and CW (thermal conductivity of walls) have a complex and non-linear relationship with Energy Use Intensity (EUI) for residential high-rise buildings in Colombo. In the case of PDS, it becomes challenging to determine the maximum reduction of EUI without testing different values of PDS variables within the minimum and maximum ranges. Hence, if such PDS is used for PDS combinations, testing numerous PDS variable values is essential. Table 11 summarizes the recommended PDS for RHBs in three climate zones. The PDSs should be addressed with the third criterion, highlighted in bold letters.

Table 10: Summary of recommended PDS

Climate zone	**Recommended Passive Design Strategy**
Colombo	• Block direct sun rays through windows using overhangs and side fins (Maximum lengths of 0.8m). • Apply solar reflective paints on exterior walls. • Reduce solar heat gain coefficient of windows by using low e-glasses. • **Use compatible thermal transmittance(U-value) of glazing by altering glazing type.** • **Select compatible thermal conductivity by altering the walling material.**

Kandy	• Block direct sun rays through windows using overhangs and side fins (Maximum lengths of 0.8m). • Apply solar reflective paints on exterior walls. • Reduce the solar heat gain coefficient of windows by using Low-e glasses.
Nuwara Eliya	• Reduce the thermal conductivity of exterior walls by introducing low-conductive walling materials. • Reduce the U-value of glasses by altering traditional glasses with multiple/thick glazing.

Several PDS combinations were simulated in the next step to identify the best energy-saving one. The following sequence was followed to form PDS combinations that matched three criteria: First, the highest sensitive PDS was added to the baseline building design. Similarly, the subsequent sensitive PDS were added to the previous combination while satisfying the first and second criteria. Finally, PDS under the third criterion were added individually with their different variable states within the minimum and maximum range. The summary of the PDS combinations and their simulated energy consumption is presented in Figure 24.

The highest sensitive PDS in Colombo was WC (Low e-glazing), which resulted in 15.8% EUI savings when used alone with a value of 0.5. The second most influential PDS was EC (Solar reflective wall paints), with 0.2 solar absorptances; it can further increase EUI savings by up to 30.5% when combined with WC. Using the third and fourth most influential PDSs, OH (0.8m long window overhang) and SF (0.8m long window side fin) with WC and EC additionally reduced EUI savings by 3.7% and 3.2%. However, these savings were less significant than those of WC and EC. Adding GU to the combination of WC, EC, OH, and SF resulted in the highest EUI savings of 40.1% when used with the minimum U-value of 1.3W/m^2/K. Increasing the GU value from 1.3 to 2.83 and 4.36 resulted in a slight drop in EUI savings to 39.9% and 38.3%, respectively. Lastly, CW, another non-linear, non-monotonic, and interactive PDS, was added to the combinations. The study found that using CW with values of 0.1 resulted in EUI savings dropping below 32%, regardless of the GU value. However, using CW values of 1.4 or 0.7 and GU values of 4.36 or 2.33 resulted in EUI savings ranging from 39.3% to 36.1%.

Integrating the most significant PDS, WC, to RHBs in Kandy (1A) saved 27% EUI. The second most influential PDS, EC, saved 29.1% of EUI, reducing the total building energy consumption by more than half of the base-case building. Adding OH and SF increased EUI savings from 56.1% to 61.3% to 63.5%, indicating the potential of PDSs to save more than 40% of building energy consumption of buildings in Kandy. In Nuwara Eliya (3A), the highest sensitive PDS, CW, with its minimum value of 0.1, saved 23.6% of EUI, which was higher than the EUI savings of the building in Colombo but less than Kandy. Integrating the only other advantageous PDS, GU, with its minimum value of 1.3, in Nuwara Eliya (3A) increased the EUI saving from 23.6% to 31.7%.

Climate Zone	Case name	Value of passive design strategy								Outputs		
		OH	SF	GW	EC	GU	WS	CW	WC	EUI	delta EUI	EUI saving %
0A	Case - 1 - 0A	0	0	0%	0.8	5.7	800	2.1	0.5	80.9	15.2	15.8
	Case - 2 - 0A	0	0	0%	0.2	5.7	800	2.1	0.5	66.8	29.34	30.5
	Case - 3 - 0A	0.8	0	0%	0.2	5.7	800	2.1	0.5	63.1	33.03	34.4
	Case - 4 - 0A	0.8	0.8	0%	0.2	5.7	800	2.1	0.5	59.8	36.3	37.8
	Case - 5 - 0A	0.8	0.8	0%	0.2	1.3	800	2.1	0.5	57.6	38.49	40.1
	Case - 6 - 0A	0.8	0.8	0%	0.2	2.83	800	2.1	0.5	57.8	38.35	39.9
	Case - 7- 0A	0.8	0.8	0%	0.2	4.36	800	2.1	0.5	59.3	36.82	38.3
	Case - 8 - 0A	0.8	0.8	0%	0.2	1.3	800	1.4	0.5	58.4	37.75	39.3
	Case - 9 - 0A	0.8	0.8	0%	0.2	2.83	800	1.4	0.5	58.4	37.66	39.2
	Case - 10 - 0A	0.8	0.8	0%	0.2	4.36	800	1.4	0.5	60.0	36.15	37.6
	Case - 11 - 0A	0.8	0.8	0%	0.2	5.7	800	1.4	0.5	60.4	35.67	37.1
	Case - 12 - 0A	0.8	0.8	0%	0.2	1.3	800	0.7	0.5	60.0	36.11	37.6
	Case - 13 - 0A	0.8	0.8	0%	0.2	2.83	800	0.7	0.5	60.0	36.11	37.6
	Case - 14 - 0A	0.8	0.8	0%	0.2	4.36	800	0.7	0.5	61.5	34.65	36.1
	Case - 15 - 0A	0.8	0.8	0%	0.2	5.7	800	0.7	0.5	61.9	34.23	35.6
	Case - 16 - 0A	0.8	0.8	0%	0.2	1.3	800	0.1	0.5	64.7	31.43	32.7
	Case - 17 - 0A	0.8	0.8	0%	0.2	2.83	800	0.1	0.5	64.4	31.66	32.9
	Case - 18 - 0A	0.8	0.8	0%	0.2	4.36	800	0.1	0.5	65.8	30.33	31.6
	Case - 19 - 0A	0.8	0.8	0%	0.2	5.7	800	0.1	0.5	66.0	30.07	31.3
1A	Case - 1 - 1A	0	0	0%	0.8	5.7	800	2.1	0.5	22.8	8.42	27
	Case - 2 - 1A	0	0	0%	0.2	5.7	800	2.1	0.5	13.7	17.51	56.1
	Case - 3 - 1A	0.8	0	0%	0.2	5.7	800	2.1	0.5	12.0	19.16	61.4
	Case - 4 - 1A	0.8	0.8	0%	0.2	5.7	800	2.1	0.5	11.4	19.82	63.5
3A	Case - 1 - 3A	0	0	0%	0.8	5.7	800	0.1	0.8	27.0	8.33	23.6
	Case - 2 - 3A	0	0	0%	0.8	1.3	800	0.1	0.8	24.1	11.22	31.7

Figure 24: EUI Summary of different PDS combinations in three climate zones.

In this section, the best energy-saving combinations for PDS have been identified and summarized in Figure 25, along with the images of updated BIM models. However, it should be noted that implementing these PDS combinations may require additional investment costs, which would have to be borne by clients. This may discourage them from investing without a complete understanding of the benefits and any potential drawbacks (Sun et al., 2018). Hence, the second stage of the study explored the PDS designs that minimize both the investment cost and building energy consumption.

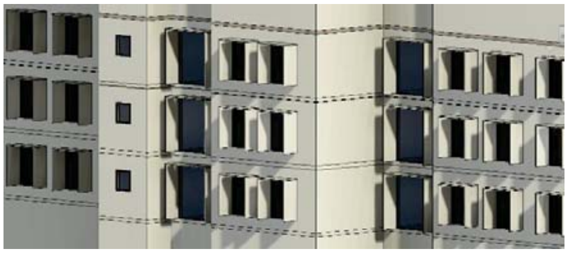

Colombo (0A)

- 0.8m window overhangs and sidefins
- Solar reflective paint on walls (Solar Absorption – 0.2)
- Multiple/thick glazing (U- 1.3W/m2)
- Low e coating on glasses (SHGC-0.5)

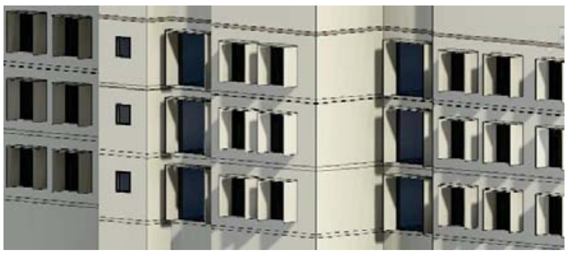

Kandy (1A)

- 0.8m window overhangs and sidefins
- Solar reflective paint on walls (Solar Absorption – 0.2)
- Multiple/thick glazing (U- 2.83W/m^2)
- Low e coating on glasses (SHGC-0.5)

Nuwara Eliya(3A)

- Multiple/thick glazing (U- 2.83W/m2)
- Low conductive walls (conductivity – 0.04 W/m-K)

Figure 25: Graphical representations of (Updated BIM models) of the best energy saving PDS combinations.

CHAPTER 7

7. MULTI-OBJECTIVE OPTIMIZATION

7.1 Choosing optimum Passive Design Strategies (PDS) design - Multi-objective Optimization approach

The previous section highlighted the importance of identifying the best PDS design that balances the trade-off between energy saving and investment costs when applied to RHBs. This task becomes a multi-objective optimization problem with two conflicting goals: minimizing operational energy and investment cost. In this phase, the study focused on the practical application of PDS and examined design options available in the market, which we will refer to as PDS design options from this point forward. By combining several PDS design options, designers can propose a PDS design for a residential high-rise building. During the sensitivity analysis, the study found that green walls and high thermal mass walls had almost no effect on reducing the operational energy consumption of the building in all three sub-climate zones. Therefore, at this phase of the study omitted these two strategies and considered the following six strategies in the optimization phase.,

1. Block direct sun rays through windows using overhangs (Maximum lengths of 0.8m)
2. Block direct sun rays through windows using side fins (Maximum lengths of 0.8m).
3. Apply solar reflective paints on exterior walls.
4. Reduce windows' solar heat gain coefficient by using Low e-glasses.
5. Use compatible thermal transmittance(U-value) of glazing by altering glazing types.
6. Select compatible thermal conductivity by altering walling materials.

Practically, each glazing design option has a solar heat gain coefficient and a U-value. Although these are two separate recommendations for operational energy reduction of buildings, this study searched for the optimal glazing option without considering these two variables separately. Similarly, each walling material has an associated thermal conductivity and thermal mass. Like the glazing options, the study followed a similar approach when considering walling material options. The final set of PDS design options is presented in Table 12. For this original design case, this study considered the design options specified for the case-study building in Section 5. These design options are highlighted in bold letters in Table 12.

Table 11: Summary of PDS design options.

Abb.	Strategy	Option Type	Description
S1	Solar Reflective Wall Paints	**Option 1**	**General emulsion paint**
		Option 2	Kraft 4 seasons paint for exterior use.
S2	Exterior Wall Material	**Option 1**	**Concrete block wall**
		Option 2	Cement Sand block wall
		Option 3	Fly ash brick
		Option 4	EPS concrete blocks
S3	Window Glazing Type	**Option 1**	**3mm float glass**
		Option 2	3mm float glass with a coating
		Option 3	6mm float glass
		Option 4	6mm float glass with a coating
		Option 5	6/16/6 Double glass
		Option 6	4/12/4/12/4 Triple glass
S4	Add Window Overhang	Continuous	**0.0m -** 0.8m
S5	Add Window Side fin	Continuous	**0.0m -** 0.8m

A detailed description of the two objective functions is presented in the subsequent sub-sections.

7.1.1 1st Objective function – Minimize Investment Cost (IC)

Property investors and housing unit clients are mainly concerned with investment cost (IC) when additional fees must be borne in integrating passive design strategies into building designs (Hamdy et al., 2011). Hence, minimizing IC is the first objective of this analysis. The proposed passive design options alter building envelope materials or assemblies while keeping internal walls, doors, and floor assemblies according to a baseline building. The function of calculating the IC of each design option ($\bar{x}$), is mathematically shown below,

$$f_{IC(\bar{x})}, \$/m^2 = \frac{\sum_{r=1}^{r} CC_r + \sum_{r=1}^{r} MC_r + OC(\$)}{FA(m^2)} \tag{8}$$

where

- CC_r – Construction Cost of r^{th} PDS design
- MC_r – Material Cost of r^{th} PDS design
- OC – Construction and Material Costs of the rest of the building element
- FA – Total area of a typical floor

7.1.2 2nd Objective function – Minimize Operational Energy Consumption

In the previous chapters, the primary goal in selecting the PDS design combination was to minimize the operational energy consumption. This goal is imperative because of the fast depletion of existing energy sources, which challenges supplying electricity to meet increasing demand. As a result, apartment owners may struggle with high electricity prices. Therefore, minimizing operational energy consumption was selected as the second optimization objective. The operational energy of each passive design option is calculated according to Eq.(9), which derives Energy Use Intensity (EUI).

$$f_{OE(\bar{x})}, kWh/m^2 = EUI = \frac{\sum (E_{hvac}(\overline{x}) + E_{lighting} + E_{equipment})\,\text{kwh}}{FA(m^2)} \tag{9}$$

- E_{hvac} – Energy consumption for HVAC for $\bar{x}$ design option
- $E_{lighting}$ – Energy consumption for artificial lighting
- $E_{equipment}$ – Energy consumption for equipment
- FA – Total area of a typical floor

The summary of the objective function is shown in Eq.(10), where the PDS design option is denoted by $\bar{x}$ with option(i) of each strategy (S1 to S6) denoted by x_{Si}.

$$Min\{\mathrm{f}_{OE}(\bar{x}), \mathrm{f}_{IC}(\bar{x})\}, \bar{x} = [\mathrm{x}_{S1i}, \mathrm{x}_{S2i}, \ldots \mathrm{x}_{S5i}] \tag{10}$$

7.1.3 Multi-objective optimization

This study used the NGSA-II algorithm and the middleware tool presented in Section 4.4 to perform multi-objective optimization. Simulation parameters were set based on Table 13.

Table 12: Multi-objective optimization parameters

Parameter	Value
Population	25
Generations	50
Crossover	0.8
Mutation	0.1

The convergence plot is a crucial indicator in multi-objective optimization as it helps determine whether the algorithm has reached global convergence. The convergence plots of this study (Figure 26) reveal two essential aspects. First, the optimization algorithm reached the global optimum value before the 50th generation in all three climate zones. This suggests that 50 generational cycles are sufficient to find the optimal solution for both objectives in this study. Second, the optimum value of operational energy was achieved in the 26th generation in Colombo, while it was completed in the 13th generation in Kandy and Nuwara Eliya. The faster convergence of Kandy and Nuwara Eliya indicates that finding a PDS design option is less complex, while the higher generations of Colombo indicate higher complexity. The reason for this scenario can be described using the global sensitivity analysis (GSA) results presented in Section 6.1.2. According to GSA, PDS in Kandy and Nuwara Eliya did not show non-linear interaction effects between their building variables. At the same time, the U value of glass and the conductivity of walls indicated non-linear interaction effects in Colombo. Additionally, only the glass's U value and the wall's conductivity effectively reduced operational energy in residential high-rise buildings in Nuwara Eliya. These reasons may underlie the faster convergence in Kandy and Nuwara Eliya and the higher number of iterations in Colombo.

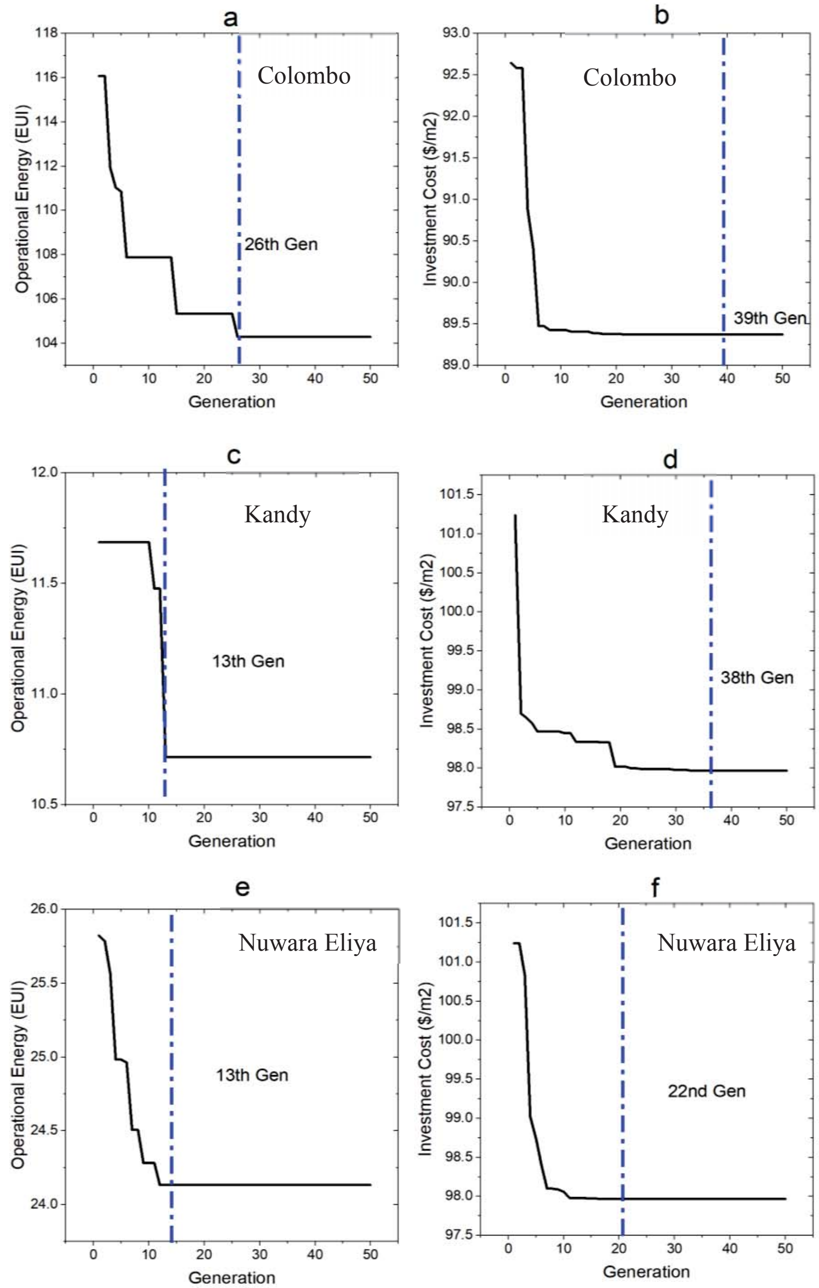

Figure 26: Convergence Plots of objective functions: Colombo - (a) Operational energy and (b) Investment Cost, Kandy- (b) Operational energy and (c) Investment Cost, Nuwara Eliya- (e) Operational energy and (f) Investment Cost

After running the optimization algorithm, the post-processing script of the Results Integrator was executed. This step involved searching for the best solutions among all options. In multi-objective optimization, the best solutions, or in other words, the solutions that cannot be further improved without compromising other objectives, are called non-dominated solutions (NDS). Figure 27 shows all designs explored by the algorithm (represented by black triangles), the non-dominated solutions (represented by red circles), and the original design (represented by blue circles). 56 NDS were found in Colombo, reduced to 34 in Kandy and 5 in Nuwara Eliya. As explained in the previous paragraph, the lower number of NDS in Kandy and Nuwara Eliya may be due to fewer energy-effective variables and the absence of nonlinear, interacting variables compared to the Colomb climate.

Although the recommended solutions are theoretically the best PDS designs, the designer must choose a single design from the suggested solutions in practice. The subsequent section of this thesis presents how to select a single PDS design.

a)

b)

c)

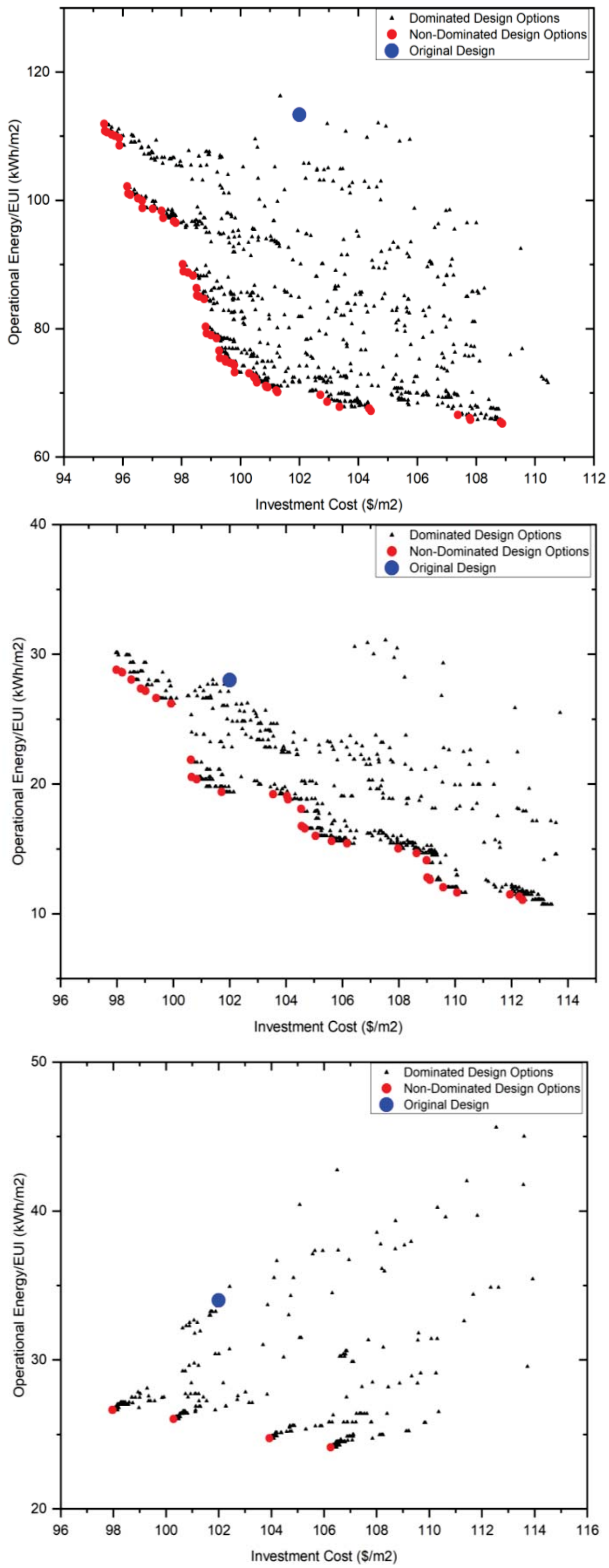

Figure 27: All solutions searched in MOO, Non-dominated solutions, and the original design case for a) Colombo, b) Kandy, and c) Nuwara Eliya.

7.2 Calculation of sustainability metrics for non-dominated solutions

Despite the need to find a single PDS design, the approach mentioned above can only search for a PDS design option that balances the investment cost and a reduction in EUI. Yet, it cannot provide insights into how each PDS design option achieves sustainability goals. Therefore, two additional metrics, lifecycle carbon emission reduction (LCCER) and Green Rating score for each PDS design option, were calculated using the Results Integrator tool introduced in Section 4.5. The following sections present a detailed explanation of the LCCER and Green Rating point calculations.

7.2.1 Life Cycle Carbon Emission Reduction (LCCER)

Policymakers are more interested in reducing the environmental impacts of buildings, explicitly reducing greenhouse gas emissions (GHG) (Röck et al., 2020). While Passive Design Strategies (PDS) can lower operational energy usage and reduce GHG emissions, incorporating additional building elements may increase GHG emissions (Elaouzy & El Fadar, 2022; Liu et al., 2023). The life Cycle Analysis (LCA) approach with a cradle-to-grave system boundary is the best way to tackle this problem. Still, limitations of available data remain a crucial challenge for LCA of Sri Lankan buildings. In particular, the maintenance and end-of-life data are hard to find and highly dynamic from project to project. Weerasinghe et al. (2021) found that the construction and utilities stages govern about 50% of the life cycle CO_2 emissions of Sri Lankan buildings. Similarly, Kumanayake & Luo (2018) show that material production, transportation, and operational phases contribute more than 90% of buildings' life cycle carbon emissions. Therefore, accounting only for GHG emissions embedded in materials and operational emissions for life-cycle carbon emission calculations is reasonable for this study.

In this study, the Life Cycle Carbon Emission Reduction (LCCER $(\bar{x})$) of $\bar{x}$ design option is calculated as follows,

$$f_{LCCE}(\bar{x}), kgCO_2eq/m^2 = OES - AUC \tag{11}$$

a. Operational Energy Saving (OES)

$$OES(\bar{x}),\ kgCO_2eq/m^2 = \Delta EUI(\bar{x}) \times EF \times n \tag{12}$$

- ΔEUI ($\bar{x}$)– Energy Use Intensity Saving (ΔEUI) by the Passive Design Strategy application of $\bar{x}$ design option.
- EF – Emission factor obtained from Sri Lankan Energy Balance Report ($0.71 kgeCO_2/kWh$).
- n – Design life considered for the building (years)

i. Energy Saving (ΔEUI) by the Passive Design Strategy application of $\bar{x}$ design option per unit floor area

$$\Delta EUI(\bar{x}), kWh/m^2/year = EUI_{baseline} - EUI_{PDS}(\bar{x}) \tag{13}$$

- $EUI_{baseline}$ – EUI of original design case
- $EUI_{PDS}(\bar{x})$ – EUI of building design option after the application of $\bar{x}$ design option

b. Additional Upfront carbon (AUC ($\bar{x}$)) due to the Passive Design Strategy application of $\bar{x}$ design option

$$AUC(\bar{x}) = UC_{PDS}(\overline{x}) - UC_{Originalcase} \tag{14}$$

Upfront Carbon (UC) was calculated using EPD (Environmental Product Declaration data). The global warming potential (GWP) values of each building assembly are shown in Annexure 03.

7.2.2 Green Building Rating Score

Green Building rating systems are widely used to evaluate and recognize sustainable building practices. These rating systems consider various sustainability parameters, including sustainable sites, management, indoor air quality, water efficiency, and social aspects. Sri Lanka has a green rating system developed by the Green Building Council of Sri Lanka. However, the local system falls short of the high energy and environmental performance standards set by LEED, a popular green rating system. Therefore, this study considers the LEED rating system (U.S. Green Building Council, 2016) as a proof of concept. The study focuses on two metrics and calculates the maximum score that can be achieved based on these metrics.

$$EA\,Credit: \%\ \text{Improvement in Energy Consumption} = \frac{EUI_{baseline} - EUI_{PDS}}{EUI_{baseline}} \times 100\% \quad (15)$$

$$MR\,Credit: \%\ \text{Reduction LCCE} = \frac{LCCE_{baseline} - LCCE_{PDS}}{LCCE_{baseline}} \times 100\% \quad (16)$$

7.3 Selection of the PDS Design

Various mathematical techniques are available to choose a single solution from a set of non-dominated solutions. Some commonly used methods are the Technique for Order Preference by Similarity to Ideal Solution (TOPSIS) (Srinivasan & Shocker, 1973), Linear Programming for multi-dimensional analysis of preference (LINMAP) (Tzeng & Huang, 2011), and Shannon's Entropy Method (Chakrabarti & Chakrabarty, 2005). This study initially used the LINMAP method to determine a single PDS design from the solutions presented in the previous chapter (Section 6.3.5.1). In addition to that, two extreme solutions (PDS designs) were tested: one with the lowest investment cost and the other with the lowest operational energy (EUI). The details of the three selected design options are presented in the subsequent sections.

7.3.1 LINMAP option

The LINMAP method first calculates the Euclidian distance using the distances to each Pareto solution from the ideal point. This ideal point is determined by intersecting the optimum values of two objectives. Then, the solution with the minimum Euclidian distance is selected as the PDS design option. The following equation calculates the Euclidian distance.

$$D_i = \sqrt{\sum_{j=1}^{n} (F_i - F_{ideal})^2} \quad (17)$$

This study had two objectives (j), so n =2 in the above equation. F_{ideal} denotes the ideal solutions or the minimum values of the objective functions. The Euclidean distance of the i[th] solution is the square of the difference between each of the solution's objective values (F_i) and the ideal solution's objective values (F_{ideal}) was calculated. The square root of the summation of both objective values was then calculated as the PDS design option's Euclidian distance (D_i).

For Colombo, the PDS design obtained from the LINMAP method resulted in a 33.4% decrease in operational and a 3.4% reduction in investment costs compared to the original design. Additionally, this design option lowered the life-cycle carbon emissions by 1280 $kgCO_2eq/m^2$ and could earn 15 points from the LEED v4.0 green rating system. Figure 28(a) shows a snapshot of the updated BIM model with this PDS option.

For Kandy, the LINMAP method suggests a PDS design (Figure 29(a)) that can reduce operational energy by 28.5% and investment cost by 1% compared to the original design. This option saves 83 $kgCO_2eq/m^2$ while achieving 6 LEED green rating points.

The PDS design option (Figure 30(a)) suggested for Nuwara Eliya can reduce 23.4% in operational energy and nearly 1% of investment cost compared to the original design option. This option saves 325 $kgCO_2eq/m^2$ while achieving 14 LEED green rating points.

7.3.2 Lowest Operational Energy option

This option explores the PDS design with the lowest operational energy. For Colombo, the lowest operational energy PDS design reduces operational energy (EUI) by 42.4% from the original design, an additional 10% reduction compared to the LINMAP solution. However, this option requires a 6.5% higher investment cost than the original design. It saves about 1754 $kgCO_2eq/m^2$ of life cycle carbon emissions and potentially earns 18 LEED green rating points. This option achieves higher sustainability goals than the solution obtained from the LINMAP method. Figure 28(b) shows a snapshot of the updated BIM model with the second PDS design option.

For Kandy, this design option (Figure 29(b)) reduces about 61% of operational energy compared to the original design. Like in the Colombo climate, this design increases the investment cost by 10.7%. Yet, it saves 441 $kgCO_2eq/m^2$ of life cycle carbon emissions and potentially earns 18 LEED green rating points.

For Nuwara Eliya, a 29.4% operational energy reduction can be observed for the PDS design (Figure 30(b)), while it increases investment costs by 4.1% compared to the original design. This option saves 420 $kgCO_2eq/m^2$ of life cycle carbon emissions and potentially earns 16 LEED green rating points.

7.3.3 Lowest Investment Cost Option

The third option selected the PDS design with the lowest investment cost (IC). In Colombo, it saves 13.7% of IC compared to the PDS design option, with the highest IC (selected option 02) and 7.5% less IC than the original design. Additionally, this option saves 1.2% operational energy compared to the original design. However, this design option failed to reduce life-cycle carbon emissions and received no LEED green rating points. Figure 28(c) shows a snapshot of the updated BIM model with the third PDS design option.

In Kandy, the PDS design (Figure 29(c)), with the lowest IC compared with the original design, saves nearly 4% of investment cost while the operational energy requirement increases by 7.1%. Like in Colombo, this option does not reduce life-cycle carbon emissions or achieve LEED green rating points.

In Nuwara Eliya, the PDS option (Figure 30(c)) with the lowest IC saves 4%, but unlike Kandy and Colombo, this option can save operational energy by 21.4%. This option saves 218 $kgCO_2eq/m^2$ of life cycle carbon emissions and potentially earns 10 LEED green rating points.

Figures 28 to 30 illustrate the impact of three different PDS designs on the appearance of buildings. In Colombo and Kandy, residential high-rise buildings (RHB) should incorporate window overhangs and side fins when opting for the lowest operational energy option. However, in Nuwara Eliya, none of the selected options include window overhangs, side fins, or reflective paints, as revealed by sensitivity analysis, indicating that these PDS designs are not practical for the climate of Nuwara Eliya. It is worth noting that for all three climates, the low investment cost option recommends using EPS concrete block as the exterior wall material and 3mm single glass as the window glazing option.

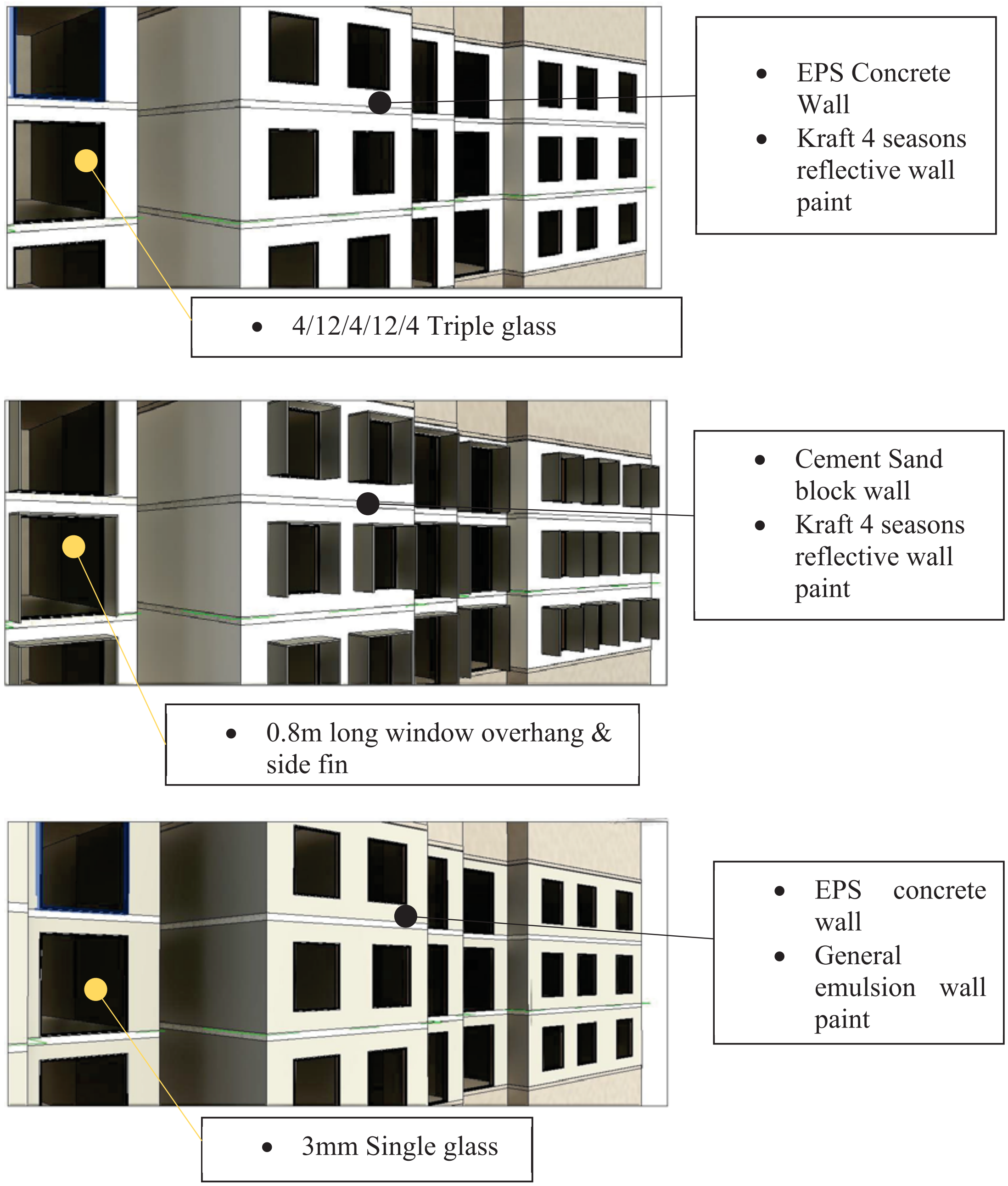

Figure 28: Updated BIM model visuals of selected PDS design options for Colombo. a) Selected PDS design option 01, b) Selected PDS design option 02, c) Selected PDS design option 03.

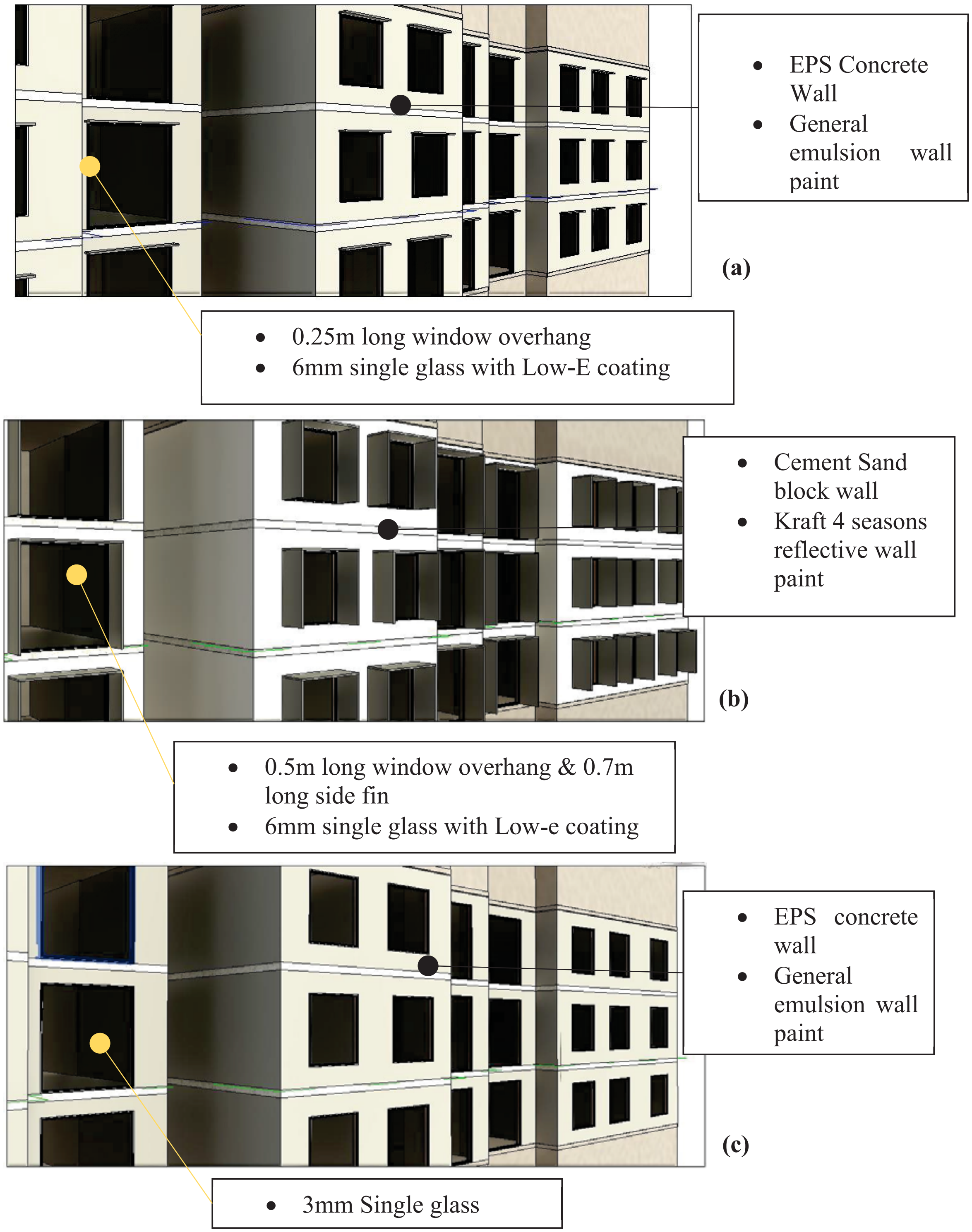

Figure 29: *Updated BIM model visuals of selected PDS design options for Kandy. a) Selected PDS design option 01, b) Selected PDS design option 02, c) Selected PDS design option 03.*

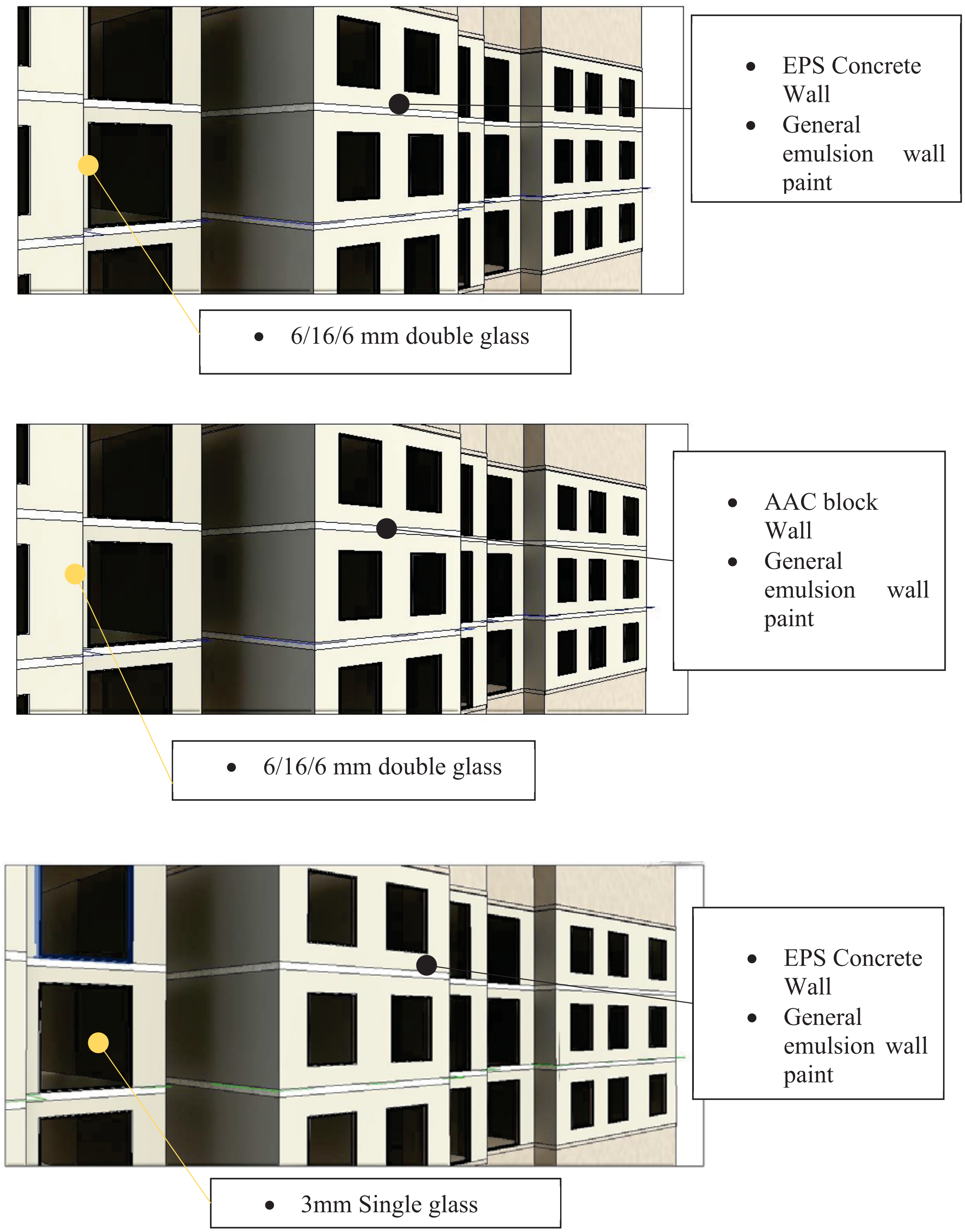

Figure 30 : *Updated BIM model visuals of selected PDS design options for Nuwara Eliya. a) Selected PDS design option 01, b) Selected PDS design option 02, c) Selected PDS design option 03.*

Figure 31 summarizes selected PDS designs, non-dominated PDS designs obtained from MOO, and the original design option with two objectives. The figure explains influential considerations designers should consider when choosing a single PDS design from non-dominated solutions.

The PDS design with the lowest investment cost (IC) only reduces IC by 4 % to 7.5% in all three regions, which may not be significant. However, this design increases operational energy in Colombo and Kandy and fails to achieve green rating points or GHG emission reduction. Despite the low IC savings, the PDS design for residential high-rise buildings (RHB) in Nuwara Eliya indicates that it can reduce GHG emissions and achieve some marks from green ratings.

Figure 31 indicates that despite the increased investment, a PDS design with the lowest operational energy can achieve high green rating scores and low GHG emissions in all three regions. Therefore, designers aiming for higher sustainability in their buildings should focus on PDS designs that achieve the lowest operational energy. However, the drawback of high IC can be overcome if designers choose a PDS design using the LINMAP method. Thus, designers considering sustainability and investment costs are recommended when selecting the LINMAP method.

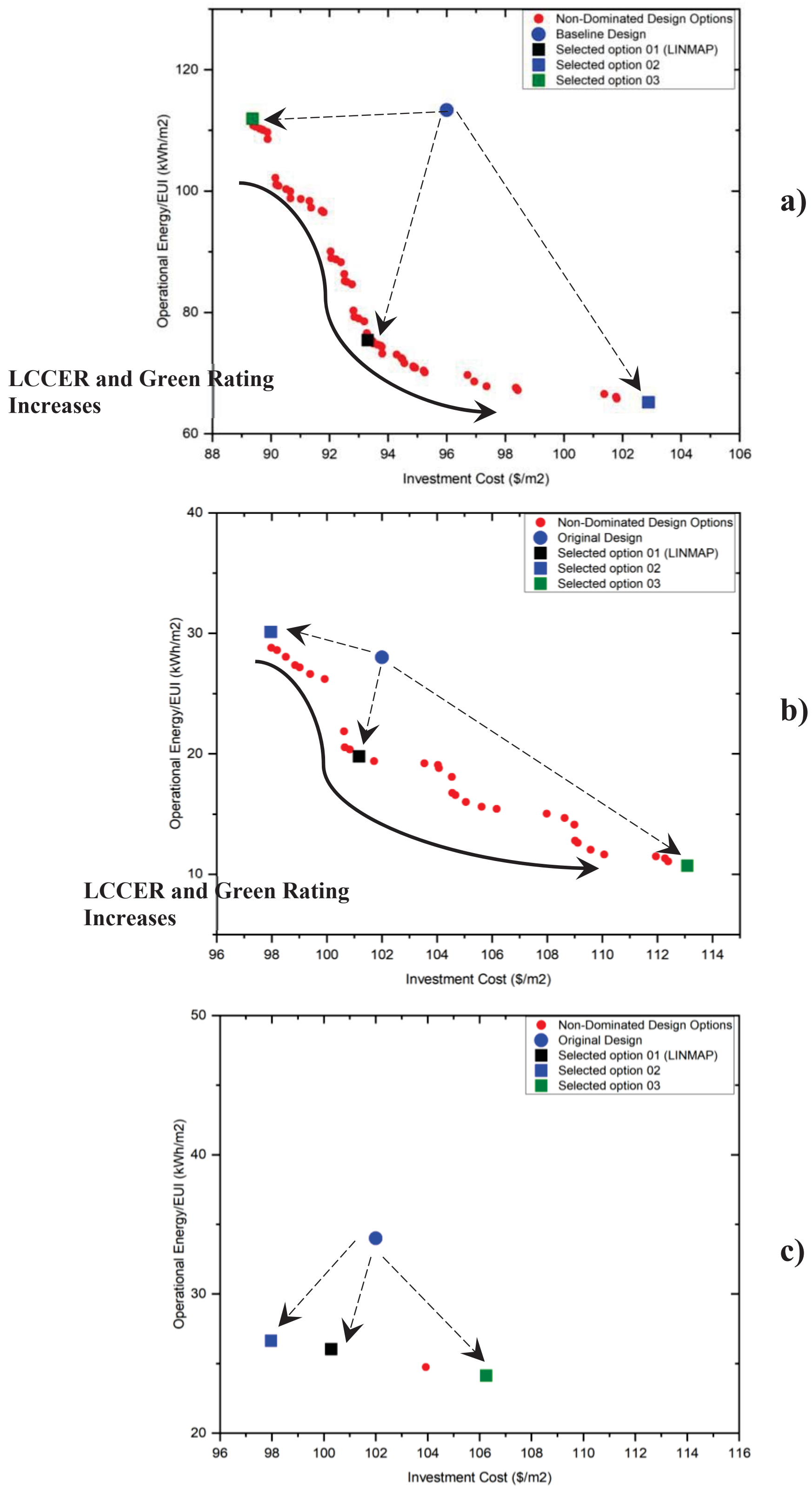

Figure 31: Selected PDS design options, non-dominated solutions, and baseline design of Colombo (a), Kandy(b) and Nuwara Eliya (c)

CHAPTER 8

8.1.LIMITATIONS OF THE STUDY

This study has introduced a new BIM-based building performance analysis (BPA) framework to support sustainable building design workflows. The study tested the framework by investigating the energy efficiency of passive design strategies (PDS) for a residential high-rise building in Sri Lanka. The case study results demonstrate that the BIM-based BPA enhances both the efficiency of the design process and the sustainability of building designs. However, it is essential to consider some limitations identified in the study for future adoptions of the framework.

- A field measurement campaign was conducted for 10 to 10 days in May and June to record data during some of the year's hottest days. However, the campaign was conducted for a shorter period as entry to the apartment was restricted. As a result, measurements in some weather and climate conditions, such as rainy days or cooler months, could not be recorded. Therefore, this study's validation of the building energy model was limited to the weather conditions observed during the measurement week.
- The study assumed a fixed natural ventilation rate for all spaces in the apartments on different floors without considering that ventilation rates vary with wind speed, which increases along the building's height. Weerasuriya et al. (2019b)demonstrated that apartments on the top floors have higher natural ventilation potential, leading to lower electricity consumption for space cooling. They also emphasized the importance of calculating ventilation rates of individual spaces using multi-zone airflow modeling rather than assuming a constant ventilation rate for all spaces. Therefore, the magnitudes of ventilation rates may differ from actual conditions.
- The study considered a consistent schedule for occupants and consistent levels of anthropogenic and equipment-related heat gains throughout the year to estimate EUI. However, the number of occupants and the usage patterns of electric and electronic appliances vary monthly, affecting energy use. Therefore, the effectiveness of the estimates may slightly differ from the real-world scenario.

- The study did not differentiate between the effectiveness of energy-saving measures during the day and night. For instance, shading devices that limit direct solar gains are only effective during the daytime, while devices that control heat transfer are beneficial throughout the day. Therefore, the research findings only apply to an overall view of annual energy consumption when using these devices in buildings.
- The scope of the daylight analysis in this study was restricted to evaluating the design day daylight condition of a PDS design with three daylight-blocking PDS and its extreme values. However, in a real-world scenario, an optimal value of PDS variables may exist other than its extreme value that can minimize EUI and maximize daylight.
- The proposed BIM-based BPA framework only partially automates the building design workflow. Designers must still switch between different interfaces, such as BIM and energy simulation, and manually input some data. Further technical developments are required to enable designers to use a fully automated workflow.
- The original multi-objective optimization was limited to only two objective functions: minimizing investment costs and operational energy. However, selecting PDS design options should be a many-objective optimization task that includes indoor air quality, daylight, and other factors.

8.2.CONCLUSIONS AND RECOMMENDATIONS

To the best of the author's knowledge, this study is the first to create a BIM-based framework that investigates the effectiveness of PDS in saving energy in residential high-rise buildings in Sri Lanka. The results of this study can assist building designers in selecting the ideal energy-saving PDS design option with the most environmentally friendly designs at the least investment cost. The study's output and recommendations are presented below:

- The study found that PDS like window overhangs, side fins, low e-coating, and exterior walls painted with reflective paints can significantly reduce operational energy consumption in residential high-rise buildings (RHBs) in Colombo and Kandy. For RHBs in Colombo, it is recommended to carefully choose compatible wall conductivities and U-value of window glasses to ensure maximum energy saving. In Nuwara Eliya, multiple/thick window glazing and low conductive walling materials are the effective PDSs. These recommendations can assist government authorities in making decisions about future residential high-rise building expansions in other areas of Sri Lanka.
- According to the study, adding green walls and high thermal mass walls does not significantly reduce operational energy consumption in any of the three climate zones in Sri Lanka. However, it is worth noting that green walls can improve indoor air quality, so they should not be ignored entirely in building designs.
- Proper selection of Passive Design Strategies (PDSs) and their properties can lead to significant energy savings in RHBs in different climate zones in Sri Lanka. The potential savings are estimated to be around 40.1%, 63.5%, and 31.7% in Colombo (0A), Kandy (1A), and Nuwara Eliya (3A), respectively. Local climate conditions should guide the selection of PDSs, their impact on energy efficiency, how they work together, building regulations, and constructability limitations.
- Using a multi-objective optimization technique, this study found an optimum PDS design for RHBs in Colombo, Kandy, and Nuwara Eliya that balances two objectives: minimize energy consumption and reduce investment cost. The optimum design for RHBs in Colombo, Kandy, and Nuwara Eliya can save

operational energy up to 42.4%, 61%, and 21.4%. Optimum designs can save investment costs up to 7.5%, 4%, and 4% in respective regions.

- The optimization further reveals that the designers should focus on PDS design options that minimize operational energy consumption, even if it requires a high investment cost, to achieve higher values for sustainability metrics. The LINMAP method has been proven effective in finding the best PDS design among non-dominated solutions obtained from a multi-objective optimization algorithm.
- According to this study, there is a weak connection between the popularity of PDSs and their energy-saving efficiency. This suggests that construction industry professionals might not have adequate knowledge of the most appropriate PDSs for different climate conditions. Therefore, the study recommends using its suggestions as a starting point for selecting suitable PDSs for RHBs in Sri Lanka rather than relying on popular opinions of construction industry professionals.
- The proposed BIM-based building performance analysis framework addresses technical gaps in the building design workflow, which requires several hundreds of building performance simulations (E.g., energy simulations). However, the study suggests further improving the framework to build a one-click tool for a fully-fledged BIM-based workflow.

REFERENCES

Afzal, A., Kim, K. Y., & Seo, J. W. (2017). Effects of latin hypercube sampling on surrogate modeling and optimization. *International Journal of Fluid Machinery and Systems*, *10*(3), 240–253. https://doi.org/10.5293/IJFMS.2017.10.3.240

Ahn, K. U., Kim, Y. J., Park, C. S., Kim, I., & Lee, K. (2014). BIM interface for full vs. semi-automated building energy simulation. *Energy and Buildings*, *68*(PART B), 671–678. https://doi.org/10.1016/j.enbuild.2013.08.063

Alsharif, R., Arashpour, M., Golafshani, E., Rashidi, A., & Li, H. (2023a). Multi-objective optimization of shading devices using ensemble machine learning and orthogonal design of experiments. *Energy and Buildings*, *283*, 112840. https://doi.org/10.1016/j.enbuild.2023.112840

Alwan, Z., & Ilhan Jones, B. (2022). IFC-based embodied carbon benchmarking for early design analysis. *Automation in Construction*, *142*(December 2021), 104505. https://doi.org/10.1016/j.autcon.2022.104505

Amoruso, F. M., Dietrich, U., & Schuetze, T. (2019). Integrated BIM-parametric workflow-based analysis of daylight improvement for sustainable renovation of an exemplary apartment in Seoul, Korea. *Sustainability (Switzerland)*, *11*(9). https://doi.org/10.3390/su11092699

ANSI/ASHRAE. (2021). Standard 169-2020, Climatic data for building design standards. *ANSI/ASHRAE Standard 169-2020*, *8400*, 1–387.

Anwar, M. W., Ali, Z., Javed, A., Din, E. U., & Sajid, M. (2021). Analysis of the effect of passive measures on the energy consumption and zero-energy prospects of residential buildings in Pakistan. *Building Simulation*, *14*(4), 1325–1342. https://doi.org/10.1007/s12273-020-0729-8

Bhamare, D. K., Rathod, M. K., & Banerjee, J. (2019). Passive cooling techniques for building and their applicability in different climatic zones—The state of art. *Energy and Buildings*, *198*, 467–490. https://doi.org/10.1016/j.enbuild.2019.06.023

Bracht, M. K., Melo, A. P., & Lamberts, R. (2021). A metamodel for building information modeling-building energy modeling integration in early design stage. *Automation in Construction*, *121*(September 2020), 103422. https://doi.org/10.1016/j.autcon.2020.103422

Chakrabarti, C. G., & Chakrabarty, I. (2005). Shannon entropy: axiomatic characterization and application. *International Journal of Mathematics and Mathematical Sciences*, *2005*(17), 2847–2854. https://doi.org/10.1155/IJMMS.2005.2847

Chang, Y. T., & Hsieh, S. H. (2020). A review of building information modeling research for green building design through building performance analysis. *Journal of Information Technology in Construction*, *25*, 1–40. https://doi.org/10.36680/j.itcon.2020.001

Charoenkit, S., & Yiemwattana, S. (2016). Living walls and their contribution to improved thermal comfort and carbon emission reduction: A review. *Building and Environment*, *105*, 82–94. https://doi.org/https://doi.org/10.1016/j.buildenv.2016.05.031

Chen, X., Yang, H., & Sun, K. (2017). Developing a meta-model for sensitivity analyses and prediction of building performance for passively designed high-rise residential buildings. *Applied Energy*, *194*, 422–439. https://doi.org/10.1016/j.apenergy.2016.08.180

Chen, Y., Mae, M., Taniguchi, K., Kojima, T., Mori, H., Trihamdani, A. R., Morita, K., & Sasajima, Y. (2021). Performance of passive design strategies in hot and humid regions. Case study: Tangerang, Indonesia. *Journal of Asian Architecture and Building Engineering*, *20*(4), 458–476. https://doi.org/10.1080/13467581.2020.1798775

Cheung, C. K., Fuller, R. J., & Luther, M. B. (2005). Energy-efficient envelope design for high-rise apartments. *Energy and Buildings*, *37*(1), 37–48. https://doi.org/10.1016/J.ENBUILD.2004.05.002

Chong, A., Xu, W., Chao, S., & Ngo, N. (2019a). *Energy & Buildings Continuous-time Bayesian calibration of energy models using BIM and energy data*. *194*, 177–190. https://doi.org/10.1016/j.enbuild.2019.04.017

CIBSE. (2015). Enviromental Design: CIBSE Guide A. *CIBSE Guide*, 239–254.

Crawley, D. B., Linda, K., & Lawrie. (2022). *Development of Global Typical Meteorological Years (TMYx)*. Climate.Onebuilding.Org. http://climate.onebuilding.org

Dahanayake, K. C., & Chow, C. L. (2018). Comparing reduction of building cooling load through green roofs and green walls by EnergyPlus simulations. *Building Simulation*, *11*(3), 421–434. https://doi.org/10.1007/s12273-017-0415-7

Dahanayake, K. W. D. K. C., & Chow, C. L. (2017). Studying the potential of energy saving through vertical greenery systems: Using EnergyPlus simulation program. *Energy and Buildings*, *138*, 47–59. https://doi.org/10.1016/j.enbuild.2016.12.002

Dias, D., Machado, J., Leal, V., & Mendes, A. (2014). Impact of using cool paints on energy demand and thermal comfort of a residential building. *Applied Thermal Engineering*. https://doi.org/10.1016/j.applthermaleng.2013.12.056

Elaouzy, Y., & El Fadar, A. (2022). Energy, economic and environmental benefits of integrating passive design strategies into buildings: A review. *Renewable and Sustainable Energy Reviews*, *167*, 112828. https://doi.org/10.1016/J.RSER.2022.112828

Elshafei, G., Negm, A., Bady, M., Suzuki, M., & Ibrahim, M. G. (2017). Numerical and experimental investigations of the impacts of window parameters on indoor natural ventilation in a residential building. *Energy and Buildings*, *141*, 321–332. https://doi.org/https://doi.org/10.1016/j.enbuild.2017.02.055

Energy Efficiency Building Code of Sri Lanka. (2021). Sri Lanka Sustainable Energy Authority. In *Web : www.energy.gov.lk +94* (Vol. 11).

Filho, J. P. B., & Santos, T. V. O. (2014a). *Thermal analysis of roofs with thermal insulation layer and reflective coatings in subtropical and equatorial climate regions in Brazil*. *84*, 466–474.

Freewan, A. A. Y. (2014a). Impact of external shading devices on thermal and daylighting performance of offices in hot climate regions. *Solar Energy*, *102*, 14–30. https://doi.org/10.1016/J.SOLENER.2014.01.009

Gamero-Salinas, J., Monge-Barrio, A., Kishnani, N., López-Fidalgo, J., & Sánchez-Ostiz, A. (2021). Passive cooling design strategies as adaptation measures for lowering the indoor overheating risk in tropical climates. *Energy and Buildings*, *252*, 111417. https://doi.org/10.1016/j.enbuild.2021.111417

Garcia Sanchez, D., Lacarrière, B., Musy, M., & Bourges, B. (2014). Application of sensitivity analysis in building energy simulations: Combining first- and second-order elementary effects methods. *Energy and Buildings*, *68*(PART C), 741–750. https://doi.org/10.1016/j.enbuild.2012.08.048

González-Torres, M., Pérez-Lombard, L., Coronel, J. F., Maestre, I. R., & Yan, D. (2022). A review on buildings energy information: Trends, end-uses, fuels and drivers. *Energy Reports*, *8*, 626–637. https://doi.org/10.1016/J.EGYR.2021.11.280

Hamdy, M., Hasan, A., & Siren, K. (2011). Applying a multi-objective optimization approach for Design of low-emission cost-effective dwellings. *Building and Environment*, *46*(1), 109–123. https://doi.org/https://doi.org/10.1016/j.buildenv.2010.07.006

Harkouss, F., Fardoun, F., & Biwole, P. H. (2018a). Passive design optimization of low energy buildings in different climates. *Energy*, *165*, 591–613. https://doi.org/10.1016/j.energy.2018.09.019

Heiselberg, P., Brohus, H., Hesselholt, A., Rasmussen, H., Seinre, E., & Thomas, S. (2009). Application of sensitivity analysis in design of sustainable buildings. *Renewable Energy*, *34*(9), 2030–2036. https://doi.org/10.1016/j.renene.2009.02.016

Hou, F., Ma, J., Kwok, H. H. L., & Cheng, J. C. P. (2022). Prediction and optimization of thermal comfort, IAQ and energy consumption of typical air-conditioned rooms based on a hybrid prediction model. *Building and Environment*, *225*(November). https://doi.org/10.1016/j.buildenv.2022.109576

Huang, K. T., & Hwang, R. L. (2016). Future trends of residential building cooling energy and passive adaptation measures to counteract climate change: The case of Taiwan. *Applied Energy*, *184*, 1230–1240. https://doi.org/10.1016/j.apenergy.2015.11.008

Ilhan, B., & Yaman, H. (2016). Green building assessment tool (GBAT) for integrated BIM-based design decisions. *Automation in Construction*, *70*, 26–37. https://doi.org/10.1016/j.autcon.2016.05.001

Jayasinghe, M. T. R., & Attalage, R. (1999). *Passive Techniques for Residential Buildings in Low Altitudes of Sri Lanka*. *January*.

Jayasinghe, M. T. R., & Priyanvada, A. K. M. (2002). Thermally comfortable passive houses for tropical uplands. *Energy for Sustainable Development*, *6*(4), 45–54. https://doi.org/10.1016/S0973-0826(08)60446-9

Jin, R., Zhong, B., Ma, L., Hashemi, A., & Ding, L. (2019). Integrating BIM with building performance analysis in project life-cycle. *Automation in Construction*, *106*(May), 102861. https://doi.org/10.1016/j.autcon.2019.102861

Judkoff, R., Wortman, D., O'Doherty, B., & Burch, J. (2008). A methodology for validating building energy analysis simulations. *NREL Technical Report 550-42059*, *April*, 1–192.

Jung, Y., Heo, Y., & Lee, H. (2021). Multi-objective optimization of the multi-story residential building with passive design strategy in South Korea. *Building and Environment*, *203*(April), 108061. https://doi.org/10.1016/j.buildenv.2021.108061

Karunathilake, W. K. U. V., Halwatura, R. U., & Pathirana, S. M. (2018). Optimization of thermal comfort in Sri Lankan residential buildings. *MERCon 2018 - 4th*

International Multidisciplinary Moratuwa Engineering Research Conference, 150–155. https://doi.org/10.1109/MERCon.2018.8421978

Kota, S., Haberl, J. S., Clayton, M. J., & Yan, W. (2014). Building Information Modeling (BIM)-based daylighting simulation and analysis. *Energy and Buildings*, *81*, 391–403. https://doi.org/10.1016/j.enbuild.2014.06.043

Krüger, E., & Givoni, B. (2008). Thermal monitoring and indoor temperature predictions in a passive solar building in an arid environment. *Building and Environment*, *43*(11), 1792–1804. https://doi.org/10.1016/j.buildenv.2007.10.019

Kumanayake, R., & Luo, H. (2018). A tool for assessing life cycle CO2 emissions of buildings in Sri Lanka. *Building and Environment*, *128*, 272–286. https://doi.org/10.1016/j.buildenv.2017.11.042

Liu, S., Kwok, Y. T., Lau, K. K. L., Ouyang, W., & Ng, E. (2020). Effectiveness of passive design strategies in responding to future climate change for residential buildings in hot and humid Hong Kong. *Energy and Buildings*, *228*. https://doi.org/10.1016/j.enbuild.2020.110469

Liu, S., Kwok, Y. T., Lau, K., & Ng, E. (2021). Applicability of different extreme weather datasets for assessing indoor overheating risks of residential buildings in a subtropical high-density city. *Building and Environment*, *194*(February), 107711. https://doi.org/10.1016/j.buildenv.2021.107711

Liu, S., Wang, Y., Liu, X., Yang, L., Zhang, Y., & He, J. (2023). How does future climatic uncertainty affect multi-objective building energy retrofit decisions? Evidence from residential buildings in subtropical Hong Kong. *Sustainable Cities and Society*, *92*(December 2022), 104482. https://doi.org/10.1016/j.scs.2023.104482

Mahar, W. A., Verbeeck, G., & Reiter, S. (2020). *Sensitivity Analysis of Passive Design Strategies for Residential Buildings in Cold Semi-Arid Climates*. *4*.

Malys, L., Musy, M., & Inard, C. (2014). A hydrothermal model to assess the impact of green walls on urban microclimate and building energy consumption. *Building and Environment*, *73*, 187–197. https://doi.org/10.1016/j.buildenv.2013.12.012

Manso, M., & Castro-Gomes, J. (2015). Green wall systems: A review of their characteristics. *Renewable and Sustainable Energy Reviews*, *41*, 863–871. https://doi.org/https://doi.org/10.1016/j.rser.2014.07.203

Mehjabeen Ratree, S., Farah, N., & Shadat, S. (2020). *Vernacular Architecture of South Asia: Exploring Passive Design Strategies of Traditional Houses in Warm Humid Climate of Bangladesh and Sri Lanka*. *May*, 216–226. https://doi.org/10.38027/n212020iccaua316262

Mendis, M. S., Rajapaksha, M., & Halwatura, R. U. (2020). Unleashing the potentials of traditional construction technique in bio-climatic building designs: A case of Ambalam, Sri Lanka. *International Journal of Environmental Science and Development*, *11*(6), 298–304. https://doi.org/10.18178/ijesd.2020.11.6.1266

Muñoz, P., González, C., Recio, R., & Gencel, O. (2022). The role of specific heat capacity on building energy performance and thermal discomfort. *Case Studies in Construction Materials*, *17*(May). https://doi.org/10.1016/j.cscm.2022.e01423

Nandapala, K., Chandra, M. S., & Halwatura, R. U. (2020a). A study on the feasibility of a new roof slab insulation system in tropical climatic conditions. *Energy and Buildings*, *208*, 109653. https://doi.org/10.1016/j.enbuild.2019.109653

Neale, J., Shamsi, M. H., Mangina, E., Finn, D., & O’Donnell, J. (2022). Accurate identification of influential building parameters through an integration of global sensitivity and feature selection techniques. *Applied Energy*, *315*(March), 118956. https://doi.org/10.1016/j.apenergy.2022.118956

Nguyen, A. T., & Reiter, S. (2014). A climate analysis tool for passive heating and cooling strategies in hot humid climate based on Typical Meteorological Year data sets. *Energy and Buildings*, *68*(PART C), 756–763. https://doi.org/10.1016/j.enbuild.2012.08.050

Nguyen, A. T., Tran, Q. B., Tran, D. Q., & Reiter, S. (2011a). An investigation on climate responsive design strategies of vernacular housing in Vietnam. *Building and Environment*, *46*(10), 2088–2106. https://doi.org/10.1016/j.buildenv.2011.04.019

Ohene, E., Hsu, S. C., & Chan, A. P. C. (2022). Feasibility and retrofit guidelines towards net-zero energy buildings in tropical climates: A case of Ghana. *Energy and Buildings*, *269*(June). https://doi.org/10.1016/j.enbuild.2022.112252

Ohlsson, K. E. A., & Olofsson, T. (2021). Benchmarking the practice of validation and uncertainty analysis of building energy models. *Renewable and Sustainable Energy Reviews*, *142*(December 2020), 110842. https://doi.org/10.1016/j.rser.2021.110842

Østergård, T., Jensen, R. L., & Maagaard, S. E. (2018). A comparison of six metamodeling techniques applied to building performance simulations. *Applied Energy*, *211*, 89–103. https://doi.org/https://doi.org/10.1016/j.apenergy.2017.10.102

Pathirana, S., Rodrigo, A., & Halwatura, R. (2019). Effect of building shape, orientation, window to wall ratios and zones on energy efficiency and thermal comfort of naturally ventilated houses in tropical climate. *International Journal of Energy and Environmental Engineering*, *10*(1), 107–120. https://doi.org/10.1007/s40095-018-0295-3

Prathapasinghe, D., Perera, M. P. R. I., & Ariyawansa, R. G. (2018). *Evolution of Condominium Market in Sri Lanka: A Review and Predict*. https://en.wikipedia.org/wiki/List_of_house_types,

Prieto, A., Knaack, U., Auer, T., & Klein, T. (2018). Passive cooling & climate responsive façade design exploring the limits of passive cooling strategies to improve the performance of commercial buildings in warm climates. *Energy and Buildings*, *175*, 30–47. https://doi.org/10.1016/j.enbuild.2018.06.016

Rad, M. A. H., Jalaei, F., Golpour, A., Varzande, S. S. H., & Guest, G. (2021). BIM-based approach to conduct Life Cycle Cost Analysis of resilient buildings at the conceptual stage. *Automation in Construction*, *123*(January), 103480. https://doi.org/10.1016/j.autcon.2020.103480

Rajapaksha, I., Nagai, H., & Okumiya, M. (2003). A ventilated courtyard as a passive cooling strategy in the warm humid tropics. *Renewable Energy*, *28*(11), 1755–1778. https://doi.org/10.1016/S0960-1481(03)00012-0

Ramaji, I. J., Messner, J. I., & Mostavi, E. (2020). IFC-Based BIM-to-BEM Model Transformation. *Journal of Computing in Civil Engineering*, *34*(3). https://doi.org/10.1061/(asce)cp.1943-5487.0000880

Rana, M. J., Hasan, M. R., Sobuz, M. H. R., & Sutan, N. M. (2021). Evaluation of passive design strategies to achieve NZEB in the corporate facilities: the context of Bangladeshi subtropical monsoon climate. *International Journal of Building Pathology and Adaptation*, *39*(4), 619–654. https://doi.org/10.1108/IJBPA-05-2020-0037

Röck, M., Saade, M. R. M., Balouktsi, M., Rasmussen, F. N., Birgisdottir, H., Frischknecht, R., Habert, G., Lützkendorf, T., & Passer, A. (2020). Embodied GHG emissions of buildings – The hidden challenge for effective climate change mitigation. *Applied Energy*, *258*, 114107. https://doi.org/10.1016/J.APENERGY.2019.114107

Royapoor, M., & Roskilly, T. (2015). Building model calibration using energy and environmental data. *Energy and Buildings*, *94*, 109–120. https://doi.org/10.1016/j.enbuild.2015.02.050

Saltelli, A., Ratto, M., Andres, T., Campolongo, F., Cariboni, J., Gatelli, D., Saisana, M., & Tarantola, S. (2008). *Global Sensitivity Analysis: The Primer*. Wiley.

Santy, Matsumoto, H., Tsuzuki, K., & Susanti, L. (2017). Bioclimatic analysis in pre-design stage of passive house in Indonesia. *Buildings*, *7*(1). https://doi.org/10.3390/buildings7010024

Seghier, T. E., Lim, Y. W., Harun, M. F., Ahmad, M. H., Samah, A. A., & Majid, H. A. (2022). BIM-based retrofit method (RBIM) for building envelope thermal performance optimization. *Energy and Buildings*, *256*. https://doi.org/10.1016/j.enbuild.2021.111693

Shen, Y., & Pan, Y. (2023). BIM-supported automatic energy performance analysis for green building design using explainable machine learning and multi-objective optimization. *Applied Energy*, *333*(December 2022). https://doi.org/10.1016/j.apenergy.2022.120575

Shiveswarran, R., Athukorala, N., & Jayasinghe, M. T. R. (2023). Embodied Energy and Lifecycle Assessment of EPS based Light-weight Panel Apartments in Tropical Uplands. *Lecture Notes in Civil Engineering*, *266*(September), 783–798. https://doi.org/10.1007/978-981-19-2886-4_55

Singh, M. M., Deb, C., & Geyer, P. (2022a). Early-stage design support combining machine learning and building information modelling. *Automation in Construction*, *136*(January), 104147. https://doi.org/10.1016/j.autcon.2022.104147

Singh, M. M., Singaravel, S., Klein, R., & Geyer, P. (2020). Quick energy prediction and comparison of options at the early design stage. *Advanced Engineering Informatics*, *46*(September), 101185. https://doi.org/10.1016/j.aei.2020.101185

Sri Lanka Sustainable Energy Authority. (2019). *Guideline for Sustainable Energy Residences in Sri Lanka*.

Srinivasan, V., & Shocker, A. D. (1973). Linear programming techniques for multidimensional analysis of preferences. *Psychometrika*, *38*(3), 337–369. https://doi.org/10.1007/BF02291658

Sun, X., Gou, Z., & Lau, S. S. Y. (2018). Cost-effectiveness of active and passive design strategies for existing building retrofits in tropical climate: Case study of a zero energy building. *Journal of Cleaner Production*, *183*, 35–45. https://doi.org/10.1016/j.jclepro.2018.02.137

Thapa, S., Rijal, H. B., Pasut, W., Singh, R., Indraganti, M., Bansal, A. K., & Panda, G. K. (2023). Simulation of thermal comfort and energy demand in buildings of sub-Himalayan eastern India - Impact of climate change at mid (2050) and distant

(2080) future. *Journal of Building Engineering*, *68*(January). https://doi.org/10.1016/j.jobe.2023.106068

Trucano, T. G., Swiler, L. P., Igusa, T., Oberkampf, W. L., & Pilch, M. (2006). Calibration, validation, and sensitivity analysis: What's what. *Reliability Engineering & System Safety*, *91*(10–11), 1331–1357. https://doi.org/10.1016/J.RESS.2005.11.031

Truong, H., Francisco, A., Khosrowpour, A., Taylor, J. E., & Mohammadi, N. (2017). Method for visualizing energy use in building information models. *Energy Procedia*, *142*, 2541–2546. https://doi.org/10.1016/j.egypro.2017.12.089

Tzeng, G.-H., & Huang, J.-J. (2011). *Multiple Attribute Decision Making*. Chapman and Hall/CRC. https://doi.org/10.1201/b11032

Udawattha, C., & Halwatura, R. (2018a). Thermal performance and structural cooling analysis of brick, cement block, and mud concrete block. *Advances in Building Energy Research*, *12*(2), 150–163. https://doi.org/10.1080/17512549.2016.1257438

U.S. Green Building Council. (2016). *LEED 2009 for New Construction and Major Renovations Rating System*. www.usgbc.org

Weerasinghe, A. S., Ramachandra, T., & Rotimi, J. O. B. (2021). Comparative life-cycle cost (LCC) study of green and traditional industrial buildings in Sri Lanka. *Energy and Buildings*, *June*, 1–26. https://doi.org/10.1038/s41598-022-07229-w

Weerasuriya, A. U., Zhang, X., Gan, V. J. L., & Tan, Y. (2019a). A holistic framework to utilize natural ventilation to optimize energy performance of residential high-rise buildings. *Building and Environment*, *153*(February), 218–232. https://doi.org/10.1016/j.buildenv.2019.02.027

Wong, I., & Baldwin, A. N. (2016a). Investigating the potential of applying vertical green walls to high-rise residential buildings for energy-saving in sub-tropical region. *Building and Environment*, *97*, 34–39. https://doi.org/10.1016/j.buildenv.2015.11.028

World Bank. (2022). *Urban Development*. https://www.worldbank.org/en/topic/urbandevelopment/overview#1

Yan, H., Ji, G., & Yan, K. (2022). Data-driven prediction and optimization of residential building performance in Singapore considering the impact of climate change. *Building and Environment*, *226*(November), 109735. https://doi.org/10.1016/j.buildenv.2022.109735

Yew, M. C., Sulong, N. H. R., Chong, W. T., Poh, S. C., Ang, B. C., & Tan, K. H. (2013). *Integration of thermal insulation coating and moving-air-cavity in a cool roof system for attic temperature reduction*. *75*, 241–248. https://doi.org/10.1016/j.enconman.2013.06.024

Zhang, D., Zhang, J., Guo, J., & Xiong, H. (2019). A Semantic and Social Approach for Real-Time Green Building Rating in BIM-Based Design. *Sustainability*, *11*(14). https://doi.org/10.3390/su11143973

Zhang, J., Liu, N., & Wang, S. (2021). Generative design and performance optimization of residential buildings based on parametric algorithm. *Energy and Buildings*, *244*, 111033. https://doi.org/10.1016/j.enbuild.2021.111033

Zhong, X., Hu, M., Deetman, S., Steubing, B., Lin, H. X., Hernandez, G. A., Harpprecht, C., Zhang, C., Tukker, A., & Behrens, P. (2021). Global greenhouse gas emissions from residential and commercial building materials and mitigation strategies to 2060. *Nature Communications*, *12*(1). https://doi.org/10.1038/s41467-021-26212-z

Zhuang, D., Zhang, X., Lu, Y., Wang, C., Jin, X., Zhou, X., & Shi, X. (2021). A performance data integrated BIM framework for building life-cycle energy efficiency and environmental optimization design. *Automation in Construction*, *127*(December 2020), 103712. https://doi.org/10.1016/j.autcon.2021.103712

ANNEXURE 01 – DETAILS OF THE BASELINE BUILDING

Building energy model parameters of the validation model are presented in the following table,

Type	Variable	Value
Orientation	Longer axis direction	North-South
Exterior wall (Reinforced concrete with plasters in both sides)	Conductivity of core walling material Conductivity of plasters	2.1 W/m-K 0.72 W/m-K
Partition wall (Cement-sand block wall with plasters both sides)	Conductivity of core walling material	1.2 W/m-K
Interior floor (Reinforced concrete with tile bed)	Conductivity of core floor material Conductivity of floor finishes	2.1 W/m-K 1.2 W/m-K
External window	U-value of glass SHGC of glass	5.0 W/m^2-K 0.6 (ratio)
Window overhang	Overhang length	0.55m

3D view, typical floor layout and the sensor location of the field-study model is shown below,

ANNEXURE 02 – DESCRIPTIVE STATISTICS OF ML-MODEL TRAINING DATASET

Descriptive statistics of the dataset used for training the Machine-Learning model

	OH	SF	GW	EC	GU	WS	CW	WC
Count	200	200	200	200	200	200	200	200
Min	0	0	0	0.1	0.81	800.1	0.04	0.2
25% percentile value	0.30	0.30	0.33	0.28	2.04	1052.25	0.64	0.38
50% percentile value	0.60	0.60	0.33	0.45	3.25	1300.44	1.22	0.55
75% percentile value	0.90	0.90	1.00	0.62	4.47	1549.55	1.81	0.72
Max	1.20	1.20	1.00	0.80	5.70	1796.07	2.40	0.90
Mean	0.60	0.60	0.50	0.45	3.25	1300.07	1.22	0.55
Standard Deviation	0.35	0.35	0.37	0.20	1.41	288.62	0.68	0.20

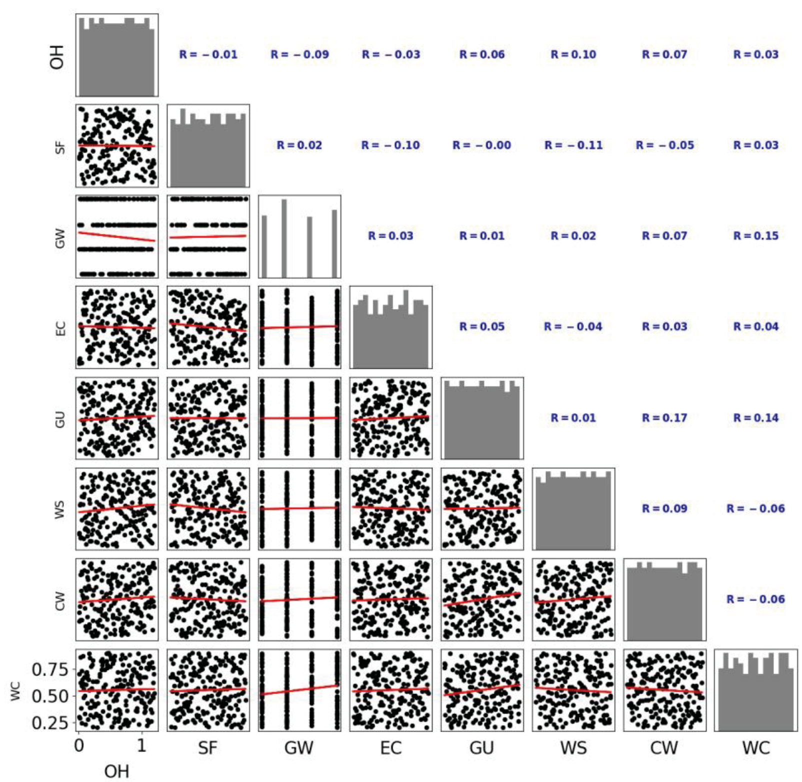

ANNEXURE 03 – GLOBAL WARMING POTENTIAL DATA OF BUILDING ELEMENTS

Strategy	Option	Description	GWP (kgCO2eq/m2)
EC	Option 1	Kraft 4 seasons paint for exterior use	0.35
	Option 2	General emulsion paint	0.206
CW	Option 1	Concrete block wall	16
	Option 2	Cement Sand block wall	30.38
	Option 3	Flash brick	17.55
	Option 4	EPS panel wall	71
GU	Option 1	3mm float glass	8.97
	Option 2	3mm float glass with a coating	9.745
	Option 3	6mm float glass	17.94
	Option 4	6mm float glass with a coating	18.715
	Option 5	6/16/6 Double glass	47.6
	Option 6	4/12/4/12/4 Triple glass	47.8
WC	Option 1	Coating on glasses	0.775
OH	Option 1		65.2
SF	Option 1		65.2